

Erosional Processes along Salt Marsh Edges
on the Eastern Shore of Virginia

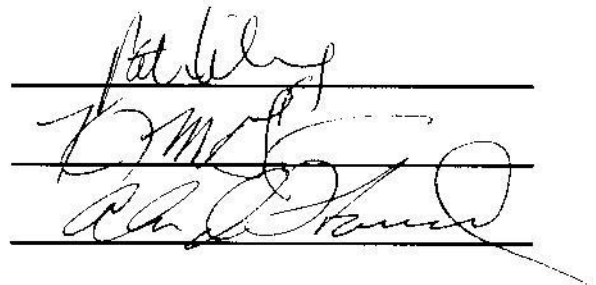
Sean Michael McLoughlin
Leonardo, New Jersey

B.A., University of Connecticut, 2008

A Thesis presented to the Graduate Faculty
of the University of Virginia in Candidacy for the Degree of
Master of Science

Department of Environmental Sciences

University of Virginia
December 2010



Three handwritten signatures are written on three horizontal lines. The top signature is 'Pat Kelly', the middle one is 'C. M. S.', and the bottom one is 'Ch. J. ...'.

ABSTRACT

Erosion and landward retreat of marsh edges has led to land loss in many marshes along the Atlantic Coast of the United States. Four salt marshes in a shallow, coastal lagoon on the Eastern Shore of Virginia were studied to determine long-term rates-of-change along the edges and to investigate the specific processes that contribute to erosion. Analysis of aerial photographs over a fifty-year period (1957-2007) using Geographic Information Systems (GIS) indicated that the marsh edge eroded rapidly at three of the marsh sites. Matulakin Marsh (a mid-lagoon peninsular marsh) experienced the greatest erosion at $1.62 \text{ m}\cdot\text{yr}^{-1}$, followed by Chimney Pole (a large marsh island) at $1.28 \text{ m}\cdot\text{yr}^{-1}$, and Hog Island (a backbarrier marsh) at $0.98 \text{ m}\cdot\text{yr}^{-1}$. Significant variability in erosion rates existed along the edge at each of the sites due to differences in wave energy, local bathymetry, and internal properties of the marsh edge (sediment, vegetation, and invertebrate characteristics). The edge at a fourth, mainland marsh, Fowling Point, remained relatively stable, with an erosion rate of $0.02 \text{ m}\cdot\text{yr}^{-1}$ over the study period. This is the result of a large mudflat that shields the marsh from high wave energy.

Sediment, vegetation, and invertebrate properties were sampled to make comparisons between sites and evaluate their effects on erosion. While wind-driven waves provide the force necessary to erode the marsh edge, other factors are important in controlling the rates and mechanisms of erosion. Results indicated that both the internal properties of the marsh edge and the specific mechanisms of erosion varied among the three eroding sites. Erosion at Matulakin Marsh was facilitated by widespread crab burrowing, which led to block detachment and slumping along the edge. At Chimney Pole, removal of the dense root mat by waves was followed by erosion of the weaker,

underlying sediment; this process was documented by a “webcam” installed on the marsh. Two erosion processes were evident at Hog Island. The southern portion of the site experienced significant undercutting and root mat toppling, which was facilitated by the marsh’s sandy substrate. The removal of the root zone by waves led to the formation of terraces at the northern end of the site, which are likely to erode gradually over time. Despite their location within a single lagoon system, the erosion of salt marsh edges may be controlled by significantly different processes. Sea-level rise is predicted to increase wave energy in the bay, leading to an acceleration of these erosion processes.

ACKNOWLEDGEMENTS

This research would not have been possible without the help of many individuals. First, I would like to thank my advisors, Pat Wiberg and Karen McGlathery, for their incredible support and generosity throughout this process. Together, they have made this a truly rewarding and enjoyable experience. I would also like to thank the third member of my committee, Alan Howard, for all of his helpful feedback. I would especially like to thank John Porter, who has had an instrumental role in much of this project, particularly with regards to GIS analysis and the camera design and setup; John has always made time to answer my questions and I am extremely grateful for all he has done. I am also appreciative of Dave Carr for providing assistance with statistical analyses and Rachel Michaels for teaching me about the ecology of salt marshes. The hydrodynamic data and wave model estimates presented here were provided by Sergio Fagherzazzi and Giulio Mariotti, who are collaborators on this project at Boston University.

I would like to thank the staff at the ABCRC field station for both logistical and field support, and particularly Art Schwarzschild and Chris Buck for assisting in the camera installation. I am grateful for field assistance from Dana Gulbransen, Kelly Hondula, Gavin Bruno, Jenny Shultis, Austin Riopel, James Self, and David Boyd, as well as lab assistance by Carlos Disla. Thanks to the McG lab group for their support, enthusiasm, and friendship. I would also like to thank my officemates, Dana Gulbransen, Dirk Koopmans, and Sara Taube for making the days more enjoyable, as well as Cat Wolner, Owen Brenner, and Clara Funk for providing helpful comments in discussing similar research issues. Finally, I would like to thank my friends and family, especially

my parents (Tom and Flo) and brothers (Pat and Tommy) for their unending support and encouragement in everything I do.

Funding for this project was provided by the US Department of Energy through the National Institute for Climatic Change Research (NICCR) program. An Exploratory Research Award from the Department of Environmental Sciences at the University of Virginia provided funding for the erosion camera. This research was conducted in the Virginia Coast Reserve, a National Science Foundation Long Term Ecological Research site.

TABLE OF CONTENTS

Abstract.....	ii
Acknowledgements.....	iv
Table of Contents.....	vi
List of Figures.....	viii
List of Tables.....	ix
Chapter 1: Introduction.....	1
Marsh Ecosystems and Edge Erosion.....	1
Hydrological Influences on Erosion.....	2
Sediment Properties and Erosion.....	4
Marsh Vegetation.....	5
The Role of Invertebrates in Marsh Ecosystems.....	7
Crabs.....	7
Mussels.....	10
Snails.....	10
Site Description.....	11
Significance.....	12
Chapter 2: Marsh Shoreline Change.....	17
Objective.....	17
Methods.....	17
Image Quality and Error Assessment.....	21
Sources of Error.....	21
Methodology.....	22
Error Results and Interpretation.....	23
Results.....	27
Discussion.....	40
Chapter 3: Effects of Marsh Edge Characteristics on Erosion.....	45
Objective.....	45
Methods.....	45
Lagoon Hydrodynamics.....	45
Edge Elevation and Morphology.....	46
Sediment Properties.....	46
Vegetation Characteristics.....	49
Invertebrate Characteristics.....	51
Statistical Analysis.....	52
Results.....	54
Hydrodynamics.....	54
Elevation and Morphology.....	56
Sediment Properties.....	62
Vegetation Characteristics.....	69
Crab Burrows.....	78
Mussel and Snail Densities.....	82

Discussion.....	85
Hydrodynamics.....	85
Elevation and Morphology	87
Sediment Properties	90
Vegetation Characteristics	94
Crab Burrows.....	97
Mussel and Snail Densities.....	100
Interpreting Fowling Point.....	101
Impacts on Erosion	103
Chapter 4: Mechanisms of Marsh Edge Erosion	104
Previously Observed Mechanisms of Edge Erosion.....	104
Erosion Mechanisms in Hog Island Bay	106
Matulakin Marsh.....	106
Chimney Pole.....	108
Observational Study at Chimney Pole.....	110
Hog Island.....	112
Mechanistic Significance.....	119
Future Sustainability	120
Conclusions.....	122
References.....	125
Appendix 1: Transect Regressions.....	134
Appendix 2: June and August Vegetation	138
Appendix 3: Burrow Characteristic Means.....	139
Appendix 4: Camera Design.....	140
Appendix 5: Hog Island Characteristic Comparisons.....	141
Appendix 6: Selected Marsh Characteristic Means	142
Appendix 7: Sediment Grain Size Distributions.....	145

LIST OF FIGURES

Figure 1.1	Map of Eastern Shore of Virginia	14
Figure 1.2	Map of Hog Island Bay study sites.....	15
Figure 1.3	Images of marsh edge at study sites	16
Figure 2.1	Required DSAS inputs for Chimney Pole	20
Figure 2.2	Mean rates of shoreline change	30
Figure 2.3	Edge locations at Chimney Pole.....	31
Figure 2.4	Edge locations at Matulakin Marsh.....	32
Figure 2.5	Edge locations at Hog Island.....	33
Figure 2.6	Edge locations at Fowling Point.....	34
Figure 2.7	Rates-of-change at Chimney Pole	35
Figure 2.8	Rates-of-change at Matulakin Marsh	36
Figure 2.9	Rates-of-change at Hog Island	37
Figure 2.10	Rates-of-change at Fowling Point	38
Figure 2.11	Class distributions for rates-of-change.....	39
Figure 2.12	Edge accretion at Fowling Point.....	44
Figure 3.1	Maps of survey locations.....	47
Figure 3.2	Lagoon hydrodynamics	55
Figure 3.3	Elevation profiles at Chimney Pole.....	58
Figure 3.4	Elevation profiles at Matulakin Marsh.....	59
Figure 3.5	Elevation profiles at Hog Island.....	60
Figure 3.6	Elevation profiles at Fowling Point.....	61
Figure 3.7	Sediment grain size.....	64
Figure 3.8	Sediment grain size class distributions.....	65
Figure 3.9	Organic content and grain size linear regression.....	67
Figure 3.10	Surface and scarp sediment shear strength.....	68
Figure 3.11	Aboveground and belowground vegetation biomass	71
Figure 3.12	Belowground biomass depth profiles	72
Figure 3.13	Root tensile strength and diameter linear regression.....	76
Figure 3.14	Root and rhizome tensile strength	77
Figure 3.15	Crab burrow characteristics	80
Figure 3.16	Crab burrow forms	81
Figure 3.17	Mussel and snail densities	83
Figure 3.18	Wave power and erosion rate linear regression.....	86
Figure 3.19	Flood tide and marsh flat elevations.....	89
Figure 4.1	Erosion process at Matulakin Marsh	107
Figure 4.2	Erosion process at Chimney Pole	109
Figure 4.3	Images from Chimney Pole camera	113
Figure 4.3	Images from Chimney Pole camera (cont.).....	114
Figure 4.4	Meteorological data corresponding with CP erosion event.....	115
Figure 4.5	Erosion process at southern Hog Island	117
Figure 4.6	Erosion process at northern Hog Island.....	118

LIST OF TABLES

Table 1.1	Erosion rates at marshes in previous studies	3
Table 2.1	RMS errors for rectified aerial photographs	19
Table 2.2	Image accuracy analysis	25
Table 2.3	Accuracy analysis statistical results.....	25
Table 2.4	DSAS R-squared comparisons.....	26
Table 2.5	DSAS R-squared statistical results	26
Table 2.6	Mean shoreline rates-of-change.....	29
Table 3.1	Wave powers at the marsh sites	54
Table 3.2	Welch's ANOVA for edge elevations	56
Table 3.3	Mean edge elevations.....	56
Table 3.4	Sediment property means.....	63
Table 3.5	Sediment property ANOVA results	66
Table 3.6	Sediment pairwise contrasts.....	66
Table 3.7	Vegetation characteristic means	73
Table 3.8	Vegetation characteristic pairwise contrasts.....	73
Table 3.9	Vegetation characteristic ANOVA results.....	74
Table 3.10	Upper root mat (0-5 cm) ANOVA results	75
Table 3.11	Upper root mat pairwise contrasts	75
Table 3.12	Root tensile strength ANOVA results	75
Table 3.13	Crab burrow ANOVA results	79
Table 3.14	Burrow density pairwise contrasts.....	79
Table 3.15	Crab counts and species identification.....	82
Table 3.16	Mussel and snail statistical results	84
Table 3.17	Mussel and snail pairwise contrasts.....	84

CHAPTER 1: INTRODUCTION

Marsh Ecosystems and Edge Erosion

Salt marshes are highly productive ecosystems located in intertidal zones between terrestrial and marine landscapes. As a result of this transitional location, they play a vital economic and ecological role in coastal communities. Marshes not only provide a unique habitat for an array of flora and fauna species, but they also serve as a filtration system for minerals and sediments, a breeding ground and protective nursery for many fish and bird species, and a coastal buffer against strong winds, waves, and storm flooding (Pennings and Bertness 2001). The location of salt marshes within the terrestrial-marine boundary also leaves them vulnerable to erosional processes brought on by hydrologic and geologic forces. A combination of natural and anthropogenic processes is currently leading to widespread loss of these vital ecosystems in many parts of the world. Sea-level rise is predicted to cause more rapid erosion of marsh boundaries in coastal bays due to increases in water depths and wave heights (Mariotti et al. 2010). The frequency of extra-tropical storms on the Virginia coast has also increased over the past century (Hayden and Hayden 2003). If this trend continues, it could have a large effect on erosion, as erosion events are highly associated with storms (Schwimmer 2001).

Erosion of marshes is primarily due to three processes: relative sea-level rise, land subsidence, and wave attack along the marsh edge (Day et al. 1998). Low-lying deltaic regions, such as the Louisiana Gulf Coast, experience significant erosion and wetland loss due to the effects of relative sea-level rise and natural land subsidence (DeLaune 1983, Reed 1990). Many marshes in these regions are unable to accrete enough sediment and organic material to maintain a vertical elevation that is at equilibrium with mean sea-

level. Many mid-Atlantic marshes also have been losing area due to the effects of sea-level rise and subsidence (Phillips 1986a, Finkelstein and Hardaway 1988, Kearney and Stevenson 1991). However, marshes in this area have also been shown to experience significant erosion along their boundaries, due primarily to wave attack (Downs et al. 1994, Wray et al. 1995, Schwimmer 2001, Erwin et al. 2004). Several studies have documented this form of erosion and have provided rates of shoreline retreat for marshes throughout the U.S. and Europe (Table 1.1). However, comparatively few studies have examined the mechanisms leading to erosion of the marsh edge. It is the objective of this research to examine rates of shoreline change at four Virginia salt marshes and to determine what processes and characteristics of the marsh contribute to edge erosion.

Hydrological Influences on Erosion

Previous studies have indicated that wind-induced waves appear to be the major cause of erosion of the open-water marsh edge (Wray et al. 1995, Day et al. 1998, Schwimmer 2001, Mariotti et al. 2010). Therefore, erosion rates are strongly associated with wave height and power. Wave heights in shallow coastal lagoons, such as those on the Delmarva Peninsula, are determined through the interactions of water depth, fetch, and wind speed and direction (Fagherazzi and Wiberg 2009). This is because waves grow larger as water depth increases, fetch lengthens, and wind speeds increase. Increases in wave heights and wind speeds over time have been shown to have a potentially significant effect on rates of marsh erosion (van der Wal and Pye 2004). The higher wave power associated with these larger waves is likely to increase edge erosion

Location	Erosion Rate (m yr⁻¹)	Duration of Study (yrs)	Study
<i>United States</i>			
Delaware Bay, NJ	3.21	38	<i>Phillips (1986a)</i>
Rehoboth Bay, DE	0.14 – 0.43	3	<i>Schwimmer (2001)</i>
Chesapeake Bay, MD	1.2	139	<i>Wray et al. (1995)</i>
Hog Island Bay, VA	~ 1.2	41	<i>Kastler and Wiberg (1996)</i>
York River Estuary, VA	0.21	95	<i>Byrne and Anderson (1978)</i>
Pamlico Sound, NC	0.79 – 0.91	25 – 32	<i>Phillips (1986a)</i>
Mississippi Delta, LA	~ 1	67	<i>Wilson and Allison (2008)</i>
<i>Europe</i>			
Dengie Peninsula, UK	1.1	9	<i>van der Wal and Pye (2004)</i>
Blackwater Estuary, UK	0.5 - 1	8	<i>van der Wal and Pye (2004)</i>
Foulness Point, UK	4 - 16	19	<i>Stoodley (1998)</i>
The Oosterschelde, Netherlands	~ 1	N/A	<i>van Eerd (1985a)</i>
Sado Estuary, Portugal	0.17	11	<i>Moreira (1992)</i>
Venice Lagoon, Italy	1.2 – 2.2	2	<i>Day et al. (1998)</i>

Table 1.1. Rates of edge erosion determined at marshes in previous research studies.

under these conditions (Schwimmer 2001). Therefore, marsh erosion is often positively correlated with storm events. During large storm events, when storm surge submerges the marsh, waves may overtop the edge and break and dissipate in the marsh interior; at that point, waves no longer directly impact the marsh edge. This suggests that intermediate storms, with mid-sized waves, may have a greater impact on erosion (Wray et al. 1995).

As waves impact the marsh, they dislodge sediment and degrade the edge. The persistence of the wave action causes large quantities of sediment and large blocks of the vegetation root mat to be removed from the edge (Wray et al. 1995). This leads to a horizontal retreat of the edge and a reduction in total marsh area. The eroded sediment has the potential to serve as an important source material for vertical accretion of the marsh flat (Reed 1988), however, it does not prevent the retreat of the edge.

Sediment Properties and Erosion

The sediment characteristics of a marsh are critical in determining the stability and erosion resistance of marsh ecosystems (Feagin et al. 2009). The important physical properties of sediment include grain size, bulk density, porosity, organic matter content, and soil shear strength. These soil parameters tend to be highly interrelated and together, determine the sediment's ability to resist erosion.

When examining the processes of erosion along the marsh edge, several of these parameters can be indicators of how resistant the sediment is to erosion. Bulk density has been shown to be a particularly important factor in determining sediment erosion within marshes (van der Wal and Pye 2004, Feagin et al. 2009). This may be an indication that

less consolidated, sandier sediments are more easily eroded than firmer, muddier sediments. Allen (1989) found that marsh cliffs with sandy sediments were more susceptible to undercutting from wave action than those of stronger, finer-grained marshes, though the geomorphic and environmental settings differed between sites.

Potentially the most important sediment characteristic influencing erosion rates is shear strength. Shear strength is a measure of the resistance of a soil or sediment to vertical shearing (Watts et al. 2003). According to Pestrong (1969), shear strength is “a function of the cohesion and internal friction of the soil and of the effective load directed to the plane of shear.” Sediments with higher shear strengths possess a greater resistance to erosion and are better able to withstand the impacts of waves and tidal currents (Watts et al. 2003). The presence of a dense root mat in marsh systems has the potential to increase sediment shear strength due to the strong binding of the sediment with the root system (Allen 1989, Watts et al. 2003,).

Marsh Vegetation

Salt marshes along the Atlantic and Gulf Coasts of the United States are dominated by the vegetation species *Spartina alterniflora* (smooth cordgrass). *S. alterniflora* is a perennial halophyte that is adapted to withstand high-stress environments and thrives in the intertidal zone of salt marshes. It commonly exists in two distinctive growth forms within salt marshes. The tall-form vegetation typically grows to heights greater than 1 m, has a comparatively low shoot density, and generally persists in the lower tidal zones of the marsh near creek banks (Valiela et al. 1978, Morris 1980). Short-form *S. alterniflora* exists at heights less than 90 cm (commonly 10-40 cm), has a

high shoot density, and is dominant in higher marsh elevations, landward of the tall form (Valiela et al. 1978, Gross et al. 1991). Though not clearly defined in the literature, the seaward edge of the marsh is thought to be dominated by the tall form (Ellison et al. 1986). Much of the ecological focus on *S. alterniflora* has centered on trying to explain the existence of these growth forms and their zonation within salt marshes (e.g. Morris 1980, Gallagher et al. 1988). Salinity, nitrogen supply, sediment oxidation, and drainage are a few of the likely controls on *S. alterniflora* growth form (Howes et al. 1986).

Due to its intertidal location, *Spartina* plays an important role in damping wave energy and reducing erosion along marsh edges. Aboveground vegetation canopies have the potential to reduce wave heights significantly and to dissipate wave energy in coastal marshes (Möller et al. 1999). Both stem density and canopy height play key roles in the dissipation or attenuation of wave energies, as density affects horizontal friction and vegetation height influences boundary layer depth (Möller 2006). Studies from the US (Virginia) and UK (Norfolk) found that wave energies were dissipated by 100% and 82%, respectively, as they moved through the marsh (Knutson et al. 1982, Möller et al. 1999). This is largely the result of the drag produced by plant stems, which reduces wave heights and energy (Knutson et al. 1982). Most wave energy is dissipated near the marsh edge (Möller 2006), with greater than 50% dissipation possible within the first 2.5 meters of *S. alterniflora* marshes (Knutson et al. 1982).

The stability of the marsh edge is highly dependent on the strength of the sediment at the edge (van Eerd 1985a). Sediment strength is a function of the binding capacity of the vegetation root system, which is an effect of biomass, root length, root diameter, and tensile strength (van Eerd 1985a). Therefore, marshes with a stronger root

mat are more equipped to resist wave attack and experience lower rates of erosion. Micheli and Kirchner (2002) found that herbaceous vegetation has the potential to cause as much as an eightfold increase in sediment strength along riparian banks. Sediment shear strength also increases as the ratio of belowground biomass to sediment mass increases (Micheli and Kirchner 2002). While some studies have failed to find a relationship between belowground biomass and edge erosion (Feagin et al. 2009), it has often been regarded as an important control on erosion rates (Rosen 1980, van Eerd 1985a, Allen 1989, Goodbred and Hine 1995), and merits further study.

The Role of Invertebrates in Marsh Ecosystems

Crabs

Often the most abundant and influential invertebrate groups inhabiting marsh and mangrove ecosystems are fiddler crabs (*Uca* spp.). Fiddler crabs are burrowing crab species that play a major role in the functioning of coastal marshes (Wang et al. 2010) and rework large quantities of sediment through their burrowing (McCraith et al. 2003), which softens and destabilizes the sediment and potentially affects marsh erosion (Botto and Iribarne 2000). Salt marshes along the temperate Atlantic Coast of the United States are inhabited by three species of fiddler crabs: *Uca pugnax*, *U. pugilator*, and *U. minax* (Teal 1958). These three species vary in their distributions within marshes based on substrate type, salinity, vegetation structure, and elevation (Allen and Curran 1974). Therefore, their relative importance to the marsh landscape may vary between marshes.

The most abundant and widely studied of the three Atlantic fiddler species is *U. pugnax*, commonly known as the Atlantic marsh fiddler or mud fiddler (Grimes et al.

1989). *U. pugnax* are dominant in areas with muddy sediment and intermediate root mat densities, particularly within the low marsh from creek banks to transitional zones (Montague 1980). *U. pugilator* (Atlantic sand fiddler), on the other hand, prefers marshes or beaches with sandier sediment, and often struggles to survive without its preferred substrate (Teal 1958). These two species have very similar appearances, but may be differentiated by slight differences in color and the presence of a distinguishing ridge on the cheliped palm of *U. pugilator* (Allen and Curran 1974). *U. minax* (red-jointed fiddler) is more easily distinguishable and is larger than the other two species. These fiddlers tend to be found in muddy environments with lower salinity levels. Due to their preference for brackish marshes, it is unlikely that *U. minax* have a significant presence in the lagoonal salt marshes of the Delmarva Peninsula. Therefore, this study will only focus on the Atlantic marsh and sand fiddler species.

Burrows are a critical part of a fiddler crab's existence on the salt marsh and serve a variety of purposes. They are a source of relief against unfavorable temperatures, provide protection against predators, provide necessary moisture during low tides, offer shelter during molting, and may be important for courtship and mating activities (Montague 1980). The burrows of *U. pugilator* and *U. pugnax* have average diameters of 1-2 cm and typically have J-, L-, and U-shaped geometries (Allen and Curran 1974). *U. pugnax* burrows tend to be more complex structures and often intersect each other or the burrows of other marsh crab species, creating complex, interconnected patterns (Grimes et al. 1989). Burrow densities may be high for both fiddler species, with densities greater than 40 burrows per square meter. However, *U. pugnax* burrow densities may be as much as 8 to 10 times greater than those of *U. pugilator* in some marshes (Montague

1980). Burrow densities of *U. pugnax* are typically highest near creek banks and decrease with distance towards the interior.

Along with fiddler crabs, marsh ecosystems are often inhabited by other burrowing crab species that may influence erosion through the reworking of sediment. Two species that may be found burrowing in marshes with muddy substrate are *Sesarma reticulatum* and *Panopeus herbstii*. *S. reticulatum* (purple marsh crab) is a nocturnal, herbivorous crab that often inhabits muddy or peaty marsh substrate (Bertness et al. 2009). *P. herbstii* (Atlantic mud crab) is a large marsh crab commonly found living alongside *S. reticulatum* in burrows near the marsh edge (Allen and Curran 1974). Several members of both species may communally share large, complex burrow systems that often intersect the burrows of *U. pugnax*. These burrows are much larger than those of the fiddler species with multiple openings and chambers, and may extend to depths of 75 cm (Allen and Curran 1974). Therefore, these extensive burrow systems near the marsh edge are likely to have a contributing effect on erosion.

The burrowing activity of crabs has been shown to have a significant effect on marsh ecosystems, particularly with regard to porewater chemistry (Michaels 2004), drainage (Xin et al. 2009), and vegetation growth (Bertness 1985). However, much less is known about their influence on the erosion of marsh edges. The grazing of *S. reticulatum* is causing die-off of vegetation in New England salt marshes, which has the potential to affect erosion near the edge (Holdredge et al. 2009). A more direct effect of the burrowing activity of crabs on marsh erosion has been observed in marshes in Argentina. Dense, interconnected burrows of *Chasmagnathus granulatus* near marsh edge sites decrease sediment shear strength and increase penetrability and water content,

reducing soil strength, and leading to erosion of banks through tidal creek widening (Escapa et al. 2007). The large interconnected burrows of *S. reticulatum* and *U. pugnax* have been implicated in the slumping and collapse of tidal creek banks (Edwards and Frey 1977, Bertness et al. 2009), but to the best of my knowledge, no studies have been performed directly linking edge erosion to the burrowing activity of crabs.

Mussels

The ribbed mussel, *Geukensia demissa*, is a bivalve commonly observed within salt marsh ecosystems. *G. demissa* are highly associated with *S. alterniflora*, as the mussels often maintain their position by attaching to the stems and roots of the cordgrass (Bertness 1984). Ribbed mussels are often found at very high densities near the marsh edge and their numbers tend to decrease significantly with distance from the edge (Bertness 1984, Franz 2001). Bertness (1984) has argued that the presence of *G. demissa* can increase the productivity of *S. alterniflora*. However, ribbed mussels can also be important in stabilizing marsh sediment and reducing erosion. This occurs by both slowing wave and current velocities and binding sediment to the root mat (Bertness 1984). Therefore, *G. demissa* may play an integral role in preventing erosion along marsh edges.

Snails

Another common marsh invertebrate that serves an important role in the ecosystem is the periwinkle snail (*Littoraria irrorata*). *L. irrorata* are the most abundant grazers in salt marshes along the Atlantic coast (Silliman and Bertness 2002). They have

the ability to impact the *S. alterniflora* community significantly through their grazing behavior. Although *L. irrorata* may not have a direct effect on the erosion of marsh edges, they may indirectly impact erosion processes through their alteration of the vegetation community. Silliman et al. (2005) found that high densities of snails in Georgia and Louisiana marshes led to significant die-off of marsh vegetation and the conversion of plant-dominated marsh regions to mudflats. Significant *S. alterniflora* die-off near the marsh edge may indirectly affect erosion potential by reducing vegetation cover.

Site Description

This study was conducted in salt marshes within the Virginia Coast Reserve (VCR) at the southern end of the Delmarva Peninsula (Figure 1.1). The VCR serves as a Long Term Ecological Research (LTER) site (www.vcrlter.virginia.edu). The barrier-lagoon-marsh system of the VCR is typical of the Atlantic Coast of the US. Four marshes were chosen within Hog Island Bay, a shallow coastal lagoon on the Atlantic side of the Delmarva Peninsula, for this research (Figure 1.2). The lagoon covers an approximate area of 100 km² (McGlathery et al. 2001), with a maximum fetch between mainland and island (WNW-ESE) of roughly 11.5 km. The mean tidal range and mean water depth (with respect to mean sea-level) within the lagoon are 1.2 and 2.1 m, respectively (Mariotti et al. 2010; Oertel 2001); about 50% of the surface area is less than 1 m at mean low water (McGlathery et al. 2001). Marshes are extensive within the bay, covering roughly 30% of the total area (Oertel 2001).

Four marsh sites were chosen for their varying location, directional orientation, and wind exposure within the bay, along with the physical appearance of their edge. All four marshes are dominated by *S. alterniflora*. Hog Island marsh (37°23'55" N, 75°42'39" W) is a backbarrier marsh located on Hog Island. Due to its location, this marsh has likely experienced significant overwash over the course of its lifetime. To the northwest of Hog Island sits a second site, Chimney Pole marsh (37°27'45.5" N, 75°42'58" W), which is a large marsh island near Quinby Inlet. A previous study has indicated that this marsh has been experiencing significant edge erosion (Kastler and Wiberg 1996). A third site, Matulakin Marsh (37°29'26" N, 75°44'35.5" W), lies at the northern portion of the bay. This is a peninsular marsh that extends into the lagoon from the mainland. Hog Island (HI), Chimney Pole (CP), and Matulakin Marsh (MM) are suspected to be experiencing edge erosion due to the presence of steep or nearly vertical scarps at the edge, which is a common feature of eroding marshes (Schwimmer and Pizzuto 2000). The final marsh site is located on Fowling Point (37°26'4.5" N, 75°49'4" W), which is thought to be a hammock marsh attached to the mainland peninsula (Oertel and Woo 1994). Unlike the other three sites, this marsh has a gently-sloping edge extending from mudflat to marsh interior, which indicates a stable or prograding shoreline (van Eerdt 1985a). Figure 1.3 provides representative pictures of the marsh edge at each of the four sites.

Significance

The purpose of this research was to evaluate long-term erosion or accretion along the edges of salt marshes and to determine what processes may influence these changes.

The first objective of this project was to determine rates-of-change along the edges at the four salt marshes over a fifty-year period. This was achieved using aerial photographs and Geographic Information Systems (GIS). The second objective was to examine the characteristic conditions along the marsh edge at each site to determine what internal properties or external forces may contribute to or facilitate erosion. Factors that are likely to have an effect on erosion include wave activity near the edge, sediment characteristics, and ecological communities (vegetation and infaunal activity). Both between-site and within-site comparisons of these different parameters have the potential to provide information about which properties along the marsh edge may be important to erosional processes. The third objective was to identify and describe mechanisms that appear to be responsible for erosion at each site. These mechanisms may differ based on the individual characteristics of the marshes. The results of this research provide a comprehensive look at how internal properties of the marsh may affect erosion potential.

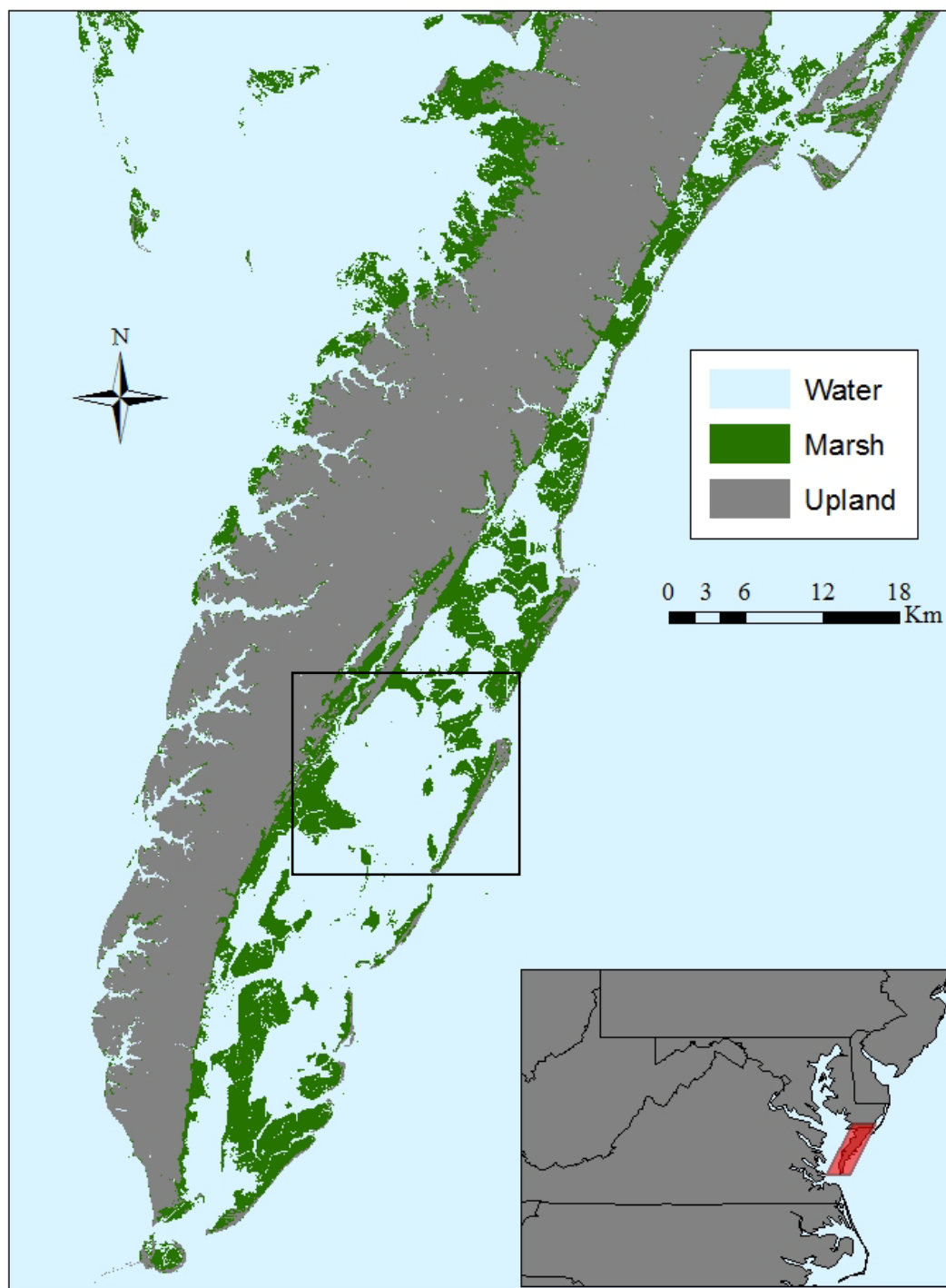


Figure 1.1. Map of the Eastern Shore of Virginia at the southern end of the Delmarva Peninsula (inset). Box indicates location of Hog Island Bay and surrounding marshes.



Figure 1.2. Locations of the four marsh sites in Hog Island Bay: Fowling Point (FP), Matulakin Marsh (MM), Chimney Pole (CP), and Hog Island (HI).

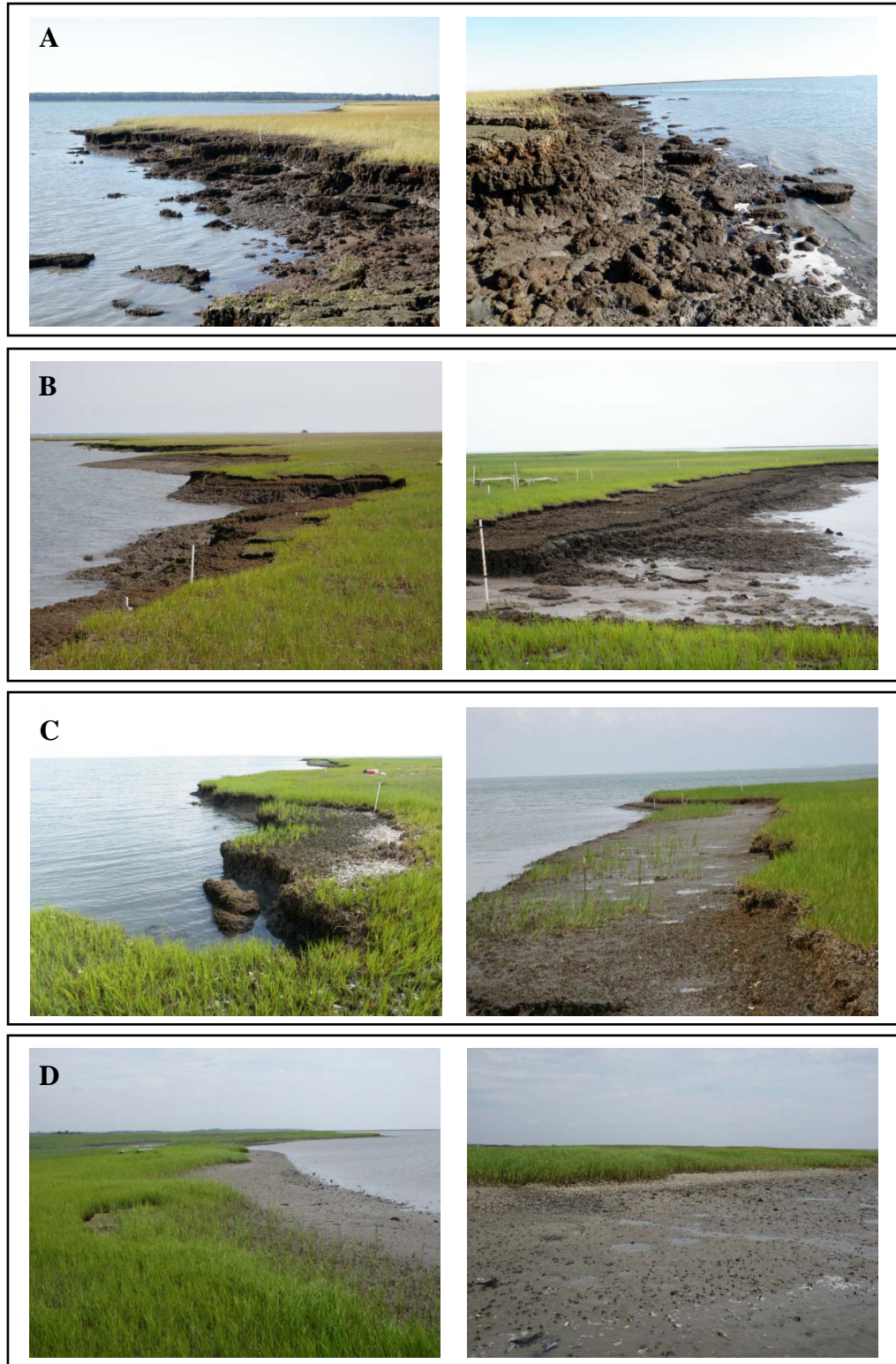


Figure 1.3. Photographs of the marsh edge at Matulakin Marsh (A), Chimney Pole (B), Hog Island (C), and Fowling Point (D).

CHAPTER 2: MARSH SHORELINE CHANGE

Objective

The first goal of this study was to determine rates-of-change along the marsh edge at the four marshes being observed. Using aerial photographs and Geographic Information Systems (GIS), average rates of shoreline movement were quantified over a fifty-year period. An accurate measurement of edge erosion or accretion allows comparisons to be made between the marshes and provides insight into how the boundaries of these systems have been altered over time. These comparisons also provide information for the development of specific hypotheses about how and why the mechanisms of change may differ between sites.

Methods

Marsh shoreline change analysis was performed using aerial photographs and the Geographic Information Systems (GIS) software ArcGIS 9.3 (ESRI, Redlands, CA). Five aerial photographs spanning a fifty-year period (1957, 1968, 1989, 2002, 2007) were chosen based on availability and image quality. The earliest images obtained were 1:20,000 black and white aerial photographs taken in 1957 under the direction of the Farm Service Agency of the USDA. The next sets of photographs were declassified defense images taken in 1968 through the Global Fiducials Program. Color-infrared photographs for 1989 were acquired from a NASA flight performed for the National Park Service. Digital orthophotographs taken in 2002 and 2007 through the Virginia Base Mapping Program (VBMP) provide the most recent images of the marshes.

While the 1968, 2002, and 2007 images had been previously georeferenced or orthorectified, the 1957 and 1989 photographs needed to be rectified in ArcMap. Traditional ground-control points (i.e., road intersections and corners of buildings) were used where present, however, these features were rare and creek intersections were used in their absence (Kastler 1993, Higinbotham et al. 2004). In the absence of permanent structures, the intersections of marsh creeks are often the most temporally stable features in these ecosystems. The 2007 digital orthophotograph was used as the base layer to which the images were rectified. Polynomial transformation was used as the rectification technique; second-order transformation was used in all cases because it provided the best results, with the exception of the 1957 Hog Island photograph, for which first-order transformation was used. The root mean square (RMS) errors for the two sets of aerial photographs are provided in Table 2.1. The RMS error is a measure of the proximity of the ground-control points (GCPs) of the transformed image to the GCPs of the original base layer, and is calculated automatically in ArcMap. An RMS error within 5 m was considered sufficient for the images to be used in the change analysis (Hughes et al. 2006). The ground resolution (as determined from pixel size) for the 1957, 1968, 1989, 2002, and 2007 images was 0.34 m, 2 m, 0.7 m, 0.6 m, and 0.3 m, respectively.

The marsh edge was digitized on-screen for each aerial photograph in ArcMap in order to create a line segment based on the shape and position of the edge. Typically, a distance between 3,400 m and 4,300 m was covered for each site. The digitized segments were then analyzed using the Digital Shoreline Analysis System (DSAS). DSAS is an ArcGIS extension specifically designed to compute shoreline rate-of-change statistics (Thieler et al. 2009). By overlaying the edge segments for each of the five years at a

particular marsh site, DSAS is able to compute an array of rate-of-change statistics for that site over the designated time period. The required inputs include a shoreline layer (consists of the five edge segments), a baseline layer (off of which transects are cast), and a transect layer (a series of adjacent lines on which statistics are calculated). An example of the necessary input features prior to running the change analysis is provided in Figure 2.1. DSAS performs a simple linear regression on the shorelines in order to determine the rate-of-change at each transect. A mean rate-of-change for each marsh was determined by averaging the rates for each transect across the length of the marsh edge. Comparisons between the marsh sites were made using the statistical software SAS 9.1 (SAS Institute, Cary, NC).

Marsh	RMS Error (m)	
	1957	1989
FP	4.89	2.30
HI	3.95	2.38
CP	4.65	1.93
MM	4.03	3.64

Table 2.1. RMS error for georectification of aerial photographs from 1957 and 1989. Second-order polynomial transformation was used for all images, except 1957 HI, where first-order transformation was used.

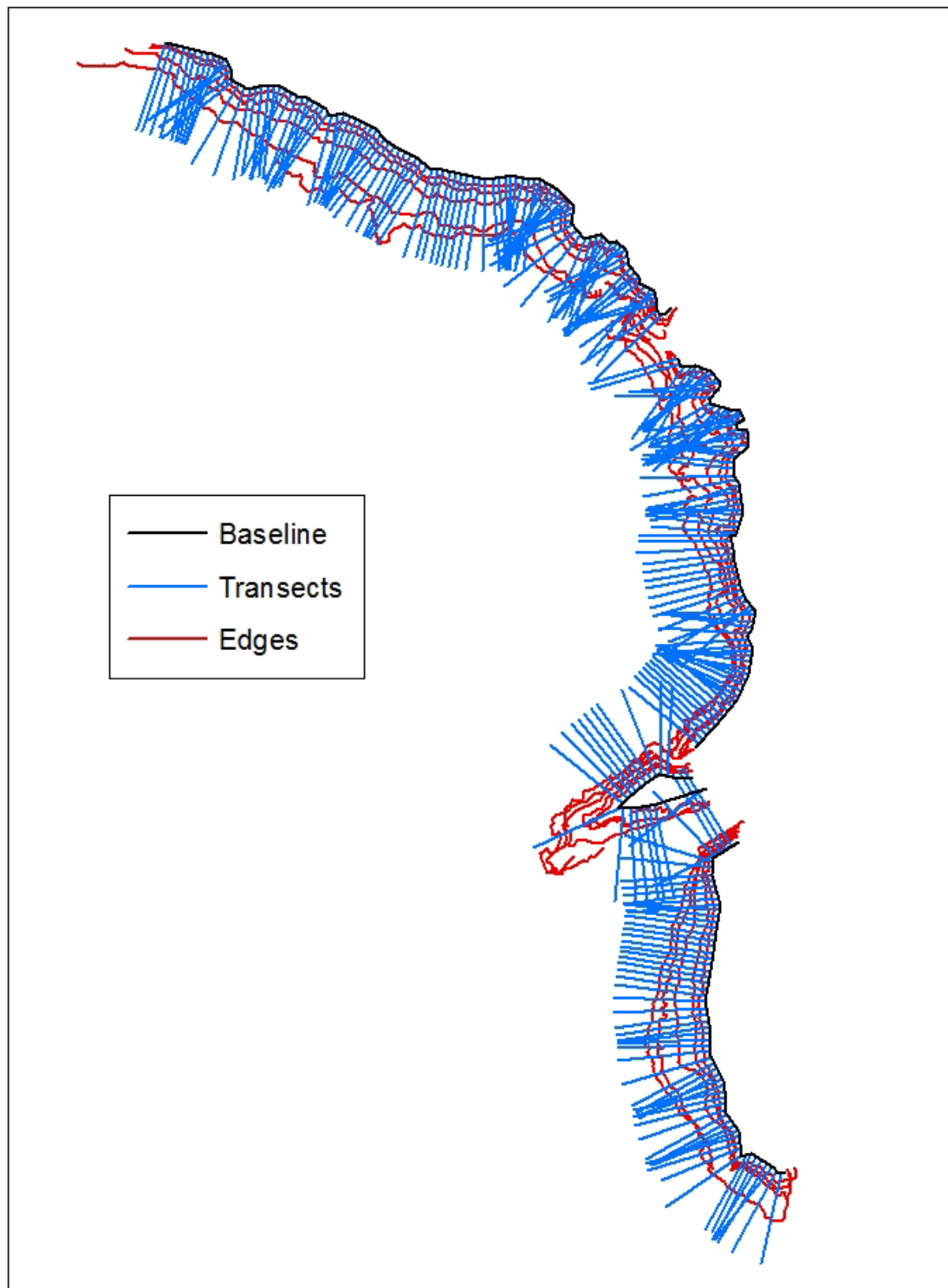


Figure 2.1. Required inputs for Chimney Pole marsh prior to running statistics in DSAS. Inputs include baseline, edge, and transect layers.

Image Quality and Error Assessment

Sources of Error

There are several sources of error that must be taken into account when using aerial photographs to map shoreline changes. There may be error associated with the photographs themselves, as lens distortion, camera tilt, and film deformation can all have an effect on the accuracy of an image (Moore 2000). Error can also be introduced during the scanning process; this can often be reduced by adjusting the resolution of the scan, however distortions may still occur if the film is not completely level on the scanning bed.

Some of the error associated with the images used in this study can certainly be attributed to the rectification process. Because this is a fairly undeveloped area, few permanent features exist to serve as ground-control points (GCPs). Therefore, creek intersections were the most prevalent GCPs used. Using features such as creek intersections as GCPs is a common method in coastal systems, however it reduces the accuracy of rectification because there is slight movement of these features over time (Higinbotham et al. 2004). While studies have not looked specifically at the stability of creek intersections, tidal creeks, in general, have been shown to be fairly stable features with reported average migration rates between 0.023 and $0.21 \text{ m}\cdot\text{yr}^{-1}$ (Gabet 1998, Garofalo 1980).

Lastly, errors can occur during digitization, which is primarily through edge interpretation for this study. In areas where there is a clear differentiation between marsh flat and mudflat, such as an eroding scarp, the location of the marsh edge is fairly simple to define. However, more complex areas tend to exist commonly along the marsh edge,

such as terraces and low-gradient edges, which provide greater difficulty and less accuracy in assessing the edge (Cox et al. 2003). Due to its gentle slope, determining the location of the edge at Fowling Point proved to be difficult. The tidal cycle can also have an impact on the accuracy of digitization (Moore 2000). Though all of the photos appear to have been taken while the marshes were exposed, the exact location within the tidal cycle is unknown; the dates and times of flyovers are not available for all of the collected photographs. This likely has the greatest effect on FP because of its low-gradient profile.

Methodology

Error analyses were performed to determine the positional accuracy of the images, as well as accuracy associated with digitization and the linear regression models. Two methods were used to accomplish this. The first involved the use of stable control points to determine how well these locations corresponded between images. Features, such as roads and houses, were digitized for each of the five images at each site; the most stable creek intersections and tree patches were used when “hard” structures were not present (Hughes et al. 2006). Five of these stable features were digitized at each site, except at FP and CP, where only four features could be accurately deciphered for 1968. The Shoreline Change Envelope (SCE) statistic in DSAS was used to determine the distance between the two farthest line segments for each feature. Averaging these distances across features provides a general assessment of how much error is associated with the positional accuracy of the images. Because the 1968 photograph seemed to invoke the most error, this procedure was also performed with the 1968 image excluded from the

analysis. A paired t-test was performed on the data with and without the 1968 image included for each of the sites to determine if significant differences existed.

Error was also analyzed by comparing the R-squared values associated with the linear regressions of the shorelines calculated in DSAS. This was done for two reasons. The first was to determine whether there truly was a linear relationship between the shorelines. The second was to determine if there was any improvement in the R-squared values when the 1968 image was excluded from analysis. Comparisons between the two sets of data (with and without 1968) were performed with paired t-tests; when the data were not normally distributed, Wilcoxon's signed-ranks test was used instead.

Error Results and Interpretation

The average distance between fixed or stable features in the images decreased at all sites when the 1968 image was removed from analysis (Table 2.2). The results of the paired t-tests for each marsh are presented in Table 2.3. Although there were decreases at all sites, HI was the only site to experience a significant change. These findings suggest that there are significant positional inaccuracies associated with the 1968 image. The analyzed features have likely remained in relatively constant locations over time, and therefore, any distinct difference in their locations between images must be attributed to one or more of the aforementioned sources of error. Distributing the error across the 50 year duration of the study provides an estimate of the yearly error associated with the positional accuracy of the images (Table 2.3). By excluding the 1968 image, there is less than a 10 cm error associated with positional differences between images from year-to-

year. That is to say that the true erosion rate differs by less than 10 cm from that determined by the DSAS analysis.

The mean R-squared values were 0.8 or greater for both sets of change analyses (with and without 1968) at HI, CP, and MM. This indicates a strong linear trend in shoreline position. Selected plots of shoreline locations along individual transects illustrate this trend (Appendix 1). The linear relationship is weaker at FP, with a mean R-squared of 0.37 ± 0.02 . The R-squared values improve at all sites when the 1968 image is excluded from analysis (Table 2.4). The most dramatic improvement occurs at FP, where the mean R-squared increases from 0.36 to 0.60. An improved linear relationship between shorelines is also evident in the plots of shoreline locations (Appendix 1). Significant differences exist between R-squared values for the two sets of images at all four sites (Table 2.5). These results suggest that the 1968 image negatively affects the relationship between the edge segments and its removal provides better model estimates for the rate-of-changes statistics.

The weaker linear relationship at FP is likely the result of the minimal movement of the edge over time. This indicates that one of two things is occurring. The first is that there is a slight net erosion of the edge, but areas of both erosion and accretion are common across the marsh. The second possibility is that any variability between the edge locations is the result of tidal differences between the images and that the edge has remained stable over the duration of the study.

Based on the results of the performed error analyses, it is not appropriate to include the 1968 image in the shoreline change analyses. The inaccuracies in the positions of stable features and the improved linear relationships through its exclusion

indicate that this image is not of the same quality as the photographs from the other four years. If the original 1968 image was available, the rectification process could be repeated in the hopes of achieving better accuracy. However, the previously-rectified photograph was the only image readily available and records of the procedures used in the rectification process were not available. Because of the relative uncertainties associated with the image and its inherent positional inaccuracies, it was excluded from the final rate-of-change analyses.

Marsh	Mean Distance Between Farthest Points (m)		Error Associated with Positional Accuracy (m·yr ⁻¹)	
	All Years	1968 Excluded	All Years	1968 Excluded
FP	7.48 ± 1.61	2.51 ± 0.49	0.15	0.05
HI	16.60 ± 1.76	1.72 ± 0.32	0.33	0.03
CP	3.62 ± 0.46	2.72 ± 0.14	0.07	0.05
MM	7.01 ± 1.02	4.64 ± 0.47	0.14	0.09

Table 2.2. Mean (± 1 SE) distance between stable features in images at each site. Mean distance divided by 50 yrs provides error attributed to differences between images (years) for a particular site.

Marsh	DF	t-value	p
FP	3	2.73	0.0722
HI	4	8.43	0.0011
CP	3	2.00	0.1395
MM	4	2.68	0.0550

Table 2.3. Results of paired t-tests for error analysis of positional accuracy of the images. Significance at $p = 0.05$.

Marsh	R-squared	
	1957 - 2007	1968 Excluded
FP	0.37 ± 0.016 (273)	0.60 ± 0.021 (273)
HI	0.80 ± 0.017 (263)	0.91 ± 0.010 (264)
CP	0.93 ± 0.007 (223)	0.95 ± 0.008 (223)
MM	0.96 ± 0.002 (231)	0.98 ± 0.003 (246)

Table 2.4. Mean (± 1 SE) R-squared values of linear regressions between shorelines. Sample sizes in parentheses.

Marsh	S	p
FP	10992.5	<0.0001
HI	8627.5	<0.0001
CP	2099.5	<0.0001
MM	7097.0	<0.0001

Table 2.5. Results of Wilcoxon's signed-ranks test comparing R-squared values when 1968 is included and excluded from analysis. Significance at $p = 0.05$

Results

Results from the shoreline change analysis indicate that significantly different rates-of-change occurred at the marsh edge between the four sites over the fifty-year period. (Figure 2.2). Due to heteroscedastic data, the Welch option in SAS was used to perform Welch's variance-weighted ANOVA. Matulakin Marsh experienced the most erosion at $1.62 \pm 0.03 \text{ m}\cdot\text{yr}^{-1}$, followed by Chimney Pole ($1.28 \pm 0.04 \text{ m}\cdot\text{yr}^{-1}$) and Hog Island ($0.98 \pm 0.04 \text{ m}\cdot\text{yr}^{-1}$). The edge at Fowling Point was much more stable than the edge at the other sites, with a mean rate of $0.02 \pm 0.02 \text{ m}\cdot\text{yr}^{-1}$. The erosion rates increased when the 1968 image was included in the change analysis (Table 2.6). The edge segments at each of the sites are presented in Figures 2.3-2.6. It is evident from these figures that the marsh edge retreated from 1957-2007 at MM, CP, and HI. On the other hand, the edge remained relatively stable at FP, with limited distance between segments.

Variability in shoreline change existed along the edge at each of the marshes. Figures 2.7-2.10 depict the individual rates-of-change for each transect included in the DSAS analyses; rates are broken down into five classes in order to observe trends. Shoreline change was not uniform across the length of the edge. Instead, the edge was dominated by smaller stretches of homogeneous rates that varied across the landscape. This was the case at all of the sites, with the exception of FP, where the majority of the shoreline was dominated by one class of erosion rates ($0-0.25 \text{ m}\cdot\text{yr}^{-1}$). The greatest within-site spatial variability existed at Hog Island. The northern end of the HI site experienced erosion rates well over $1 \text{ m}\cdot\text{yr}^{-1}$, with many areas seeing greater than $2 \text{ m}\cdot\text{yr}^{-1}$. Meanwhile, the majority of the southern portion of the site eroded at less than $1 \text{ m}\cdot\text{yr}^{-1}$.

The blue stars in Figures 2.7-2.10 indicate the study locations for the sampling of marsh characteristics and erosion mechanisms. These locations experienced mean erosion rates within the range of 0-0.025, 0.5-1.0, 0-0.5, and $>2.0 \text{ m}\cdot\text{yr}^{-1}$ at FP, HI, CP, and MM, respectively. While the sampling sites at FP and HI experienced erosion rates typical of their respective marshes, the rates at the CP sampling location tended to be lower than the average rates along the marsh edge and erosion at the MM sampling site was higher than the average rates experienced at that marsh.

The variability in rates along the edge is also indicated by the percentage of transects that fall within each class of shoreline change (Figure 2.11). MM had the greatest percentage of transects with an erosion rate greater than $2 \text{ m}\cdot\text{yr}^{-1}$ and over 95% of observations had a value greater than $1 \text{ m}\cdot\text{yr}^{-1}$. While the frequency of rates greater than $1 \text{ m}\cdot\text{yr}^{-1}$ decreased from MM to CP, the percentage of values less than $1 \text{ m}\cdot\text{yr}^{-1}$ increased. A similar trend occurred between CP and HI. This trend is a reflection of the decrease in the mean rate of erosion from MM to CP to HI. HI and FP were the only sites to exhibit areas of accretion (negative values), however these areas constituted less than 5% of the HI shoreline. The distribution was radically different for FP than at the other three sites. Greater than 95% of all transects experienced edge accretion or erosion of less than $0.5 \text{ m}\cdot\text{yr}^{-1}$ at FP. This is indicative of the stable shoreline present there.

A		
Marsh	Rate-of-Change (m·yr ⁻¹)	
	1957 – 2007 (1968 included)	1957 - 2007 (1968 excluded)
FP	0.14 ± 0.02 (273)	0.02 ± 0.02 (273)
HI	0.99 ± 0.04 (263)	0.98 ± 0.04 (264)
CP	1.29 ± 0.04 (223)	1.28 ± 0.04 (223)
MM	1.78 ± 0.03 (231)	1.62 ± 0.03 (246)
B		
Marsh	Rate-of-Change (m·yr ⁻¹)	
	1957 – 2007 (1968 included)	1957 - 2007 (1968 excluded)
FP	0.14 ± 0.31 (273)	0.02 ± 0.33 (273)
HI	0.99 ± 0.70 (263)	0.98 ± 0.67 (264)
CP	1.29 ± 0.59 (223)	1.28 ± 0.60 (223)
MM	1.78 ± 0.50 (231)	1.62 ± 0.51 (246)

Table 2.6. Mean rates-of-change with ± 1 SE (A) and ± 1 SD (B). Rates are shown for statistics performed on all 5 years and with 1968 removed from analysis. Positive values indicate erosion of the edge. Sample size (n) is in parentheses.

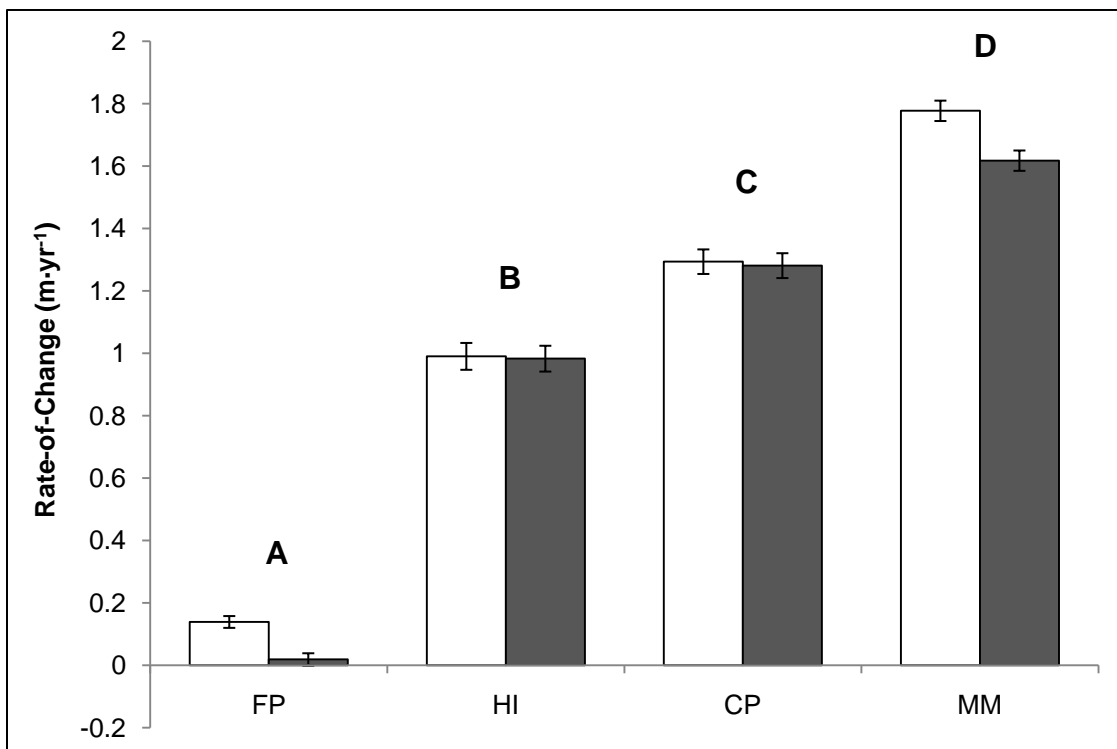


Figure 2.2. Rates-of-change at the four sites with all years included (white) and with 1968 excluded (gray). Error bars indicate ± 1 SE. Significant differences between marshes are indicated by letters ($p = 0.05$). Positive values indicate erosion.

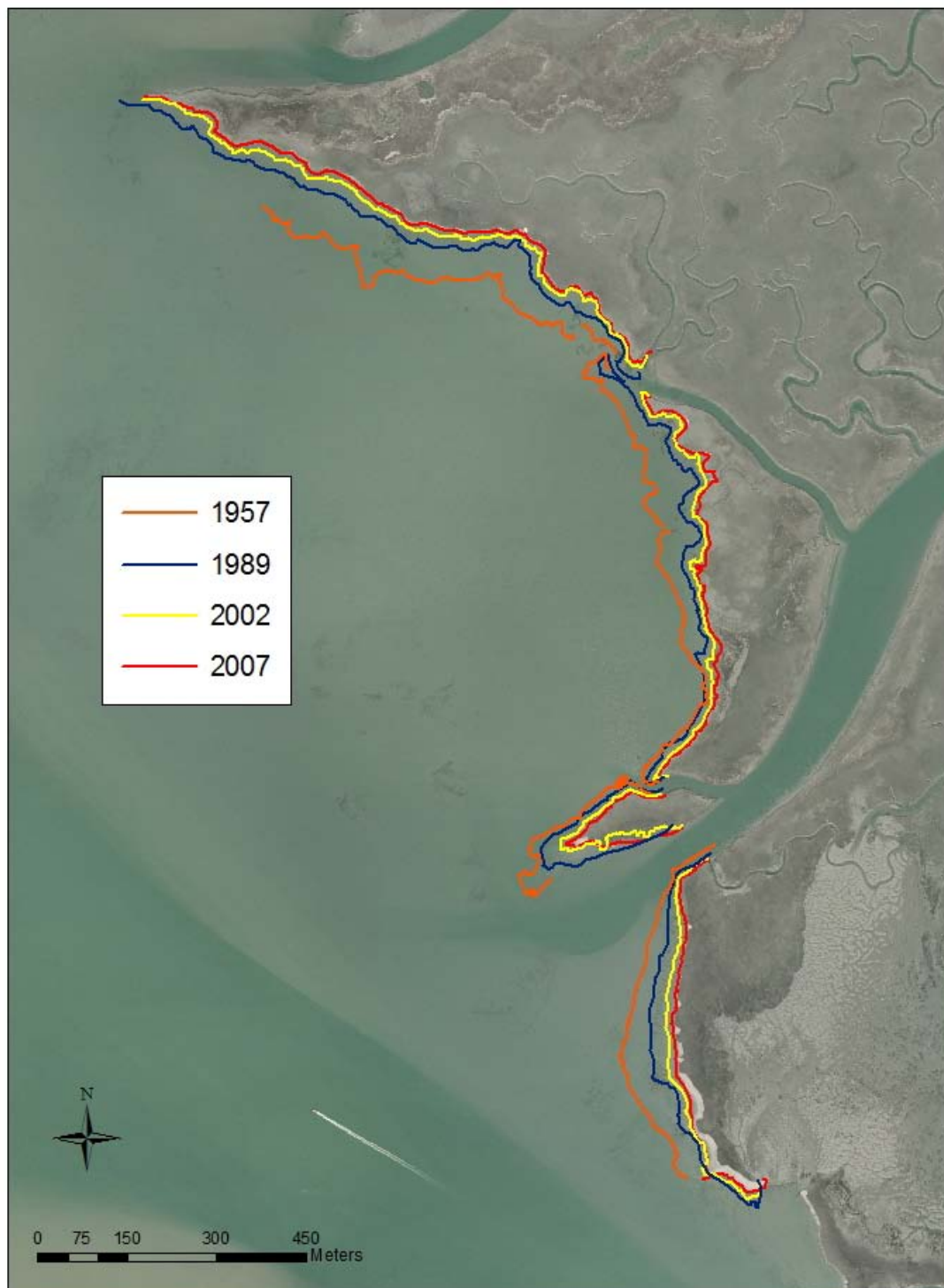


Figure 2.3. Position of the marsh edge at Chimney Pole in 1957, 1989, 2002, and 2007.

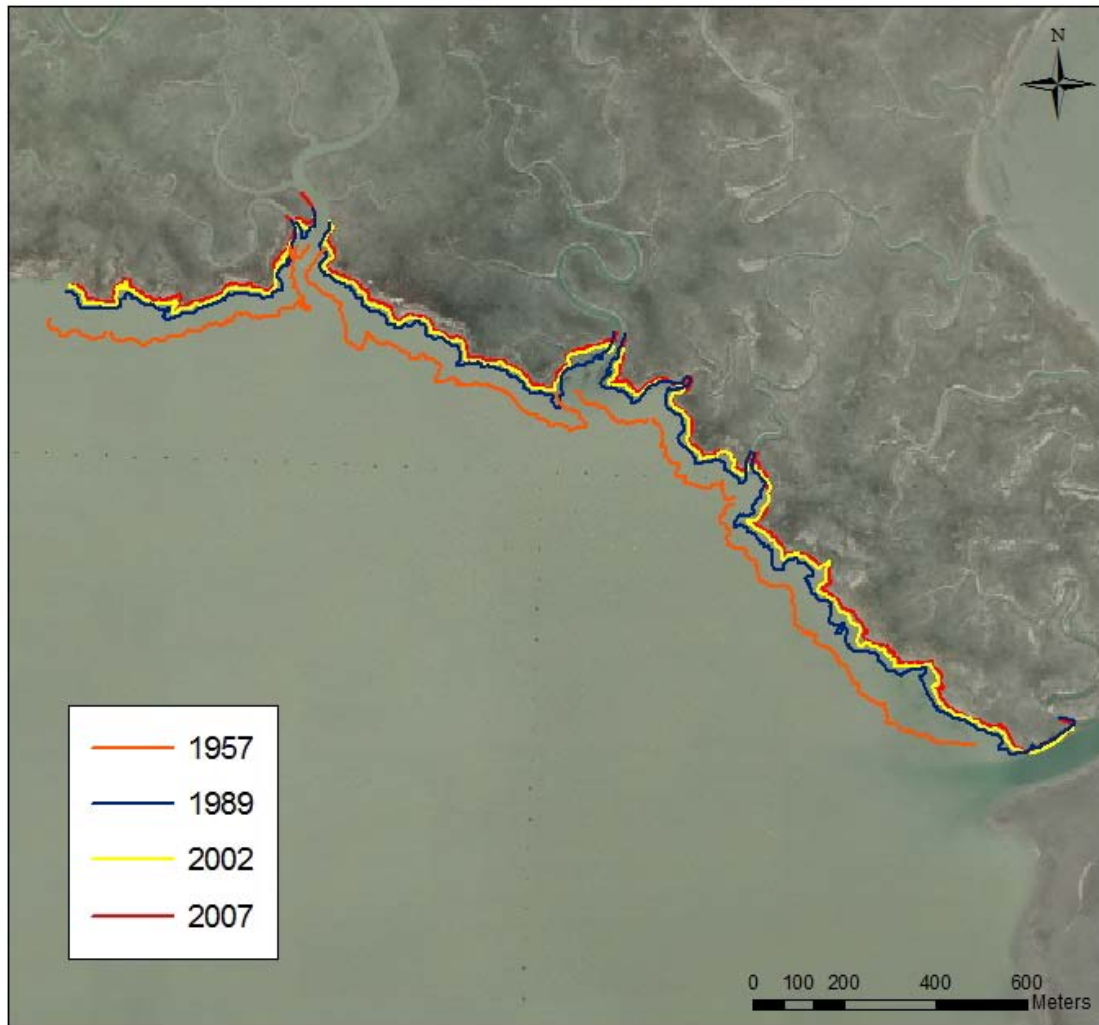


Figure 2.4. Position of the marsh edge at Matulakin Marsh in 1957, 1989, 2002, and 2007.



Figure 2.5. Position of the marsh edge at Hog Island in 1957, 1989, 2002, and 2007.

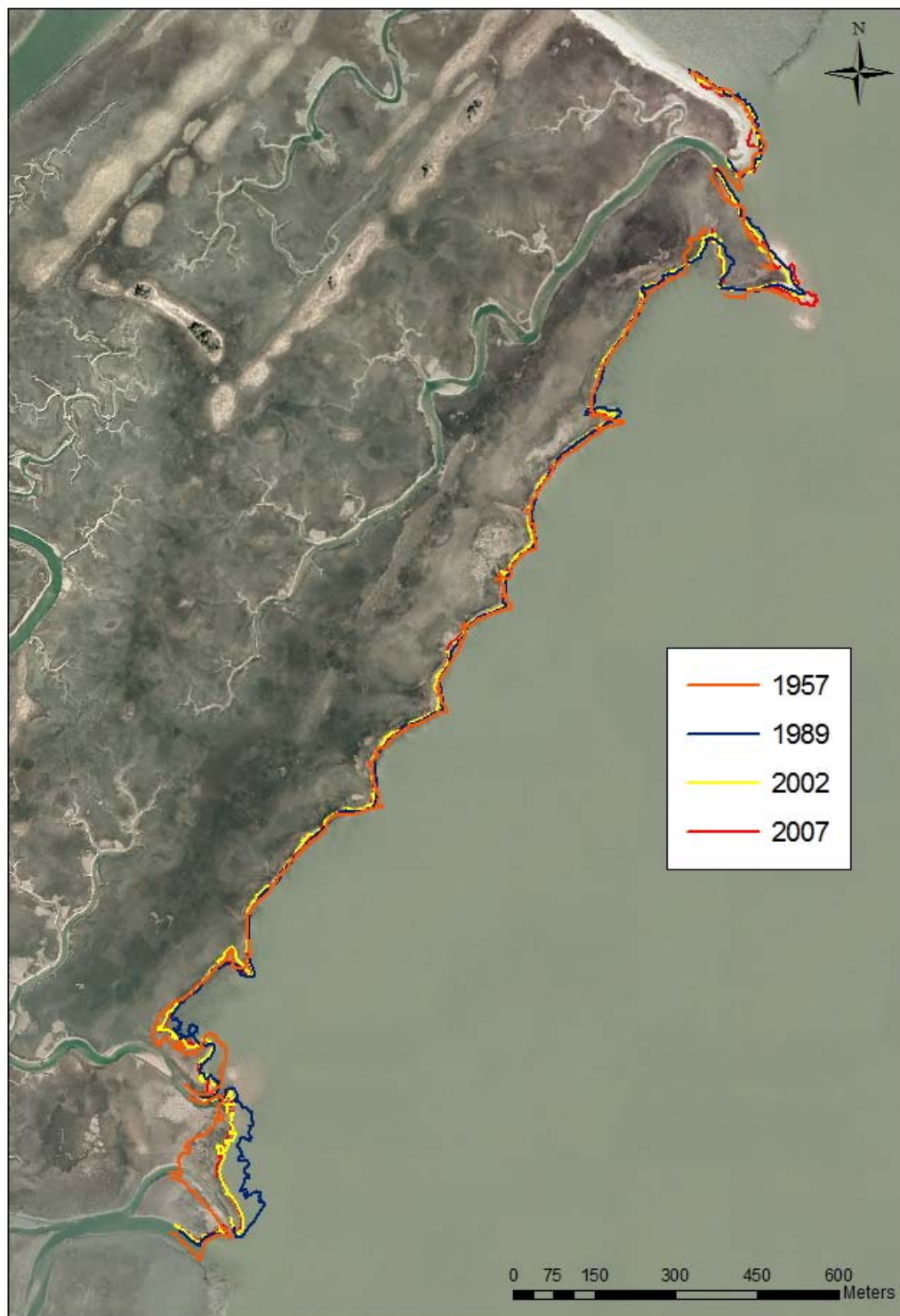


Figure 2.6. Position of the marsh edge at Fowling Point in 1957, 1989, 2002, and 2007.

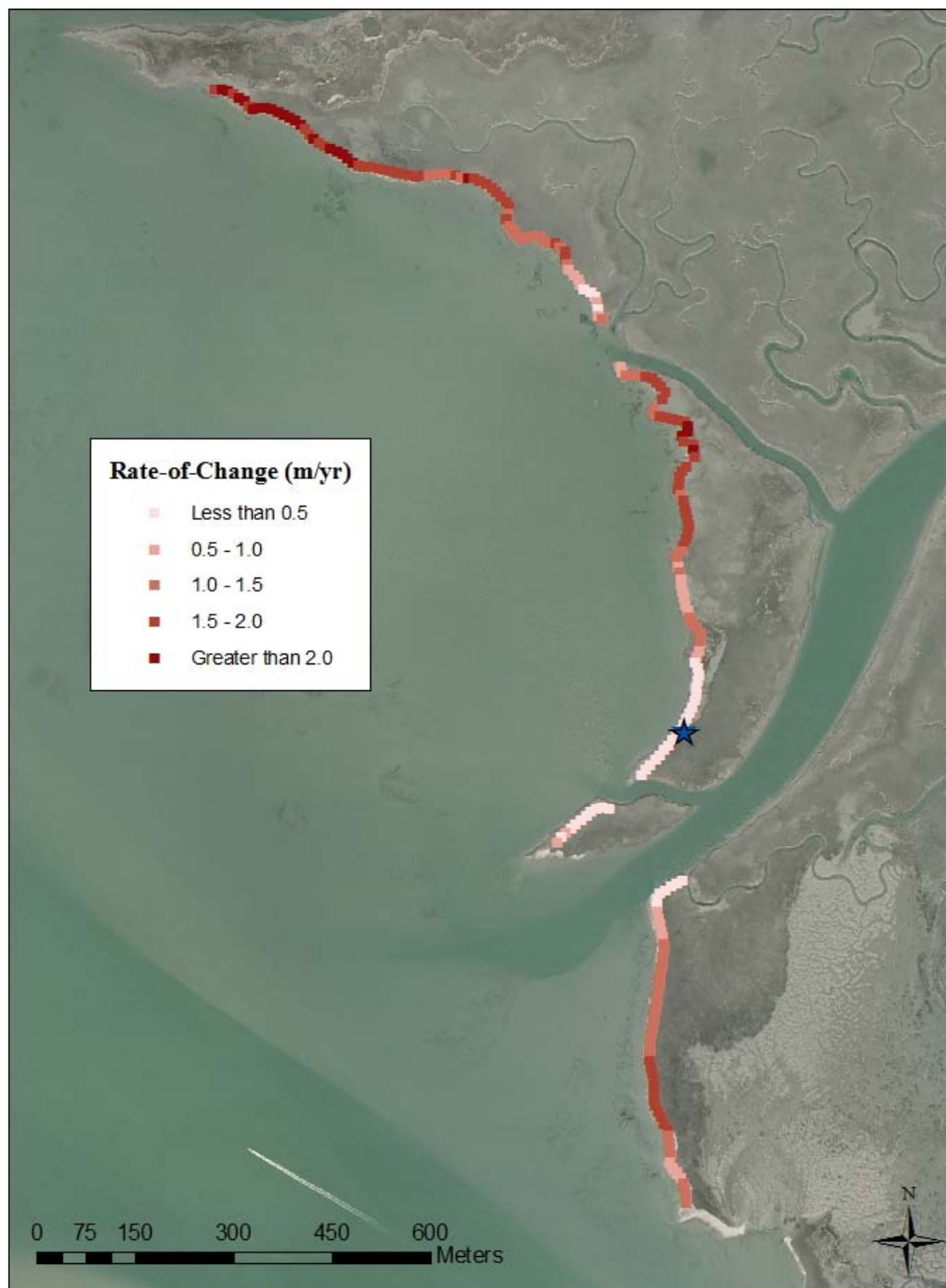


Figure 2.7. Rates-of-change along the marsh edge at Chimney Pole. Positive values indicate erosion of the edge.

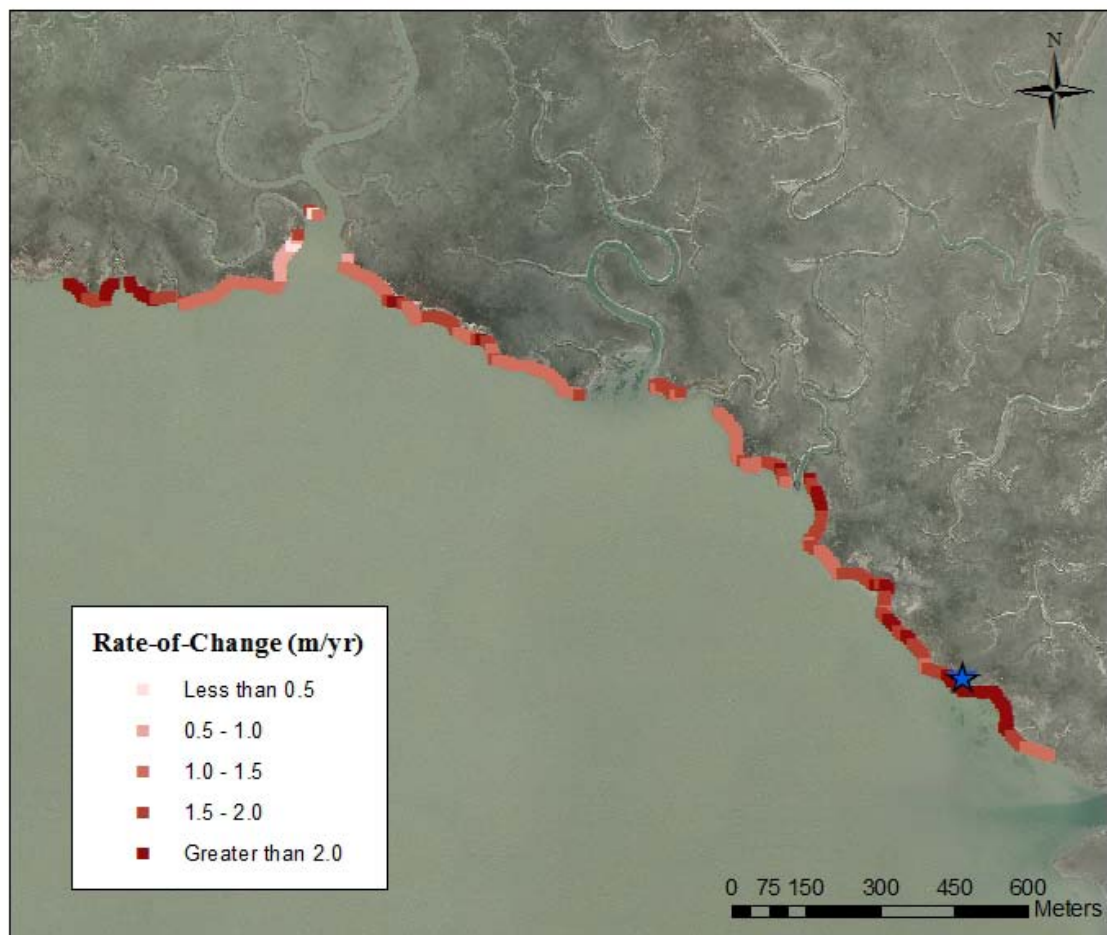


Figure 2.8. Rates-of-change along the marsh edge at Matulakin Marsh. Positive values indicate erosion of the edge.



Figure 2.9. Rates-of-change along the marsh edge at Hog Island. Positive values indicate erosion of the edge.



Figure 2.10. Rates-of-change along the marsh edge at Fowling Point. Note the change in class ranges from Figs. 2.7-2.9. Positive values indicate erosion of the edge, negative values indicate progradation.

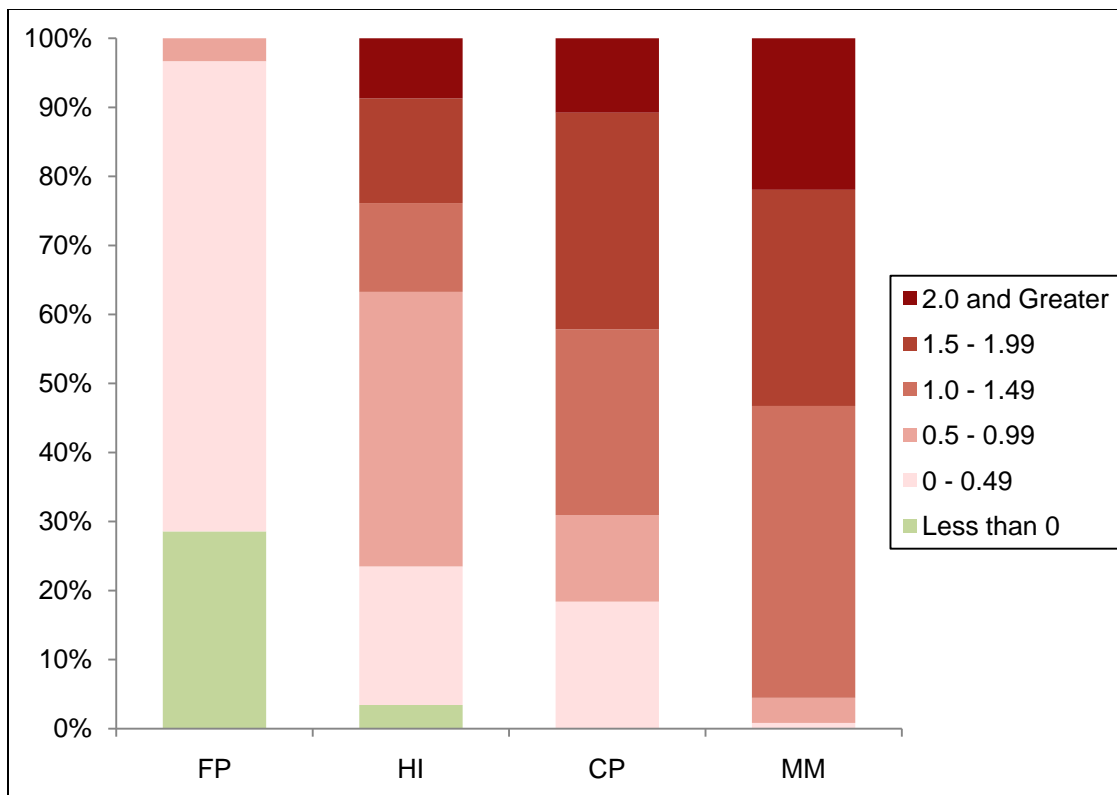


Figure 2.11. Percentage of transects within each rate-of-change class interval (m·yr⁻¹) at the four sites. Positive values indicate erosion, negative values indicate progradation.

Discussion

The edge eroded at each of the marsh sites over the fifty-year period of the study; however, this erosion occurred at significantly different rates between sites. The mean erosion rates at HI, CP, and MM fell within similar ranges as those found at eroding marshes in Chesapeake Bay and Venice Lagoon (Wray et al. 1995, Day et al. 1998). Erosion rates on Chimney Pole marsh agreed well with those of a previous study, where Kastler and Wiberg (1996) found an approximate erosion rate of $1.2 \text{ m}\cdot\text{yr}^{-1}$ at their study site. Rates between 1.0 and $1.5 \text{ m}\cdot\text{yr}^{-1}$ were recorded in the same vicinity at CP for this study.

The mean erosion rates agree with preliminary assessments of the four marshes. Though actual rates were not predicted, it was thought that the edges at MM, CP, and HI were eroding due to the presence of steep or vertical scarps at each marsh, a characteristic feature of retreating edges (Schwimmer 2001). The edge at FP remained relatively stable over time; it was originally hypothesized that this is not an eroding edge due to the gentle gradient between mudflat and marsh interior (Fagherazzi et al. 2006). The large adjacent mudflat protects the marsh from high wave energies, preventing the formation of tall scarps and subsequent erosion through wave attack.

At MM, CP, and HI erosion appears to have occurred at a consistent rate over the period of the study. This is indicated by the high mean R-squared values at the three sites, which suggests a strong linear relationship between the shorelines. Cyclic periods of erosion and accretion have been observed at some marsh sites, with rates varying between cycles (Harmsworth and Long 1986, Cox et al. 2003). Erosion was much more uniform over time at the Hog Island Bay sites, as was also noted for marsh islands in

Chesapeake Bay (Wray et al. 1995). As sea-levels rise and waves continue to attack the marsh edge, it appears unlikely that favorable conditions for marsh regrowth will be present (Phillips 1986a). Therefore, dramatic changes to environmental conditions may be required to initiate a cycle of extension and retreat, such as a shift in the tidal prism (Cox et al. 2003). Barring such a shift, the three marsh sites in Hog Island Bay will likely continue to erode at a consistent rate.

Alongshore variability in rates of shoreline change at a particular marsh can be common (Wray et al. 1995, Phillips 1986a). With the exception of FP, rates-of-change were highly variable depending on location along the edge. Phillips (1986b) argues that small-scale variability along the marsh edge is the result of the local morphology and characteristics of the edge, as well as variations in wave exposure. These factors determine the relative resistance of the edge to erosion. On the other hand, the large-scale behavior and mean rates-of-change for a marsh are more affected by its geographic setting and bay geometry (Phillips 1986b). Therefore, while the overall behavior of each marsh site may be determined by such attributes as its position within the bay and maximum fetch, local variations are more dependent on the morphology and varying characteristics of the edge. An example of this might be represented by the erosional trends along the edge at HI (Figure 2.9). On a broader scale, the marsh clearly eroded and higher rates of erosion occurred at the northern end of the site, while slower rates occurred to the south. This was likely a function of the orientation of the marsh and its effect on wave exposure and energy. However, within these regions of greater and lesser erosion, there was smaller-scale variability. This variability was likely attributed to the local morphology of the edge and the individual properties of the edge that affect marsh

resistance, such as sediment, vegetation, and invertebrate characteristics. The characteristics of the marsh edge that may affect erosion rates are examined in Chapter 3.

The ranges of erosion rates were similar at all sites, with the exception of FP. While the more eroded sites experienced greater variability and higher rates along the edge, FP was dominated by two classes of shoreline change, with the majority of the edge experiencing erosion between 0 and $0.25 \text{ m}\cdot\text{yr}^{-1}$. This is in sharp contrast to the other three marsh sites, which were dominated by rates greater than $0.5 \text{ m}\cdot\text{yr}^{-1}$. The variation in mean erosion rates at these three sites is evident by the percentage of points along the edge within a particular erosion class. While MM was dominated by high rates (greater than $1 \text{ m}\cdot\text{yr}^{-1}$), CP experienced a more evenly dispersed pattern, and HI was dominated by rates at the lower range of erosion (less than $1 \text{ m}\cdot\text{yr}^{-1}$). Significant areas of accretion were only evident at FP. Significant accretion would not be expected at the other sites due to their morphology and high rates of retreat. It is unclear whether the areas of large accretion at FP (southern end) are the result of actual depositional processes or simply a difference in tidal level between images. Evaluating the images, it seems likely it might be a combination of the two. However, this does appear to have been an area of high deposition at one time, as shown by the areas of accretion in the images in Figure 2.12. This indicates that, despite the dominance of eroding or stable edges within the lagoon, there might be localized stretches where marsh growth is still possible.

The difference in mean erosion rates between sites suggests that these marshes are exposed to differing wave exposure, directional orientation, and local bathymetry that affect the ways in which the marsh edge behaves over time. Along with wave exposure related to wind, bathymetry, and fetch, internal properties of the marsh edge may also

influence differences between sites (Schwimmer 2001, van der Wal and Pye 2004).

Studying the hydrodynamic, sedimentary, and ecological characteristics of the marsh edge should provide insight into the erosion mechanisms in play and why these particular processes may occur.

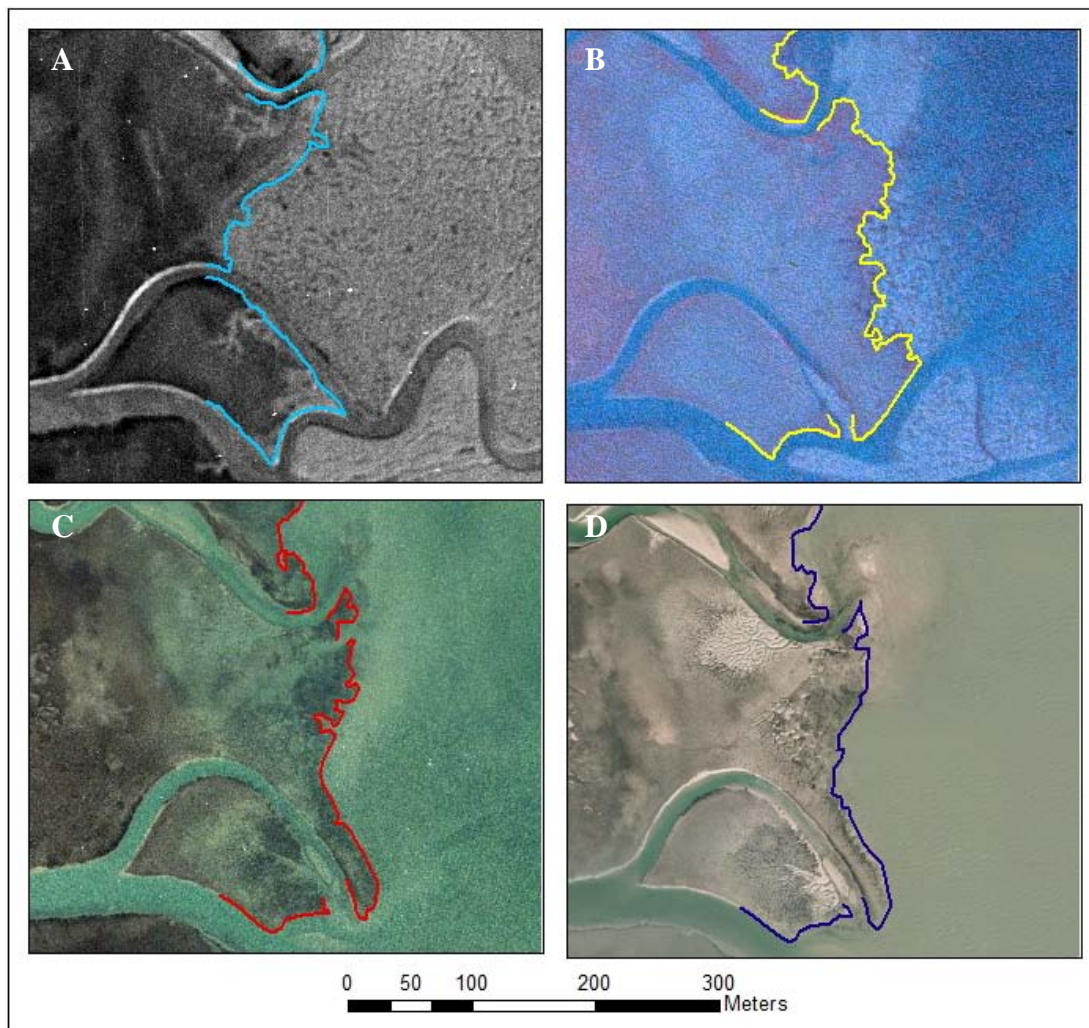


Figure 2.12. The southern portion of FP in 1957 (A), 1989 (B), 2002 (C), and 2007 (D). Line segments indicate the location of the edge. There appears to have been some accretion of the edge between 1957 and 1989.

CHAPTER 3: EFFECTS OF MARSH EDGE CHARACTERISTICS ON EROSION

Objective

After edge erosion rates were quantified at each of the sites, the next goal was to understand how and why this erosion occurs. Specific characteristics of the marsh edge may play an important role in determining mechanisms and rates of erosion. Such characteristics include the hydrodynamics acting on the edge, edge morphology, sediment properties, vegetation characteristics, and invertebrate abundance and behavior. These properties were measured and evaluated in order to determine which characteristics influence erosion at each site.

Methods

Lagoon Hydrodynamics

Wave energies acting on the marsh edge were analyzed with the WWTM2D model as discussed in Mariotti et al. (2010). The WWTM (Wind Wave Tidal Model) is a two-dimensional finite element hydrodynamic model used to estimate tidal fluxes and wave heights within shallow coastal lagoons. The model accounts for wind speeds and direction, water depth, fetch, and bathymetry within the lagoons. The model mesh covers an approximate area of 2400 km² and consists of 68000 triangular elements and 35000 nodes. Wave energies at each marsh site can be simulated under varying wind conditions, storm surge, and local sea-level (Mariotti et al. 2010). Estimates of wave power at the four marshes under typical wind conditions were calculated based on wind data from NOAA station CHLV2 (Chesapeake Light, VA) from 1996-1999. Values of wave power for each site were estimated across an approximate distance of 1500-2000 m

along the marsh edge. This provides a general estimate of typical wave energies at the marshes in order to make comparisons between sites.

Edge Elevation and Morphology

Land surveying was performed at the four sites in order to obtain precise elevations of the marshes and lateral profiles of the edge. Surveying was performed in July and August 2010 with the use of a Trimble R8 GNSS System (Trimble, Sunnyvale, CA). This is a high-accuracy survey GPS system that uses satellites to generate precise latitude, longitude, and elevation positions. Survey points were taken approximately every 2-5 m along the marsh edge in order to record its position and elevation. Points were also measured along five horizontal transects (six at HI) extending from the fronting mudflat to the marsh interior to obtain elevation profiles of each marsh. This provides information about the morphologies of the individual sites, as well as the opportunity to make morphological and elevation comparisons between sites. The locations of the survey points at each of the sites are presented in Figure 3.1. The survey locations were corrected using NOAA's Online Positioning User Service (OPUS) and processed in Trimble Geomatics Office (TGO).

Sediment Properties

Sediment samples were collected at the marsh edge and 10 m inland (hereafter referred to as "interior") of the edge at all four sites in October 2009. Five samples were collected at 15 m intervals along both the edge and interior transects. Two small (2.54 cm diameter) plastic cores were taken at each sample location to a depth of 5 cm. One

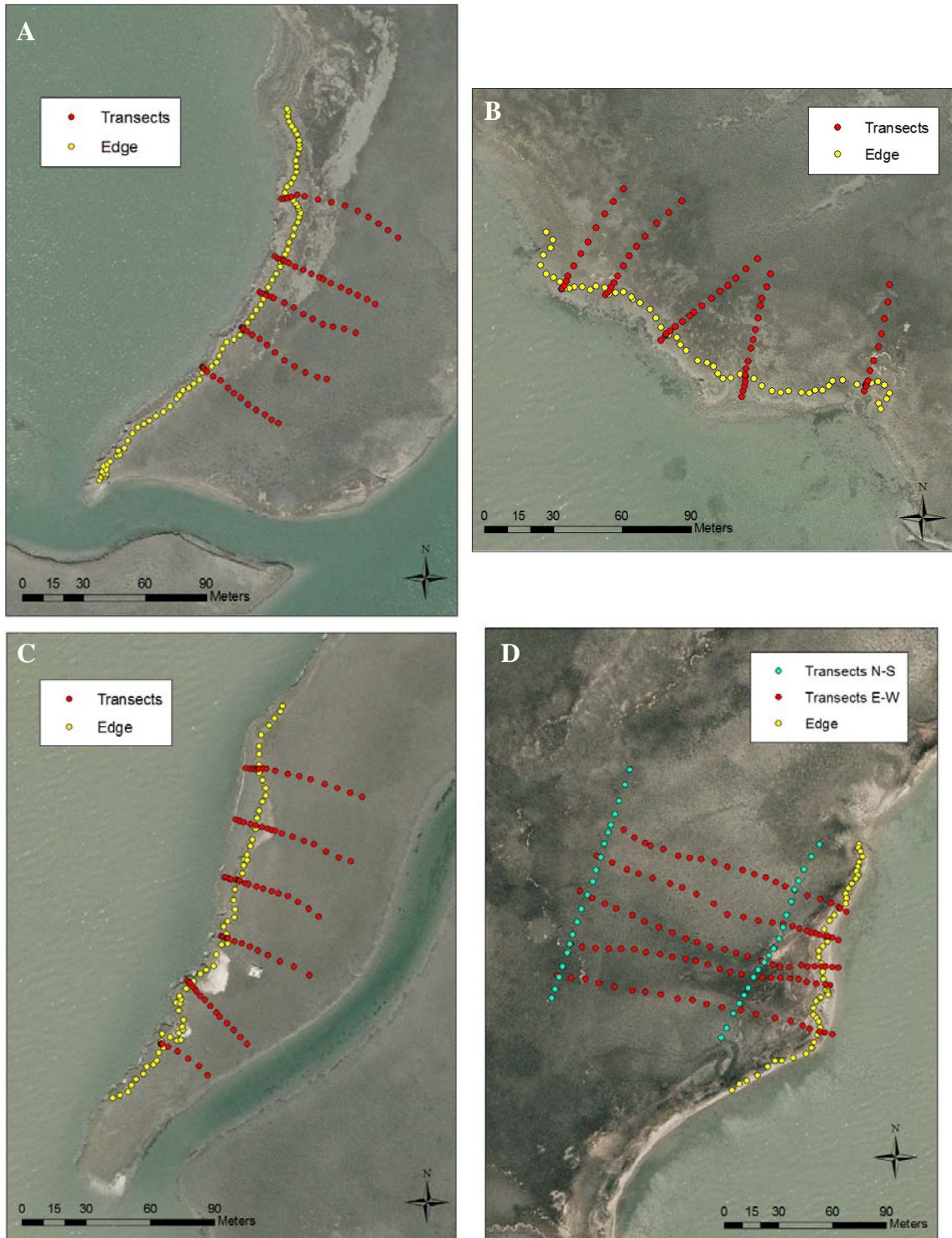


Figure 3.1. Survey locations at CP (A), MM (B), HI (C), and FP (D). Transects were run along the marsh edge (yellow) and perpendicular to the edge (red) at all sites. Transects were also run parallel to the edge at FP (blue).

core was used for grain size analysis and the other to determine porosity, bulk density, and organic content.

Prior to performing grain size analysis, the sediment samples were prepared in the lab. The bottom 2 cm of each core was sectioned off and used for analysis. The samples were rinsed over a 1 mm sieve to remove large organic material, and all water and sediment that passed through the sieve was collected and placed into a glass jar. 50 ml of bleach was added to each sample to remove any remaining organic material. Once the sediment had completely settled and there was no evidence of organic matter, the excess water was decanted. A 5% sodium hexametaphosphate solution was added to each sample as a dispersant. Grain size analysis was performed using an LS 13 320 Laser Diffraction Particle Size Analyzer (Beckman Coulter, Brea, CA). A small syringe was used to add the sediment-water mixture (approximately 0.5-1.0 cc) to the particle size analyzer (PSA) to obtain an appropriate obscuration. Three replicates were run for each sample and averaged with the machine's software; the average values were used for data analysis.

The remaining sediment cores were weighed to determine wet weight and then dried at 60 °C to a constant mass and re-weighed. Bulk density was calculated as the weight of the dry sediment divided by the sample volume. Porosity was calculated as the difference between the wet weight and dry weight divided by the volume of the sample. The samples were placed in a muffle furnace at 500 °C overnight and re-weighed. Organic content was determined as the weight of the sample lost on ignition.

Geotechnical properties of the salt marshes were also measured at the edge and interior of each site. Sediment shear strength was sampled on the marsh flat, as well as at

positions along the vertical scarp. Shear strength was estimated using a pocket vane shear tester (Geotest, Evanston, IL). This measures the maximum shear at sediment failure. The standard vane size (2.5 cm diameter) was used, except in cases where the sediment was very soft (typically in the marsh interior), for which the larger vane was needed (4.8 cm diameter). On the marsh flat, six samples were taken at 20 m intervals along both the edge and interior transects. Three replicates were taken at each sample location and the mean value was used to indicate shear strength at that location. Along the scarp, measurements were taken at a depth of 0-5 cm and 25-30 cm at the same 20 m intervals. If a clearly defined scarp was not present, no measurements were taken at that location. Scarp shear strength was not measured at FP due to the lack of a continuous edge. Sediment compaction was also determined to obtain an estimate for sediment hardness and a proxy for strength. A soil compaction tester (Dickey-John, Springfield, IL) was used to measure maximum sediment compaction and the corresponding depth. A soil compaction tester is a penetrometer, consisting of a 30-degree cone tip connected to a steel driving shaft. As the shaft is driven into the sediment, a pressure gauge measures compaction at corresponding depths. Samples were taken at the same locations as the surface shear strength tests. Three measurements were taken at each sample location and averaged to obtain a mean value.

Vegetation Characteristics

Belowground and aboveground biomass, stem density, and canopy height of *S. alterniflora* were sampled at the sites in June and August 2009. Within each marsh, 5 samples were taken at the marsh edge and 5 samples were taken in the interior (10 m

inland of the edge). Individual samples were taken at 15 m intervals along the edge and interior transects. Belowground biomass was collected using a 15 cm diameter PVC coring tube to a depth of 20 cm. The cores were placed into plastic bags and returned to the lab, where they were cut into 5 cm sections (Ellison et al. 1986). The sections were rinsed over a 2 mm sieve (overlying a 1.5 mm mesh sieve), placed into labeled paper bags, and set in a drying oven. The samples were dried at 60 °C to a constant mass and weighed (± 0.01 g).

Aboveground biomass, stem density, and canopy height were measured from the aboveground material within the diameter of each core. All aboveground material was clipped at the sediment surface and placed into plastic bags. In the laboratory, the aboveground vegetation was rinsed and separated into live standing, dead standing, and loose leaves and litter categories. All stems were counted and measured to determine density and height. The samples were placed into labeled paper bags, dried at 60 °C to a constant mass, and weighed (± 0.01 g).

Root strength was quantified by collecting 10 cores with a width of 7.62 cm and a depth of 10 cm at each of the marsh sites (5 samples at the edge and 5 samples in the interior). Samples were collected at 20 m intervals along the edge and interior transects. The cores were rinsed in the laboratory and roots and rhizomes were separated using forceps. One end of the root or rhizome was attached to a binder or alligator clip of varying sizes (depending on the width of the root or rhizome), and a spring scale was attached to the clip through looped string. Four spring scales with differing ranges of forces were used. While holding onto the opposite end of the root or rhizome, the spring scale was slowly pulled to determine the force needed to break the root or rhizome.

Approximately 10 roots and 10 rhizomes were randomly chosen from each sample, though more or less were used in a few cases based on availability. It was observed during sampling that this method has the tendency to underestimate the strength of the thickest rhizomes and overestimate the strength of the thinnest roots; this is because the thickest rhizomes may slip from the tester's hand or shred near the clip before breakage occurs, while the thinnest roots may break under very little force.

Invertebrate Characteristics

Crab burrow densities and diameters were measured at the marsh sites in July 2009. A 625 cm² quadrat was used to determine burrow densities and diameters at 10 locations within each marsh (5 edge and 5 interior). Samples were taken every 20 m along the edge and interior transects. All burrows within the quadrat were counted and the diameter of their openings measured (± 0.1 mm); only burrows with diameters greater than 5 mm were used in analysis to ensure that only openings representing burrow structures were included. Burrow coverage on the marsh surface was determined by calculating the area of each burrow opening and summing across each sample quadrat.

In order to estimate burrow volumes at the sites, polyester resin was used to create casts of the burrows (Shinn 1968). All open burrows within a 0.25 m² quadrat were filled with resin (Delvie's Plastics, Salt Lake City, UT) in July 2009. The resin was allowed to harden and the casts were retrieved the following week. Two edge and two interior samples were taken at each site, with one of each taken at opposing ends of the edge and interior transects; quadrats were placed in areas with representative burrow coverage. The casts were rinsed at the lab to carefully remove sediment and root material. Burrow

volume was determined by measuring the volume of water displaced by a submerged cast.

Pitfall traps were installed in July 2010 in order to identify crab species within the marshes. The cylinder traps had a diameter of 15 cm and depth of 20 cm and were installed flush with the marsh surface (McIvor and Smith 1995). Twelve traps were placed at each marsh (6 edge and 6 interior), and spaced 20 m along the edge and interior transects. The traps were retrieved the following day and crabs were counted, measured for carapace width, and identified to species.

The densities of ribbed mussels (*G. demissa*) and periwinkle snails (*L. irrorata*) were also measured at each site. All *G. demissa* visible at the surface of the marsh were counted within a 625 cm² quadrat. Sixteen samples (8 edge and 8 interior) were taken at each marsh at 15 m intervals. The same sampling scheme was used for *L. irrorata*; however, the snails were counted in separate quadrats from *G. demissa*.

Statistical Analysis

Statistical analyses were performed using the statistical software SAS 9.1 and SPSS 18 (SPSS, Chicago, IL). Edge elevations were compared using a one-way ANOVA. Due to heteroscedastic data, the Welch option in SPSS was used to perform Welch's ANOVA to correct for unequal variances. Post-hoc comparisons were performed using Dunnett's C test.

Analyses of sediment, vegetation, and invertebrate properties were primarily performed with a two-way (factorial) ANOVA in SAS. Since comparisons were being made to understand how the marsh characteristics differ between eroding sites, only the

three rapidly eroding sites were used for statistical computations, and the Fowling Point (FP) site was not included. A 3x2 design was used, in which two factors or main effects (marsh and location) and their interaction were tested. The marsh factor had three levels (HI, CP, and MM) and the location factor had two (edge and interior). An exception to this is the scarp shear strength measurements, where depth is used as a factor instead of location. In cases where the interaction term was significant, pairwise contrasts were performed between marsh edge sites and within the locations of an individual marsh (edge and interior). Due to the focus on the edge in this study, differences between interior sites were not of importance. If the interaction was not significant, but there was a significant main effect, post-hoc comparisons were made using either Ryan's Q (equal sample sizes) or Tukey-Kramer (unequal sample sizes) tests. A three-way ANOVA (3x2x4) was used to compare belowground vegetation by marsh site, location, and depth.

When ANOVA assumptions were not met, square-root and log10 transformations were used to satisfy assumptions. In the few cases where normality and/or homogeneity of variance were still not met, the Scheirer-Ray-Hare test was used instead. The Scheirer-Ray-Hare test is an extension of the Kruskal-Wallis test and a nonparametric alternative to a two-way ANOVA (Sokal and Rohlf 1995). In this case, post-hoc pairwise comparisons were performed with Mann-Whitney U tests.

Despite being excluded from statistical analyses, data results of the marsh properties at Fowling Point are included in tables and figures. The lone exception is for crab burrow sampling, for which FP results are presented in Appendix 3.

Results

Hydrodynamics

Wave energies differ along the marsh boundaries throughout the coastal bays of the Virginia Coast Reserve. Wave energies are largely determined by wind speeds and directions in the bays. A wind rose (Figure 3.2) depicts wind speeds and directions near the bay from 1996-1999. Winds tend to prevail from 180-210° N and 330-60° N and at speeds less than 12.5 m·s⁻¹ (Mariotti et al. 2010). These wind statistics were used to calculate a weighted Wave Factor at the marsh Boundary (WFB), predicting wave powers at locations along the marsh boundaries based on the probability of wind conditions (Figure 3.2). Average wave powers along the marsh edge at the four study sites indicate differences in probable wave energies at each site (Table 3.1). Estimated wave power is substantially less at FP (56 W·m⁻¹) than at the other three sites, all of which have average wave powers greater than 100 W·m⁻¹. CP experiences the greatest wave energies at 194 W·m⁻¹, followed by HI (147 W·m⁻¹), and MM (125 W·m⁻¹).

Marsh	Mean Wave Power (W·m ⁻¹)
FP	56
HI	147
CP	194
MM	125

Table 3.1. Mean wave power along the marsh edge at each of the sites, as estimated by the WWTM2D model.

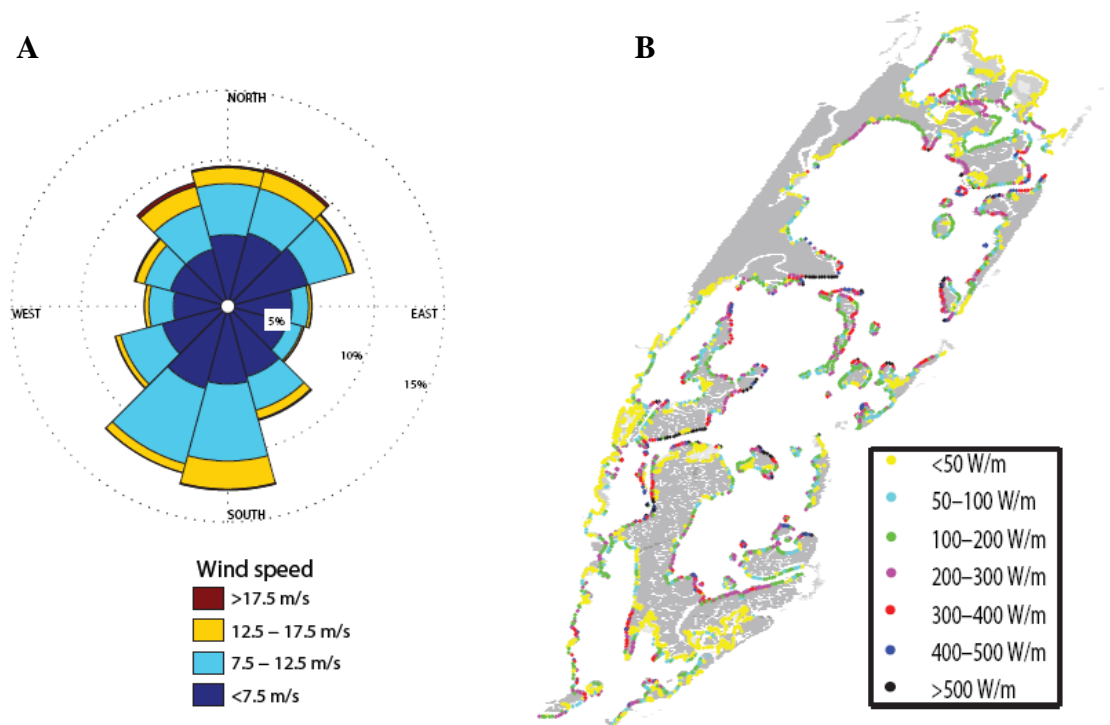


Figure 3.2. A) Wind statistics near Hog Island Bay from 1996-1999. B) Wave powers along marsh boundaries weighted with the wind statistics. Figures presented in Mariotti et al. 2010.

Elevation and Morphology

Results of Welch's ANOVA comparing edge elevations between sites are presented in Table 3.2. Significant differences existed between mean edge elevations at all four sites (Table 3.3). The marsh edges at HI, CP, and MM had elevations above mean sea-level, with CP exhibiting the greatest elevation. In contrast, the edge at FP, or at least the edge of the vegetation line, had an elevation below mean sea level. Mean elevations along the marsh flats (the portion of the transects that extended from the marsh edge to the interior) were 0.25 m, 0.37 m, 0.42 m, and 0.55 m at FP, HI, CP, and MM, respectively. Therefore, the average surface elevation of the marsh was above MSL at all four sites.

Source	df	F-Value	Pr > F
Marsh	3	160.27	<0.0001
Error	115.1		

Table 3.2. Welch's ANOVA results comparing edge elevations between sites.

Marsh	N	Mean (m)	Standard Error	Standard Deviation	Significance
FP	52	-0.09	0.03	0.22	A
HI	71	0.30	0.02	0.14	B
CP	86	0.51	0.01	0.06	D
MM	61	0.41	0.02	0.13	C

Table 3.3. Mean elevation of the marsh edge at the four sites. Letters indicate significantly different elevations.

The lateral profiles of marsh elevations indicated differences in the morphologies of the marsh at each of the sites (Figures 3.3-3.6). At all sites, elevations tended to increase within the first 10-20 m of the edge; this was followed by a decrease in elevation with distance towards the interior at CP, MM, and HI. This may suggest the presence of natural levees near the edge. There was large variability in elevations amongst the transect profiles at FP; however, their morphologies tended to be similar. The marsh elevation increased dramatically near the edge, followed by a sharp decrease in elevation, and then steadily increasing again towards the interior.

Smaller-scale profiles of the marsh edge depicted differences in edge morphologies between sites (Figures 3.3-3.6). There was variability along the edge at all sites; however, general trends in shape were apparent along each of the edges. MM had a fairly vertical scarp along most of its edge, while the scarp tended to have a rounder, gentler profile at CP. Terracing was evident at HI, with distinct platforms at varying elevations present. The edge along FP exhibited a more gradual slope and unlike the other three sites, lacked a clearly-defined edge.

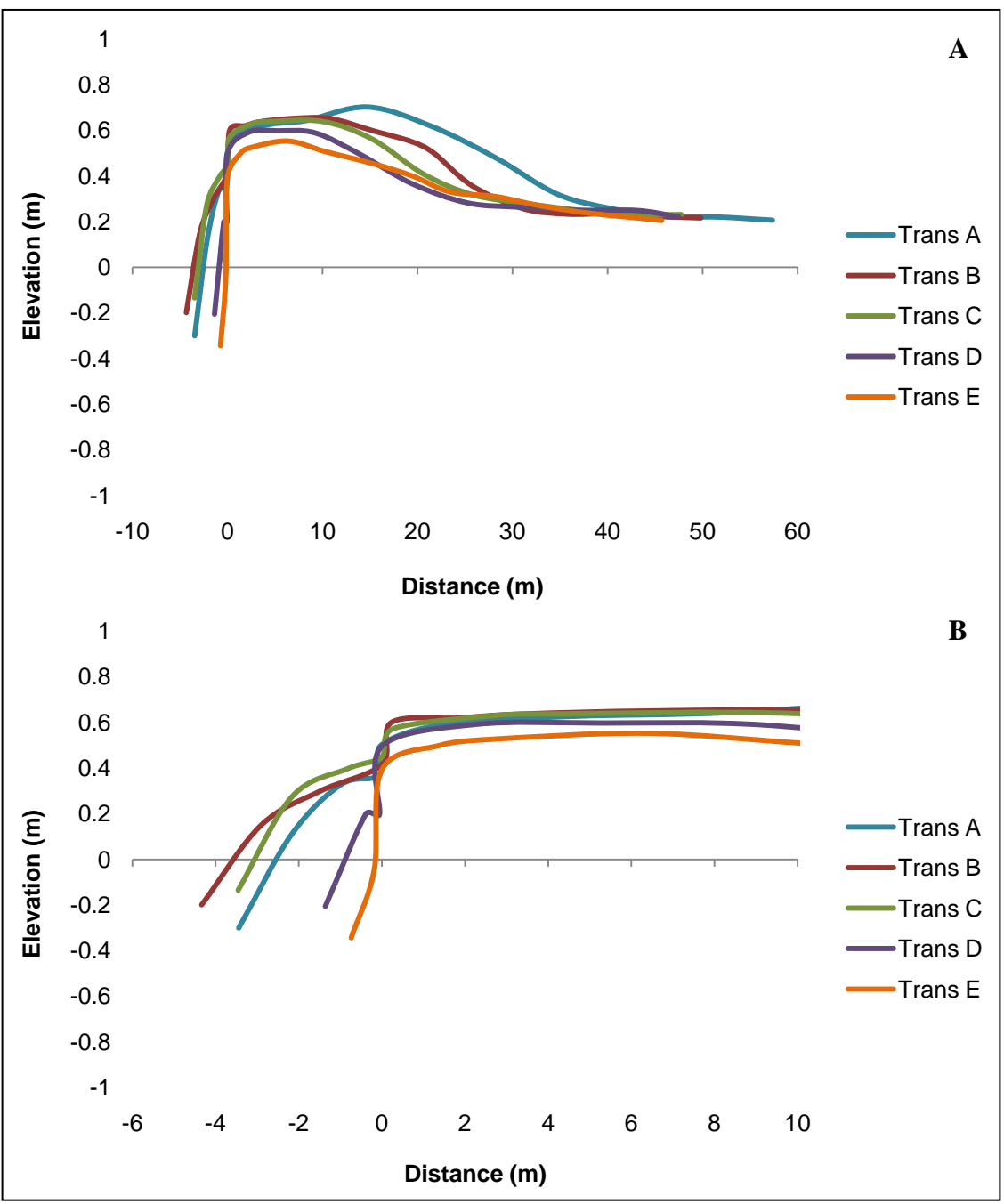


Figure 3.3. Elevation profiles of the entire length of the survey transects (A) and within the first 10 m of the edge (B) at CP. Transects are labeled alphabetically from left, A, to right, E (when facing marsh interior).

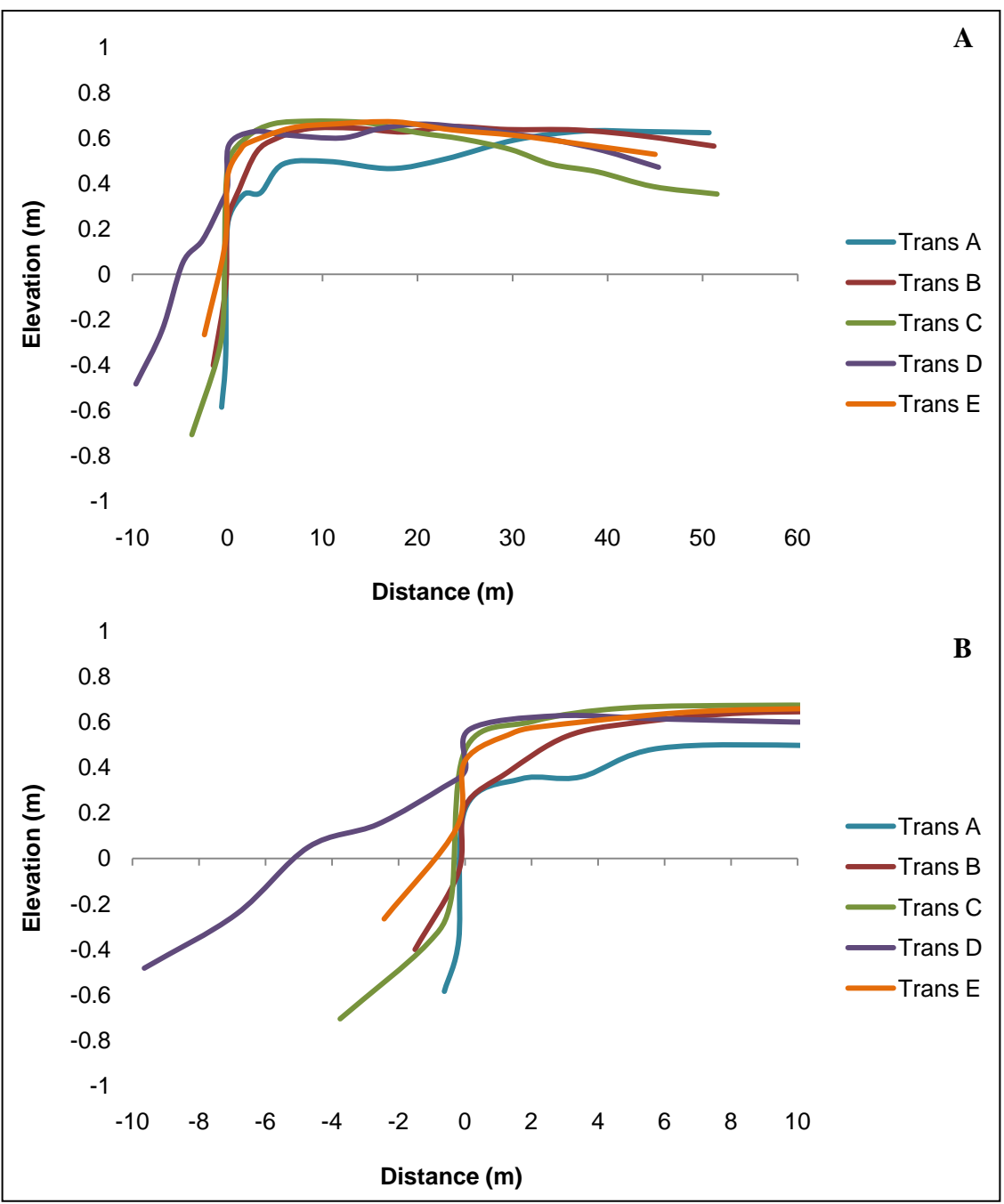


Figure 3.4. Elevation profiles of the entire length of the survey transects (A) and within the first 10 m of the edge (B) at MM. Transects are labeled alphabetically from left, A, to right, E (when facing marsh interior).

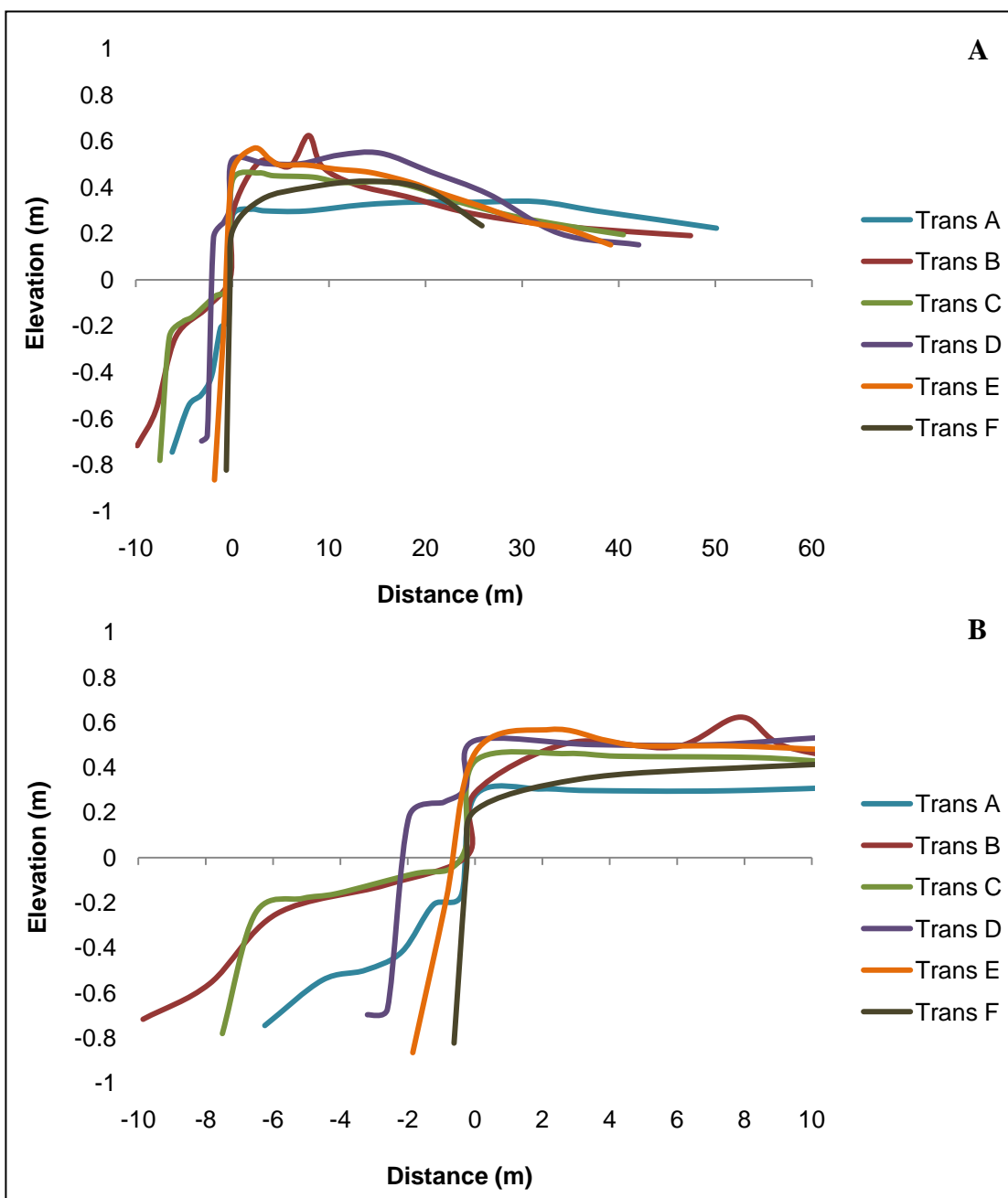


Figure 3.5. Elevation profiles of the entire length of the survey transects (A) and within the first 10 m of the edge (B) at HI. Transects are labeled alphabetically from left, A, to right, F (when facing marsh interior).

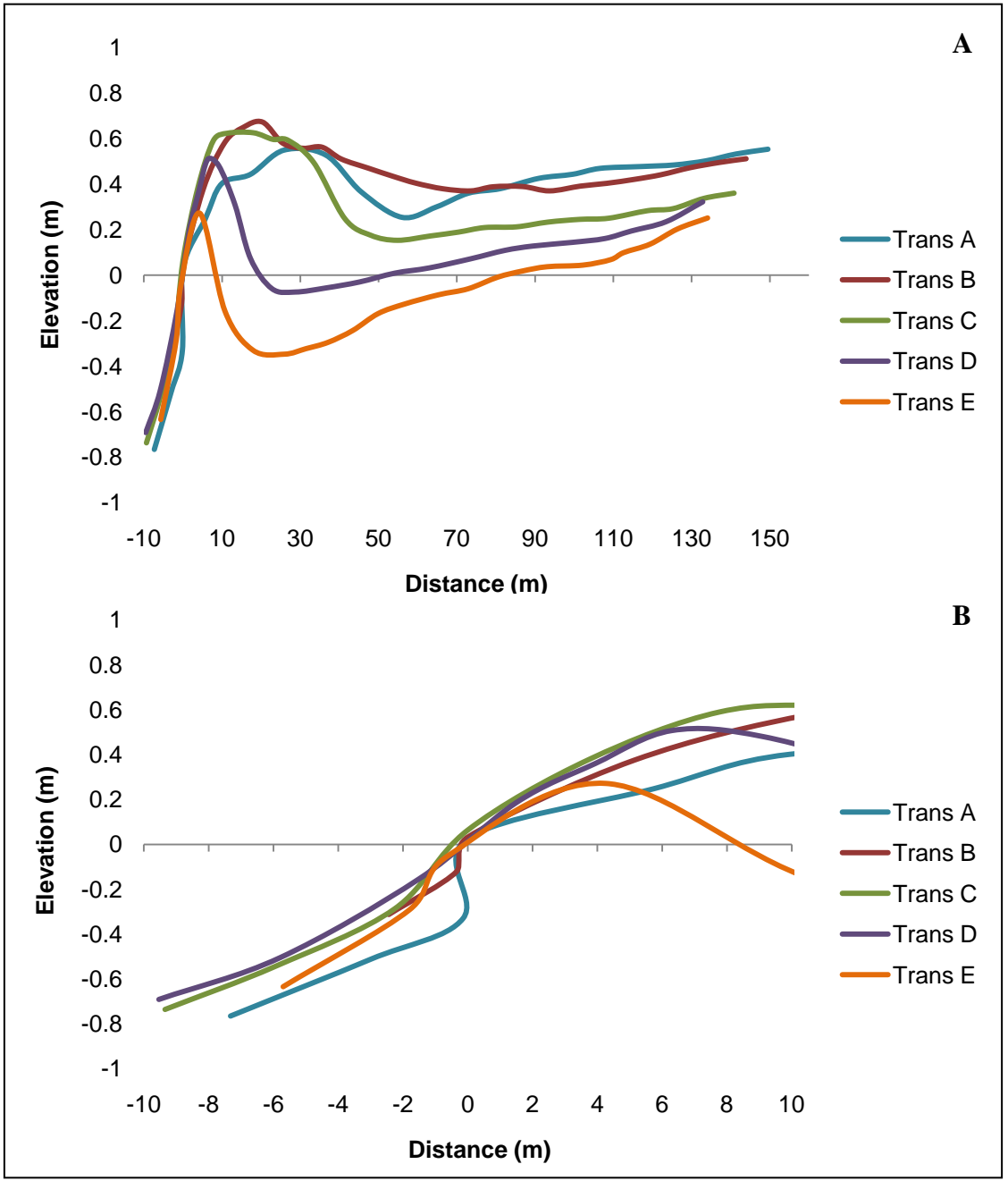


Figure 3.6. Elevation profiles of the entire length of the survey transects (A) and within the first 10 m of the edge (B) at FP. Transects are labeled alphabetically from left, A, to right, E (when facing marsh interior).

Sediment Properties

Sediment grain size differed significantly between marsh sites, but did not vary between the marsh edge and interior at any of the sites (Figure 3.7). Median grain sizes (d50) fell in the range of medium sand, fine sand, coarse silt, and fine silt at FP (254.3 μm), HI (140.3 μm), CP (46.1 μm), and MM (14.5 μm), respectively (Udden-Wentworth). The size distributions of sediment at the sampling locations are presented in Figure 3.8.

Additional properties of the marsh sediments were compared between HI, CP, and MM to analyze potential effects on erosion. Mean values of porosity, bulk density, organic content, and maximum soil compaction are presented in Table 3.4. ANOVA results are presented in Table 3.5; if a significant interaction existed between marsh sites and locations, the results of contrasts are displayed in Table 3.6. Significant interactions were found between marsh (site) and location (edge/interior) for porosity, bulk density, and surface shear strength. Significant differences in porosity existed between the edge at HI and the edges at CP and MM. Bulk density at the marsh edge differed between all three sites. HI was the only marsh to experience within site differences in porosity and bulk density between the edge and interior, with greater bulk density and lower porosity at the interior than the edge. Organic content differed significantly between the sites, with MM having the greatest percentage of organic material, followed by CP and HI. A significant negative relationship existed between organic content and grain size, with percent organic content decreasing with an increase in median grain size (Figure 3.9, $r^2 = 0.71$, $p < 0.0001$, $n = 40$, sediment size log-transformed).

Surface shear strength was significantly greater at the edge of CP than MM, but no differences were found between the edge of HI and the other two sites; shear strength was significantly less in the interior at all three sites (Figure 3.10). Scarp shear strength differed between depths (Scheirer-Ray-Hare test, $df = 1$, $SS = 286.2$, $H = 5.49$, $p < 0.05$), but there were no differences between marsh sites or the interaction between site and location (Figure 3.10). Maximum compaction did not differ between sites or locations, with little overall variability in the data ($df = 5$, $SS = 12.65$, $F = 0.88$, $p = 0.5$).

Marsh	Porosity ($\text{g}\cdot\text{cm}^{-3}$) (n = 5)	Bulk Density ($\text{g}\cdot\text{cm}^{-3}$) (n = 5)	Organic Content (%) (n = 5)	Maximum Compaction ($\text{kg}\cdot\text{cm}^{-2}$) (n = 6)
Stable Edge				
<i>Fowling Point</i>				
Edge	0.50 ± 0.03	1.19 ± 0.08	3.95 ± 0.72	6.74 ± 1.04
Interior	0.54 ± 0.03	1.15 ± 0.08	4.14 ± 0.70	4.92 ± 1.32
Eroding Edge				
<i>Hog Island</i>				
Edge	0.55 ± 0.02	0.99 ± 0.09	4.96 ± 0.76	4.41 ± 1.29
Interior	0.47 ± 0.01	1.52 ± 0.04	1.73 ± 0.17	4.37 ± 0.59
<i>Chimney Pole</i>				
Edge	0.70 ± 0.02	0.77 ± 0.06	12.22 ± 1.66	3.61 ± 0.35
Interior	0.72 ± 0.02	0.75 ± 0.07	10.55 ± 1.32	3.03 ± 0.27
<i>Matulakin Marsh</i>				
Edge	0.69 ± 0.02	0.58 ± 0.06	14.41 ± 1.47	3.03 ± 0.78
Interior	0.74 ± 0.03	0.58 ± 0.03	15.20 ± 0.83	3.16 ± 0.23

Table 3.4. Means (± 1 SE) for selected sediment characteristics at the four marsh sites. Letter superscripts indicate significant differences between marshes ($p < 0.05$).

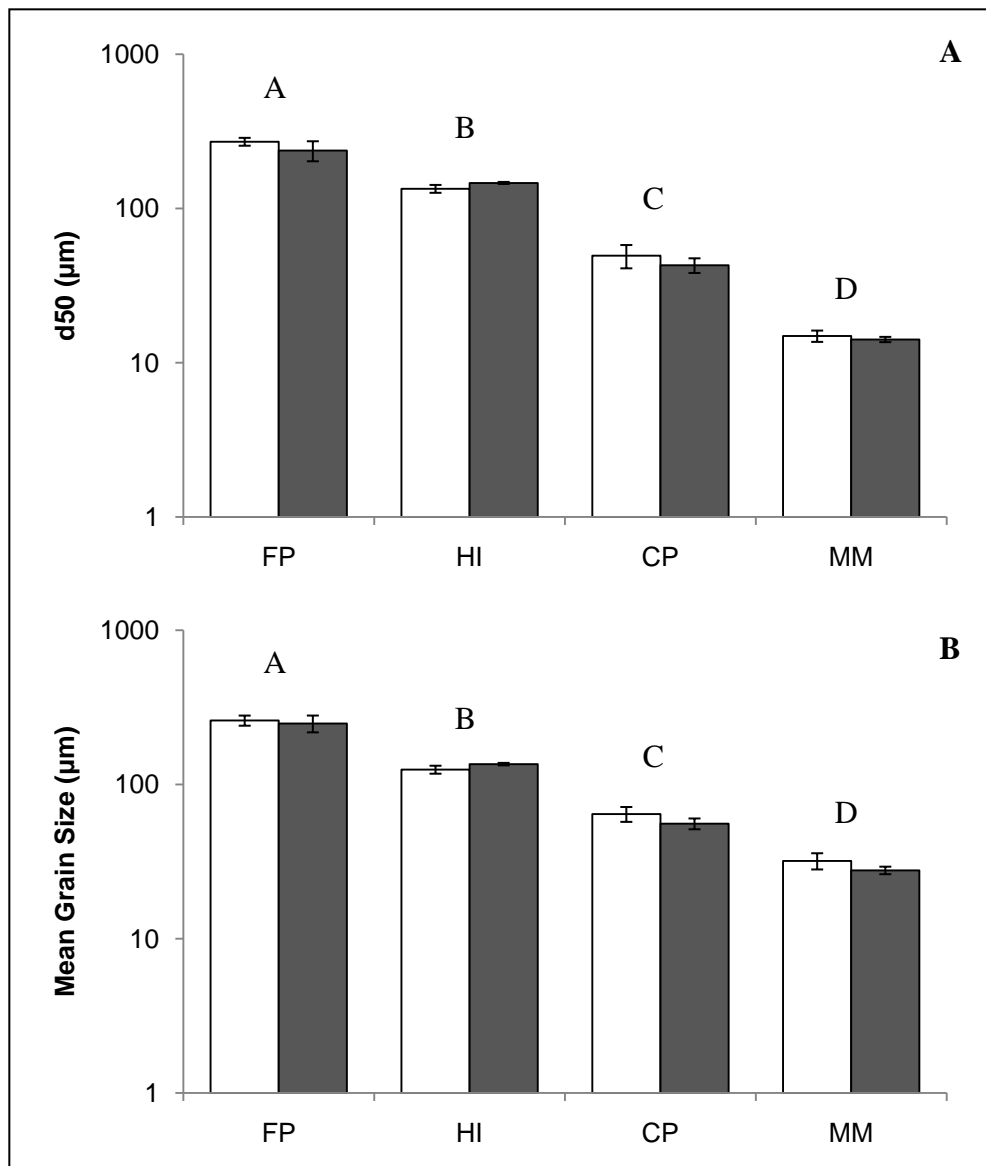


Figure 3.7. Median (A) and mean (B) sediment grain size at each study site. White and gray bars represent edge and interior locations, respectively. The y-axis is on a logarithmic scale. Letters represent significant differences between marsh sites. Error bars indicate ± 1 SE.

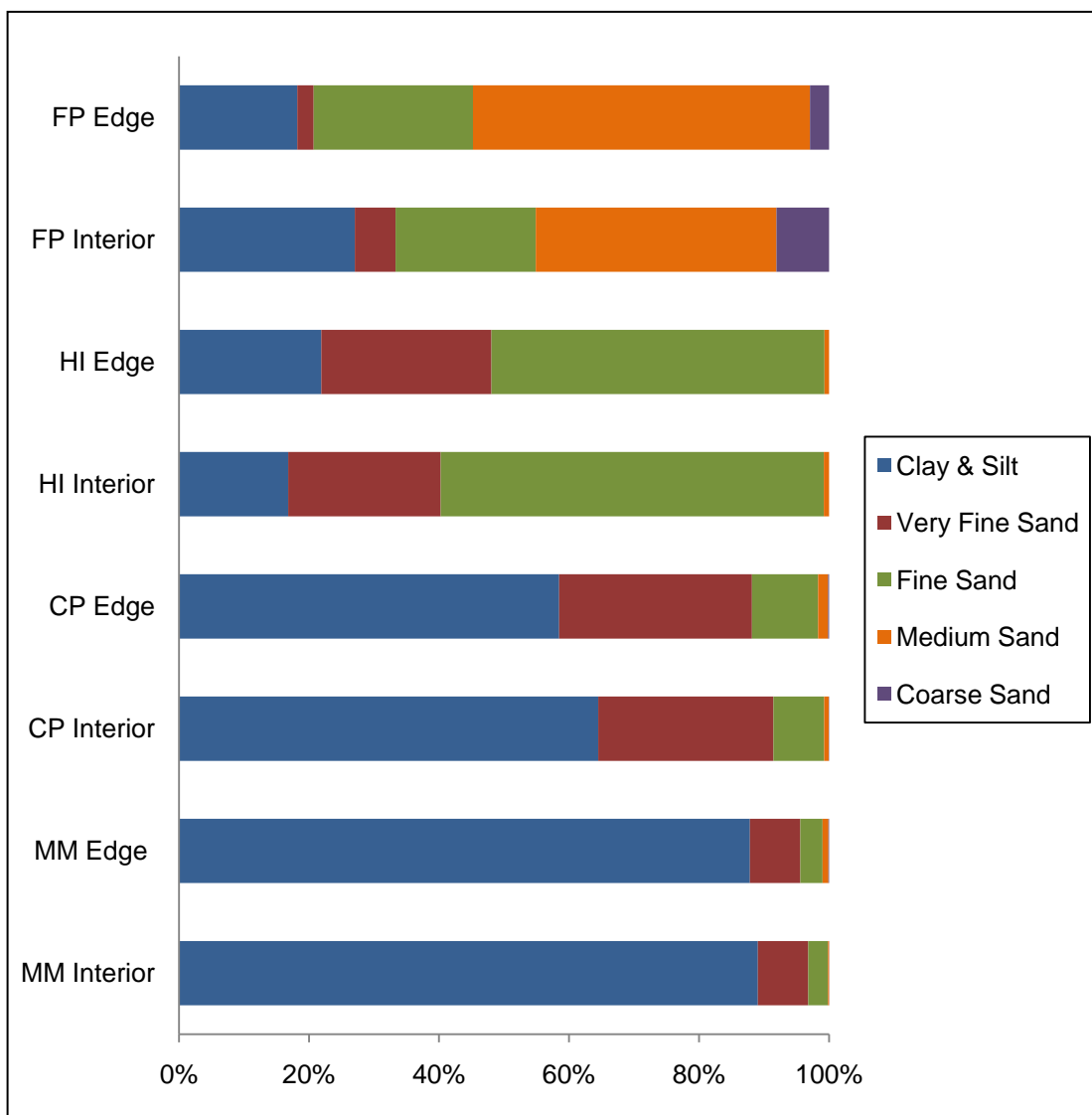


Figure 3.8. Sediment grain size distribution at the edge and interior of each site.

Parameter	df	SS	MS	F	p
Median Grain Size^{sr}					
Marsh	2	330.669	165.334	282.63	<0.0001
Location	1	0.002	0.002	0	0.9577
Marsh x Location	2	1.126	0.563	0.96	0.3962
Porosity^{sr}					
Marsh	2	0.114	0.057	64.64	<0.0001
Location	1	0.0001	0.0001	0.16	0.6902
Marsh x Location	2	0.008	0.004	4.73	0.0186
Bulk Density					
Marsh	2	2.440	1.220	68.93	<0.0001
Location	1	0.217	0.217	12.26	0.0018
Marsh x Location	2	0.486	0.243	13.72	0.0001
% Organic Matter					
Marsh	2	692.024	346.012	52.09	<0.0001
Location	1	14.075	14.075	2.12	0.1585
Marsh x Location	2	20.609	10.304	1.55	0.2325
Surface Shear Strength^{log}					
Marsh	2	0.046	0.023	1.54	0.231
Location	1	3.838	3.838	256.57	<0.0001
Marsh x Location	2	0.495	0.248	16.55	<0.0001

Table 3.5. Statistical results of two-way ANOVAs comparing main and interaction effects for sediment characteristics ($p < 0.05$). df = degrees of freedom, SS = sum of squares, MS = mean square. Superscripts indicate square-root and log₁₀ transformations.

Contrast	p		
	Porosity	Bulk Density	Surface Shear Strength
<i>Between Edge Sites</i>			
MM x CP	ns	0.0329	0.0071
MM x HI	<0.0001	<0.0001	ns
CP x HI	<0.0001	0.0154	ns
<i>Within Site Locations (Edge x Interior)</i>			
MM	ns	ns	<0.0001
CP	ns	ns	<0.0001
HI	0.0121	<0.0001	<0.0001

Table 3.6. Results of pairwise contrasts to determine between and within site differences. ns = no significant effect.

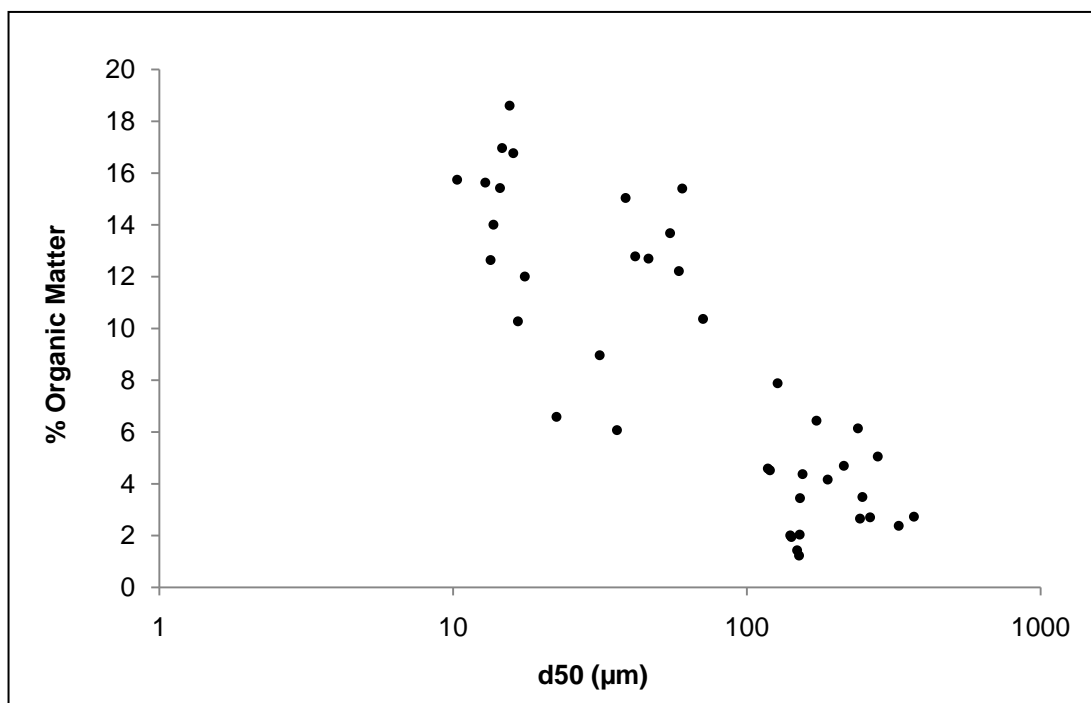


Figure 3.9. Relationship between median grain size (d50) and percent organic matter.

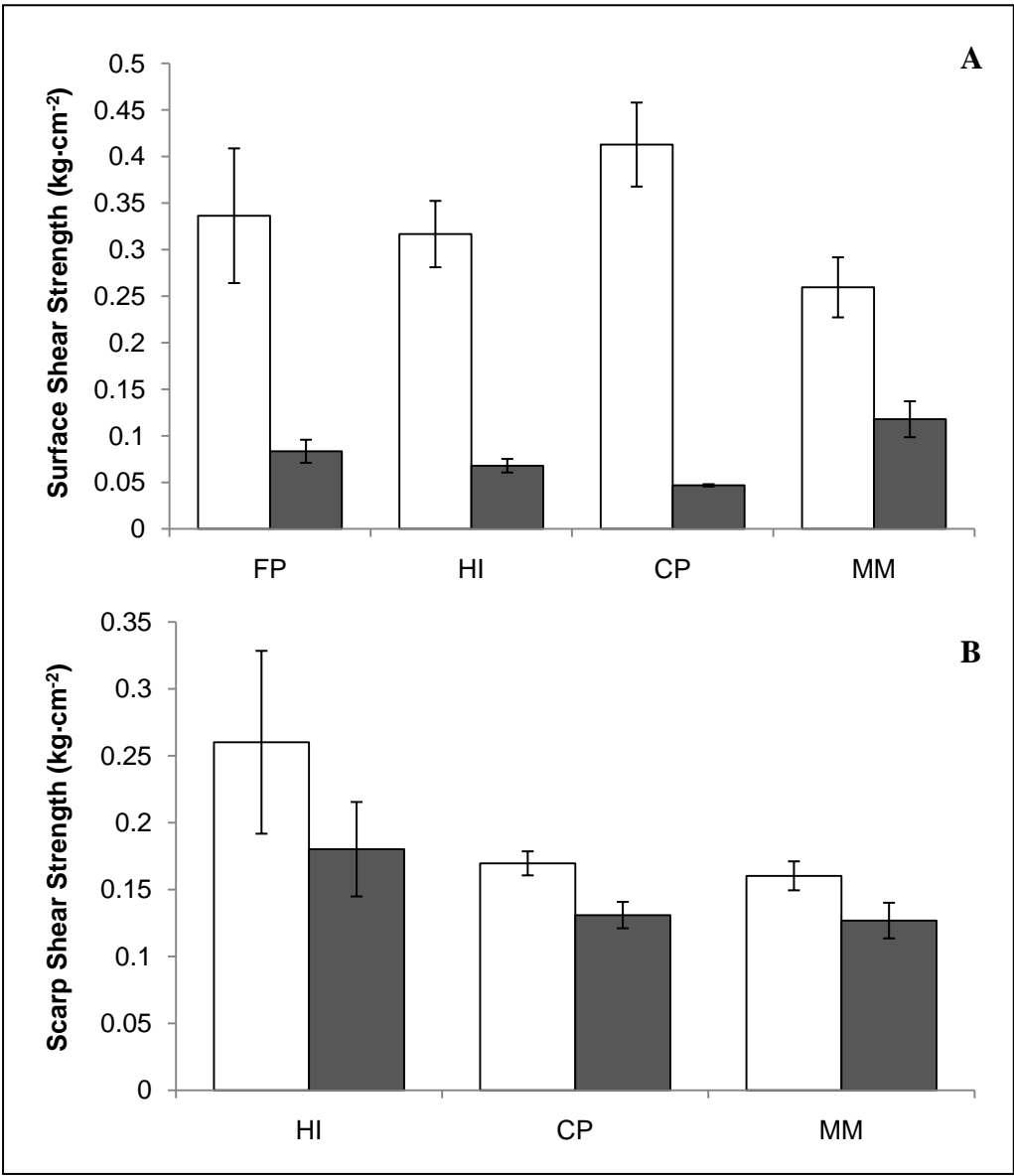


Figure 3.10. Results of mean (± 1 SE) shear strength measurements on the marsh surface (A) and scarp (B). No scarp measurements were made at FP. Surface measurements taken at the edge and interior (white and gray bars, A) and scarp measurements taken at 0-5 cm and 25-30 cm depths (white and gray bars, B).

Vegetation Characteristics

June and August vegetation samples were pooled for two reasons: (1) there were no significant differences detected between the two months and (2) pooling provides a general estimate of vegetation characteristics throughout the growing season. It is not believed that vegetation differences between the months affect erosion rates, and therefore pooling the data seemed to be an appropriate action. Above- and belowground biomass results are presented in Figures 3.11 and 3.12, while mean shoot:root ratios, canopy heights, and stem densities are provided in Table 3.7. Statistical results of the ANOVAs are presented in Table 3.8, and contrasts for significant interactions are in Table 3.9.

The two-way interaction (marsh x location) was significant for total aboveground biomass, total belowground biomass, and canopy height. Aboveground biomass at the marsh edge was statistically greater at HI than at CP and MM; there was no difference in aboveground biomass between CP and MM. MM was the only site to experience within-site variation, with the edge having less total biomass than the interior. Total belowground biomass only differed between the edges at CP and HI. Belowground biomass is greater at the edge at HI than in the interior. The edge canopy height differed among all three sites, with HI having the tallest vegetation, followed by CP and MM. Canopy height was significantly greater in the marsh interior than at the edge at CP and MM. The three-way interaction between marsh, location, and depth for belowground biomass was statistically significant. This indicates that the biomass at a particular depth may vary based on the site and location. Contrasts were not run for the three-way interaction; however, depth profiles (Figure 3.12) indicate specific trends at each of the

sites. The ratio of aboveground to belowground biomass (shoot:root) differs between marsh sites (HI > MM) and locations (interior > edge).

Because the top layer of the root mat appears to play a particularly important role in stabilizing the marsh against erosion, the top 5 cm of belowground biomass was compared between sites and locations (Table 3.10). A significant interaction indicated that the biomass in the upper root layer differed at the edge at all sites (CP > MM > HI). There was also a difference between the edge and interior at CP and HI (Table 3.11).

Root and rhizome tensile strengths were affected by the diameter of the roots/rhizomes, with diameter explaining 75% of the variation in strength (Figure 3.13, $r^2 = 0.75$, $p < 0.0001$, $n = 750$, log-transformed). Mean root and rhizome strengths both differed significantly between the marsh edge and marsh interior (Table 3.12). In both cases, strength was greater in the interior than at the edge (Figure 3.14). Between site differences only existed for rhizome strengths, with MM having a lower mean strength than CP and HI. The interaction term was not significant for either root or rhizome strength.

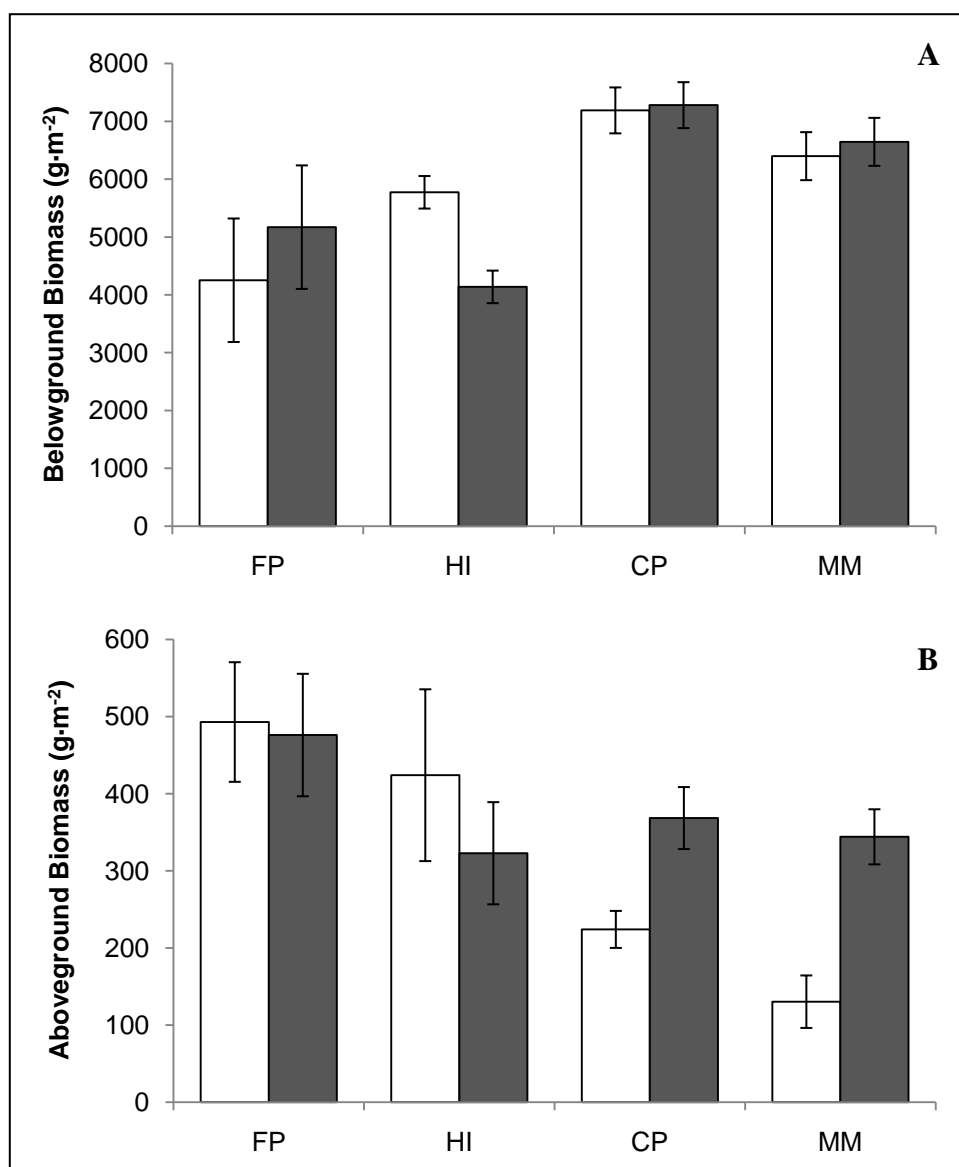


Figure 3.11. Mean (± 1 SE) total belowground (A) and total aboveground (B) biomass at the study sites. Samples taken at the marsh edge (white) and interior (gray). $n = 10$ at all aboveground locations (except FP interior, $n = 9$). $n = 10$ at all belowground sites, with the exception of CP edge ($n = 5$), CP interior ($n = 5$), and FP interior ($n = 9$).

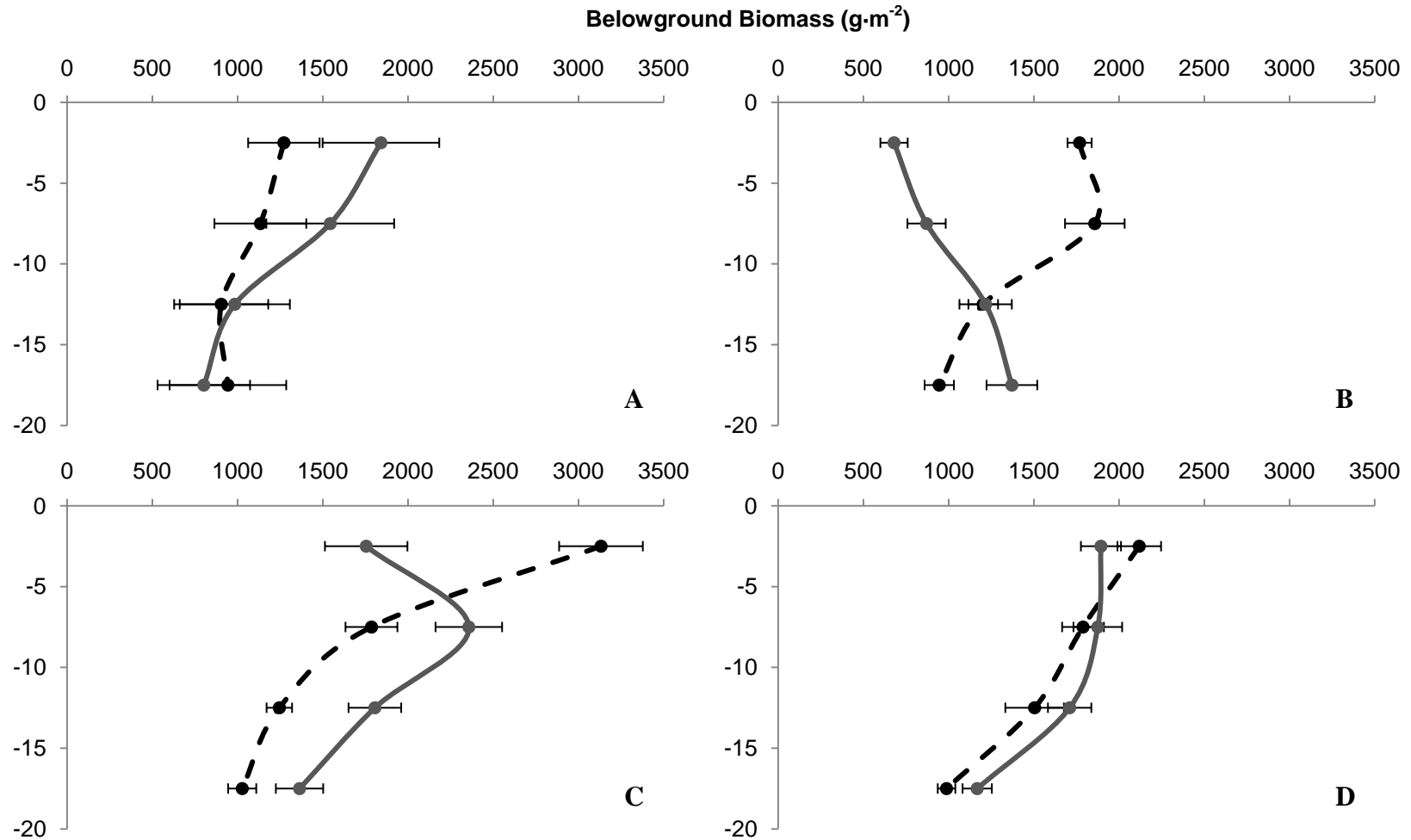


Figure 3.12. Belowground biomass depth profiles at FP (A), HI (B), CP (C), and MM (D). Dots represents mean (± 1 SE) biomass at 0-5 cm, 5-10 cm, 10-15 cm, and 15-20 cm depths. Samples taken at the marsh edge (black, dashed) and interior (gray, solid). y-axis indicates cm below the surface.

Marsh	Shoot:Root Ratio	Height (cm)	Density (m ⁻²)
Stable Edge			
<i>Fowling Point</i>			
Edge	0.160 ± 0.028	30.6 ± 3.3	990 ± 206
Interior	0.188 ± 0.081	27.9 ± 4.0	786 ± 145
Eroding Edge			
<i>Hog Island</i> ^a			
Edge	0.073 ± 0.018	20.0 ± 2.4	996 ± 130
Interior	0.081 ± 0.015	17.6 ± 1.4	877 ± 121
<i>Chimney Pole</i> ^{ab}			
Edge	0.036 ± 0.005	13.2 ± 1.1	1319 ± 153
Interior	0.047 ± 0.008	18.1 ± 1.0	934 ± 135
<i>Matulakin Marsh</i> ^b			
Edge	0.023 ± 0.007	7.7 ± 2.0	764 ± 275
Interior	0.051 ± 0.004	15.2 ± 0.9	1166 ± 110

Table 3.7. Means (± 1 SE) for selected vegetation characteristics at the four marsh sites. Letter superscripts indicate significant differences between marshes ($p < 0.05$).

Contrast	p		
	Aboveground Biomass	Belowground Biomass	Height
<i>Between Edge Sites</i>			
MM x CP	ns	ns	0.0144
MM x HI	0.0001	ns	<0.0001
CP x HI	0.0351	0.0345	0.0031
<i>Within Site Locations (Edge x Interior)</i>			
MM	0.0006	ns	0.0012
CP	ns	ns	0.0304
HI	ns	0.0035	ns

Table 3.8. Results of pairwise contrasts to determine between-site and within-site differences. ns = no significant effect.

Table 3.9. ANOVA results comparing main and interaction effects for vegetation characteristics.

Parameter	df	SS	MS	F	p
Total Aboveground Biomass^{sr}					
Marsh	2	149.765	74.882	3.21	0.0482
Location	1	150.919	150.919	6.47	0.0139
Marsh x Location	2	269.837	134.919	5.78	0.0053
Total Belowground Biomass					
Marsh	2	42450195	21225097	15.11	<0.0001
Location	1	2104251	2104251	1.5	0.2274
Marsh x Location	2	10095577	5047788	3.59	0.0358
Belowground Biomass by Depth					
Marsh	2	10612549	5306274	35.9	<0.0001
Location	1	526063	526063	3.56	0.0609
Depth	3	15026023	5008674	33.88	<0.0001
Marsh x Location	2	2523894	1261947	8.54	0.0003
Marsh x Depth	6	6773215	1128869	7.64	<0.0001
Location x Depth	3	10532760	3510920	23.75	<0.0001
Marsh x Location x Depth	6	6002548	1000425	6.77	<0.0001
Shoot:Root Ratio^{sr}					
Marsh	2	0.074	0.037	7.69	0.0014
Location	1	0.022	0.026	4.49	0.0397
Marsh x Location	2	0.016	0.008	1.64	0.2064
Height					
Marsh	2	541.851	270.926	11.33	<0.0001
Location	1	163.374	163.374	6.83	0.0116
Marsh x Location	2	265.269	132.634	5.55	0.0064

Parameter	df	SS	MS	F	p
0-5 cm Depth					
Marsh	2	11604979	5802489	41.7	<0.0001
Location	1	9051891	9051891	65.06	<0.0001
Marsh x Location	2	2905052	1452526	10.44	0.0002

Table 3.10. Results of a two-way ANOVA comparing main and interaction effects for the top 5 cm of belowground biomass.

Contrast	0-5 cm Depth p
<i>Between Edge Sites</i>	
MM x CP	<0.0001
MM x HI	0.0417
CP x HI	<0.0001
<i>Within Site Locations (Edge x Interior)</i>	
MM	ns
CP	<0.0001
HI	<0.0001

Table 3.11. Pairwise contrasts comparing between site and within site differences for the top 5 cm of belowground biomass.

Parameter	df	SS	MS	F	p
Root Strength					
Marsh	2	0.80	0.40	1.9	0.1715
Location	1	1.99	1.99	9.47	0.0052
Marsh x Location	2	0.28	0.14	0.66	0.5238
Rhizome Strength					
Marsh	2	435.71	217.85	15.47	<0.0001
Location	1	78.28	78.28	5.56	0.0269
Marsh x Location	2	4.69	2.34	0.17	0.8476

Table 3.12. Two-way ANOVA results for main and interaction effects of root and rhizome strengths.

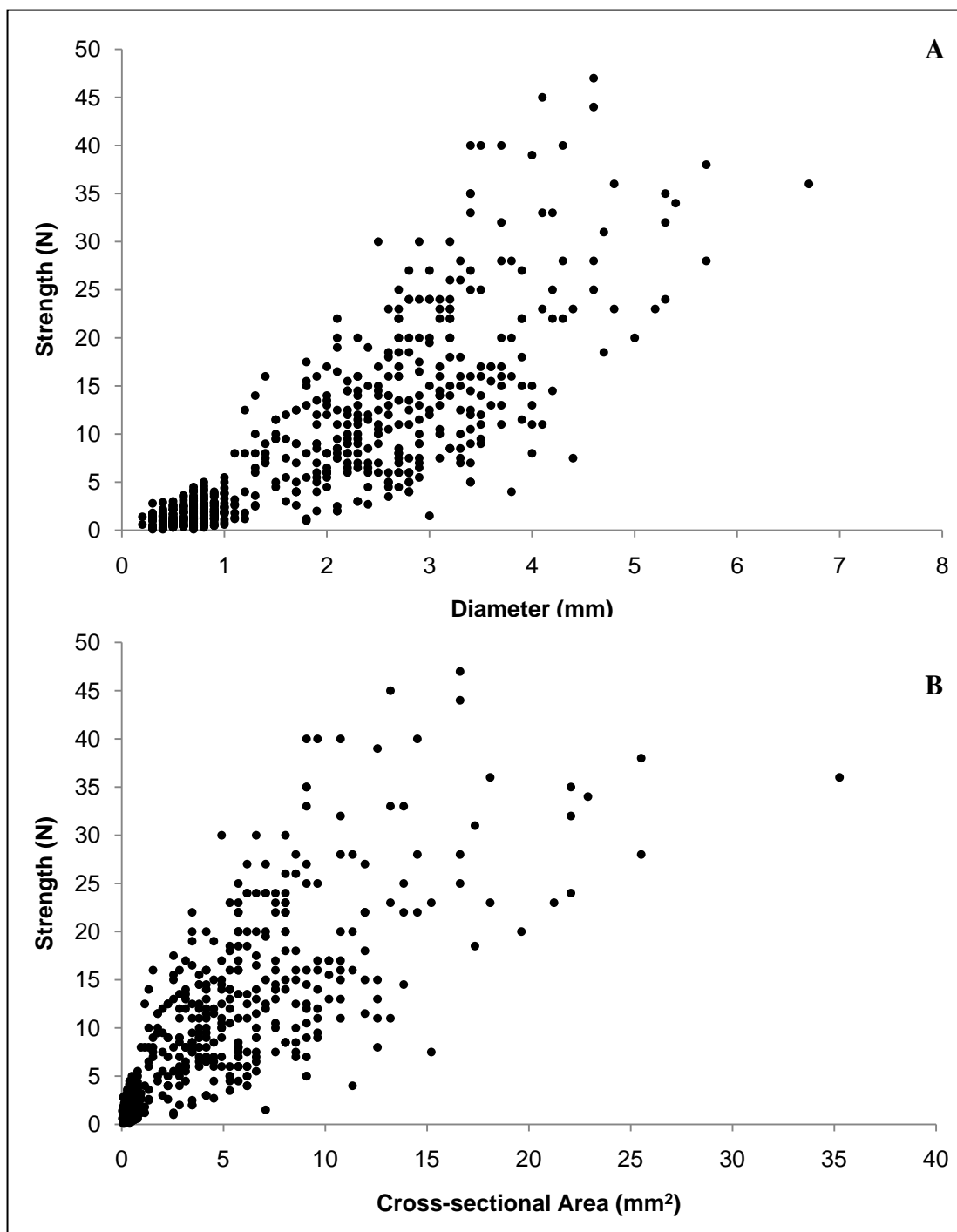


Figure 3.13. Relationship between tensile strength and diameter (A) and cross-sectional area (B) of roots and rhizomes.

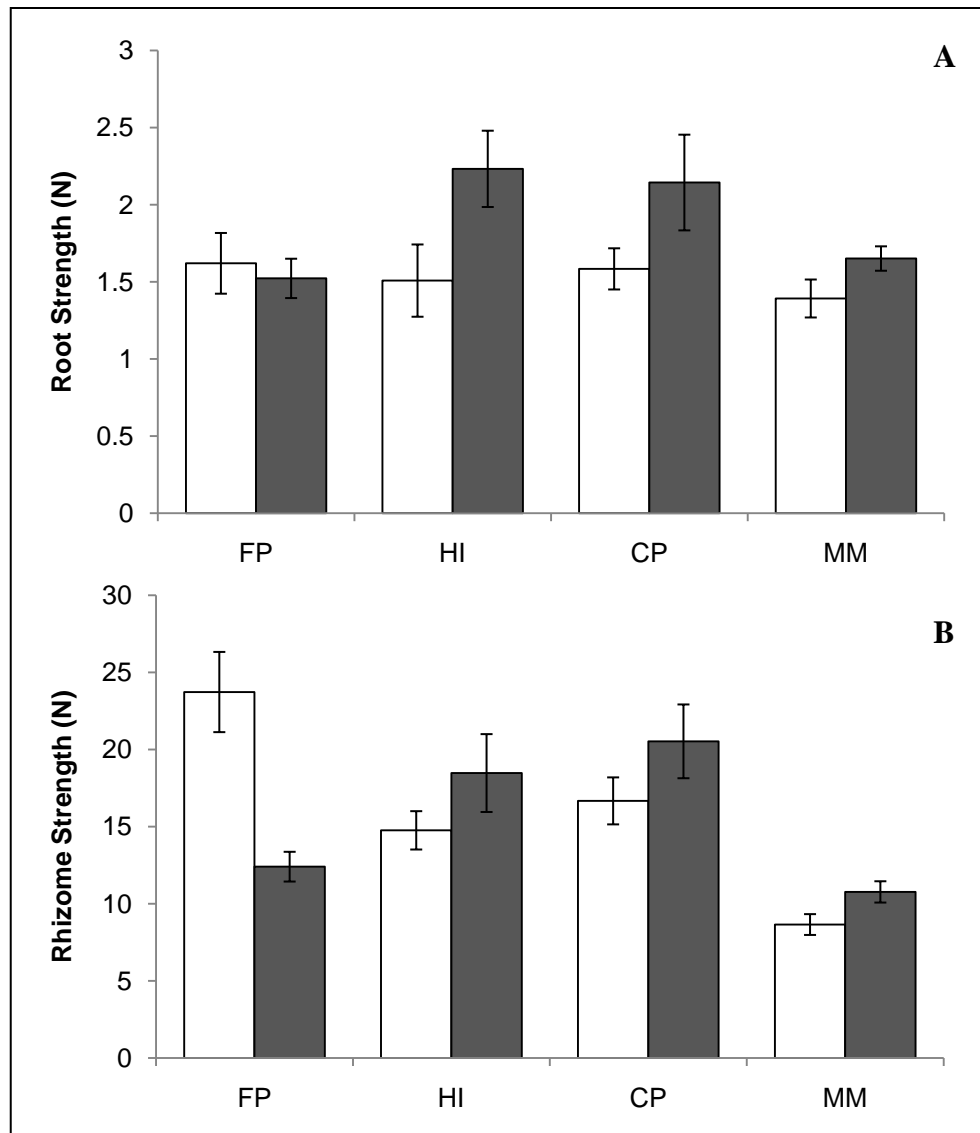


Figure 3.14. Mean (± 1 SE) strengths of roots (A) and rhizomes (B) at the study sites. Samples taken at marsh edge (white) and interior (gray) locations. $n = 5$.

Crab Burrows

Crab burrow sampling results are presented in Figure 3.15. There was a significant interaction between marsh and interior for burrow densities (Table 3.13). Burrow densities were statistically greater at the edge of MM than at the edges of CP and HI (Table 3.14). The only within site differences in burrow densities occurred at CP, where densities were greater in the interior than at the edge. Burrow diameters and surface areas differed between marsh sites, with greater burrow diameters and coverage at MM and CP than at HI. There was also a significant difference in diameters between marsh locations at CP, where edge burrows had greater average diameters than interior burrows.

Statistical analysis was not performed on the volumes of the burrow casts because locations were not chosen randomly and limited samples were taken. However, total burrow volume at each sampling location (averaged across the two quadrats) indicated the presence of much larger burrows at the edge of CP and MM compared to interior locations or the edge at HI (Figure 3.13d). Direct comparisons should not be made between CP and MM because a greater percentage of burrows within the CP edge quadrats were molded and retrieved than at MM; many of the burrows at the edge of MM opened directly into the bay (through the vertical scarp), and therefore were not able to retain the resin long enough for a cast to set. Some examples of burrow forms within the marshes are presented in Figure 3.16.

The greatest numbers of crabs were found in traps at MM, followed by CP and HI (Table 3.15). *Uca pugnax* was present at all sites and was found to have the greatest abundance of all crab species. Though much less abundant, *Sesarma reticulatum* were

also present at all three of the marshes (1 crab trapped at each site). *Panopeus herbstii* was found in a single trap at both MM and HI. Despite its sandy sediment, no sand fiddler crabs (*U. pugilator*) were found in traps at HI.

Parameter	df	SS	MS	F	p
Burrow Density					
Marsh	2	81425.07	40712.53	6.74	0.0047
Location	1	853.333	853.333	0.14	0.7103
Marsh x Location	2	52548.27	26274.13	4.35	0.0244
Burrow Diameter					
Marsh	2	238.877	119.438	4.01	0.0315
Location	1	199.755	199.755	6.7	0.0161
Marsh x Location	2	20.702	10.351	0.35	0.7101
Burrow Area^{sr}					
Marsh	2	933.270	466.635	5.88	0.0083
Location	1	247.871	247.871	3.12	0.0899
Marsh x Location	2	186.127	93.064	1.17	0.3266

Table 3.13. Two-way ANOVA results for main and interaction effects of crab burrow properties. Superscript indicates square-root transformation.

Contrast	Burrow Density p
<i>Between Edge Sites</i>	
MM x CP	0.0063
MM x HI	0.0046
CP x HI	ns
<i>Within Site Locations (Edge x Interior)</i>	
MM	ns
CP	0.018
HI	ns

Table 3.14. Pairwise contrasts of between-site and within-site differences for crab burrow densities.

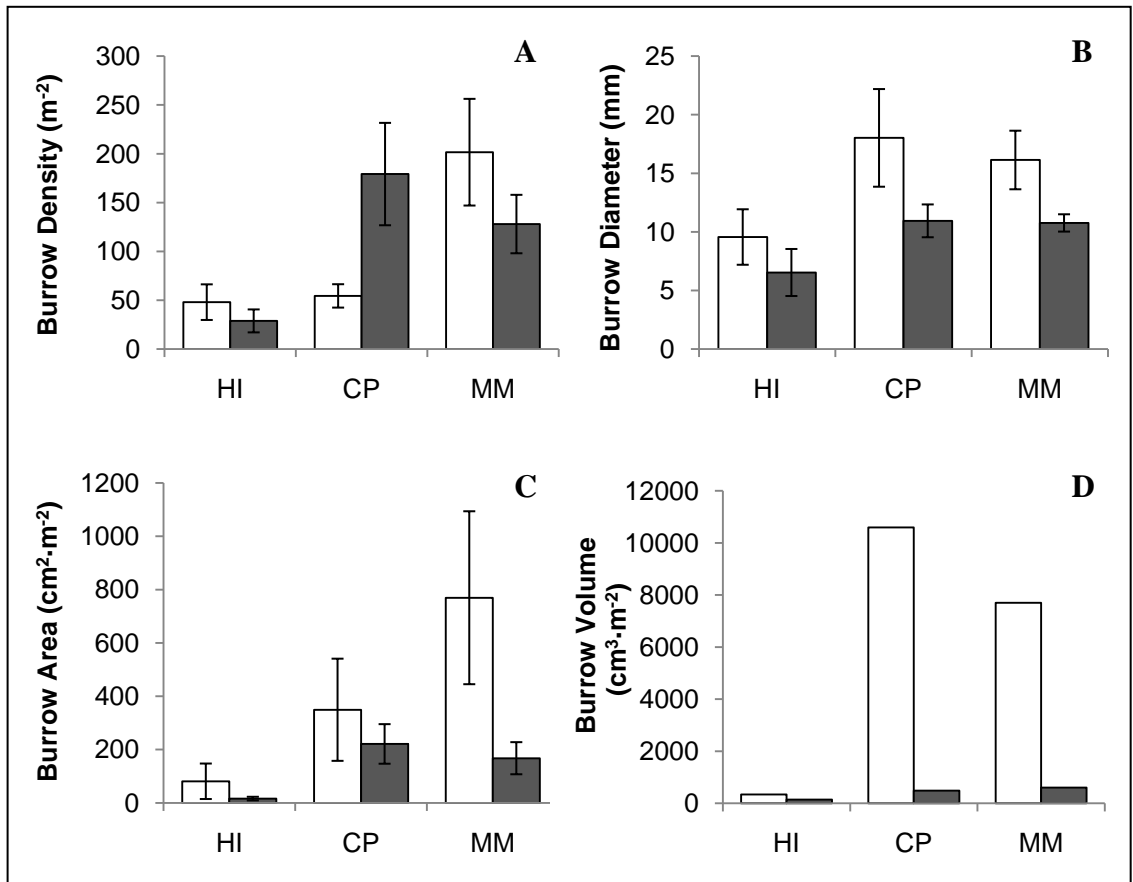


Figure 3.15. Mean crab burrow densities (A), diameters (B), coverage (C), and total volumes (D) at the study sites. Measurements made at the marsh edge (white) and interior (gray). $n = 5$ for density, diameter, and coverage; $n = 2$ for volume. Error bars indicate ± 1 SE.

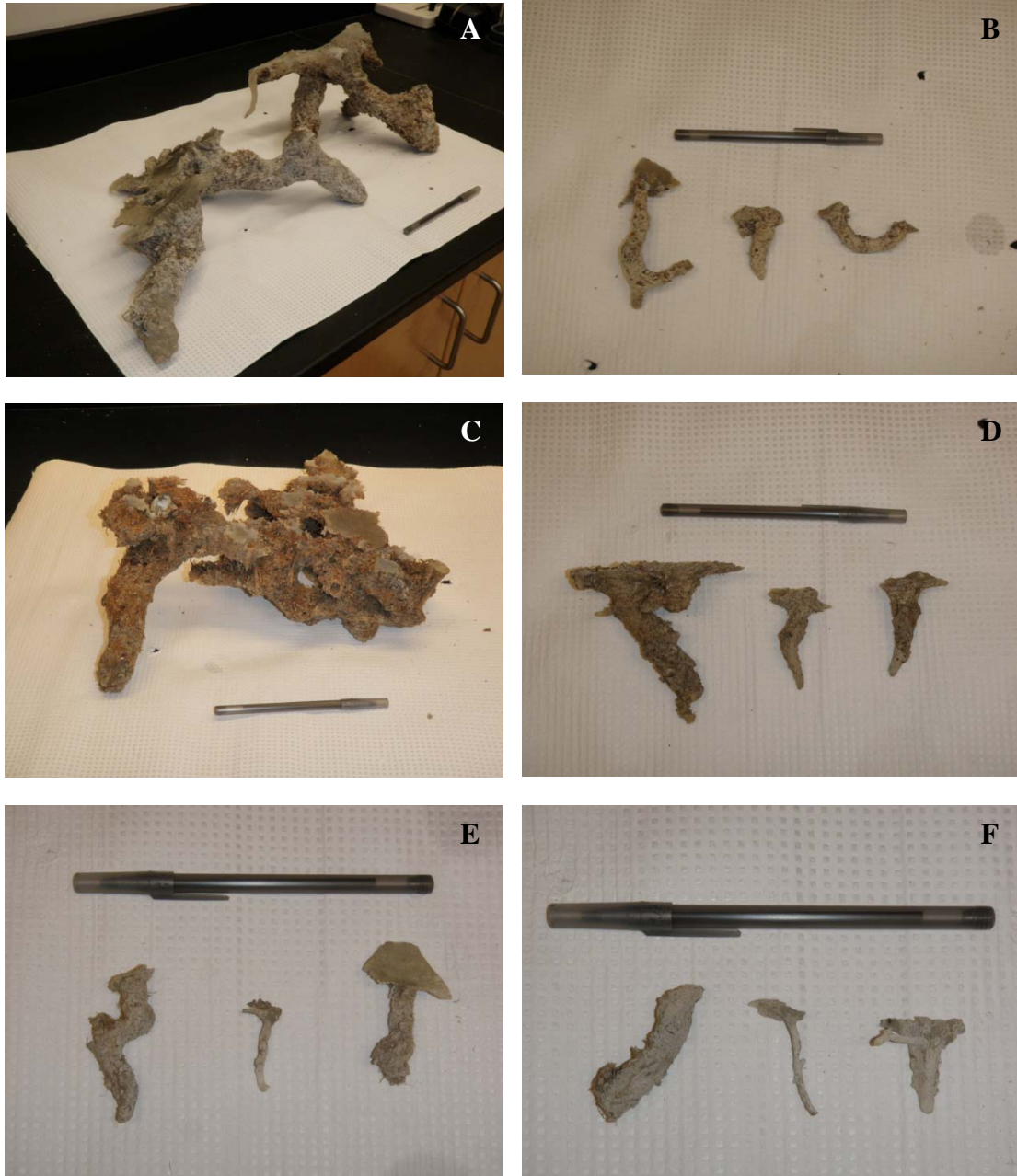


Figure 3.16. Representative burrow casts from CP Edge (A), CP Interior (B), MM Edge (C), MM Interior (D), HI Edge (E), and HI Interior (F). Pen is included for scale.

Site	Number of Crabs			
	<i>U. pugnax</i>	<i>S. reticulatum</i>	<i>P. herbstii</i>	Total per Trap
<i>Hog Island</i>				
Edge	1	1	0	0.33
Interior	3	0	1	0.5
<i>Chimney Pole</i>				
Edge	9	0	0	1.5
Interior	17	1	0	3
<i>Matulakin Marsh</i>				
Edge	16	1	1	3
Interior	23	0	0	4.6

Table 3.15. Total number of crabs of each species found in pitfall traps on the marshes. n = 6 (except at MM interior, n = 5).

Mussel and Snail Densities

Mean densities of ribbed mussels (*G. demissa*) and periwinkle snails (*L. irrorata*) at the edge and interior locations of the sites are presented in Figure 3.17. There was a significant interaction between marsh and location for mussel densities (Table 3.16). Densities were significantly greater at the edge of HI than the edge at CP; mussel densities at the edge of MM did not statistically differ from either site (Table 3.17). The marsh edge had significantly greater mussel densities than the interior at HI and CP, but no location differences existed at MM. The interaction between marsh and location was also significant for snail densities (Table 3.16). The edge at HI had significantly lower densities of snails than the edges at CP and MM; there were no differences in edge densities between CP and MM (Table 3.17). Location differences only existed at HI, where densities were greater in the interior than at the edge.

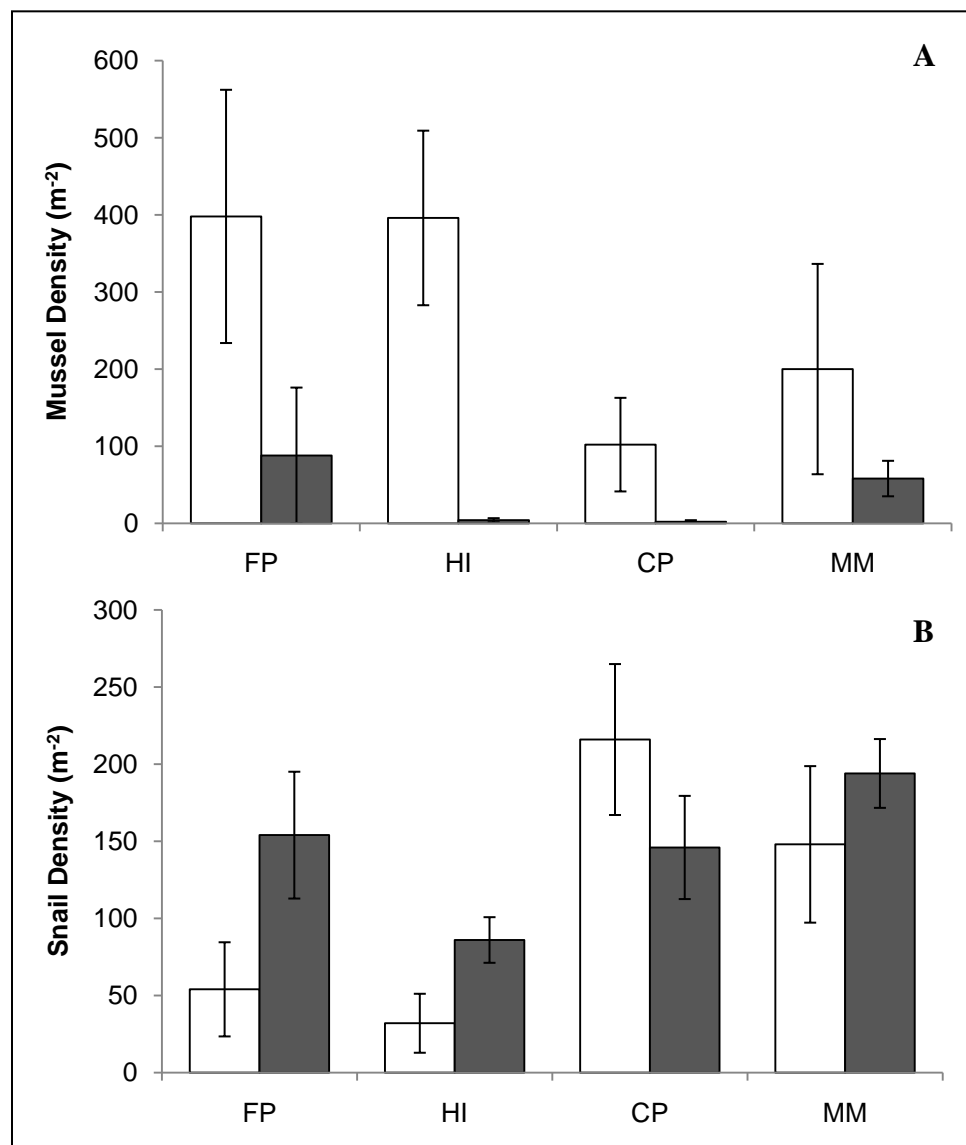


Figure 3.17. Mean (± 1 SE) densities of ribbed mussels (A) and periwinkle snails (B) at the study sites. Measurements taken at the marsh edge (white) and interior (gray). $n = 8$.

Parameter	df	SS	MS	F (or H)	p
Mussel Density*					
Marsh	2	423.1	211.5	2.31	>0.1
Location	1	2268.8	2268.8	12.41	<0.0001
Marsh x Location	2	1990.4	995.2	10.89	<0.01
Snail Density					
Marsh	2	386.5	193.3	10.99	0.0001
Location	1	43.6	43.6	2.48	0.123
Marsh x Location	2	117.1	58.6	3.33	0.0455

Table 3.16. Statistical results of main and interaction effects for mussel and snail densities.

* Scheirer-Ray-Hare test used instead of two-way ANOVA

Contrast	p	
	Mussel Density*	Snail Density
<i>Between Edge Sites</i>		
MM x CP	ns	ns
MM x HI	ns	0.0022
CP x HI	0.0206	<0.0001
<i>Within Site Locations (Edge x Interior)</i>		
MM	ns	ns
CP	0.0034	ns
HI	0.0007	0.0194

Table 3.17. Pairwise contrasts for differences between sites and within sites. ns = no significant effect.

* Pairwise comparisons made using Mann-Whitney U test

Discussion

Hydrodynamics

The importance of waves on controlling erosion of salt marsh edges has been well documented (e.g., Allen 1989, Pethick 1992, Downs et al. 1994, Wray et al. 1995, Day et al. 1998, Schwimmer 2001). As waves continually act on the marsh scarp, they remove sediment and create fractures along the edge that leads to lateral retreat and a reduction in marsh area. Model estimates of wave energies at the four study sites indicated that typical wave powers were much higher along the edge of the three rapidly eroding marshes (HI, CP, and MM) than the stable edge site (FP). The low wave power at FP reflects the large mudflat fronting this mainland marsh and the corresponding shallow water depth, which provide greater shelter against the development of large waves; this prevents the formation of steep scarps that characterize eroding edges (van Eerd 1985a).

Though it is difficult to make direct comparisons between different systems and studies, the wave powers found at the four marshes in this study were much less than those found at marshes in Rehoboth Bay, DE (Schwimmer 2001). This is relevant because erosion rates calculated at MM, CP, and HI were much greater than those found at the Rehoboth sites, despite the lower wave energies. Schwimmer (2001) found there to be a strong positive relationship between wave power and marsh shoreline erosion, with erosion rates increasing as wave energies increase. There was also a positive relationship between wave power and edge erosion at the Hog Island Bay sites; however, this relationship fell apart when FP was removed from analysis (Figure 3.18). If waves alone were responsible for edge erosion, then we would expect erosion to reflect modeled wave

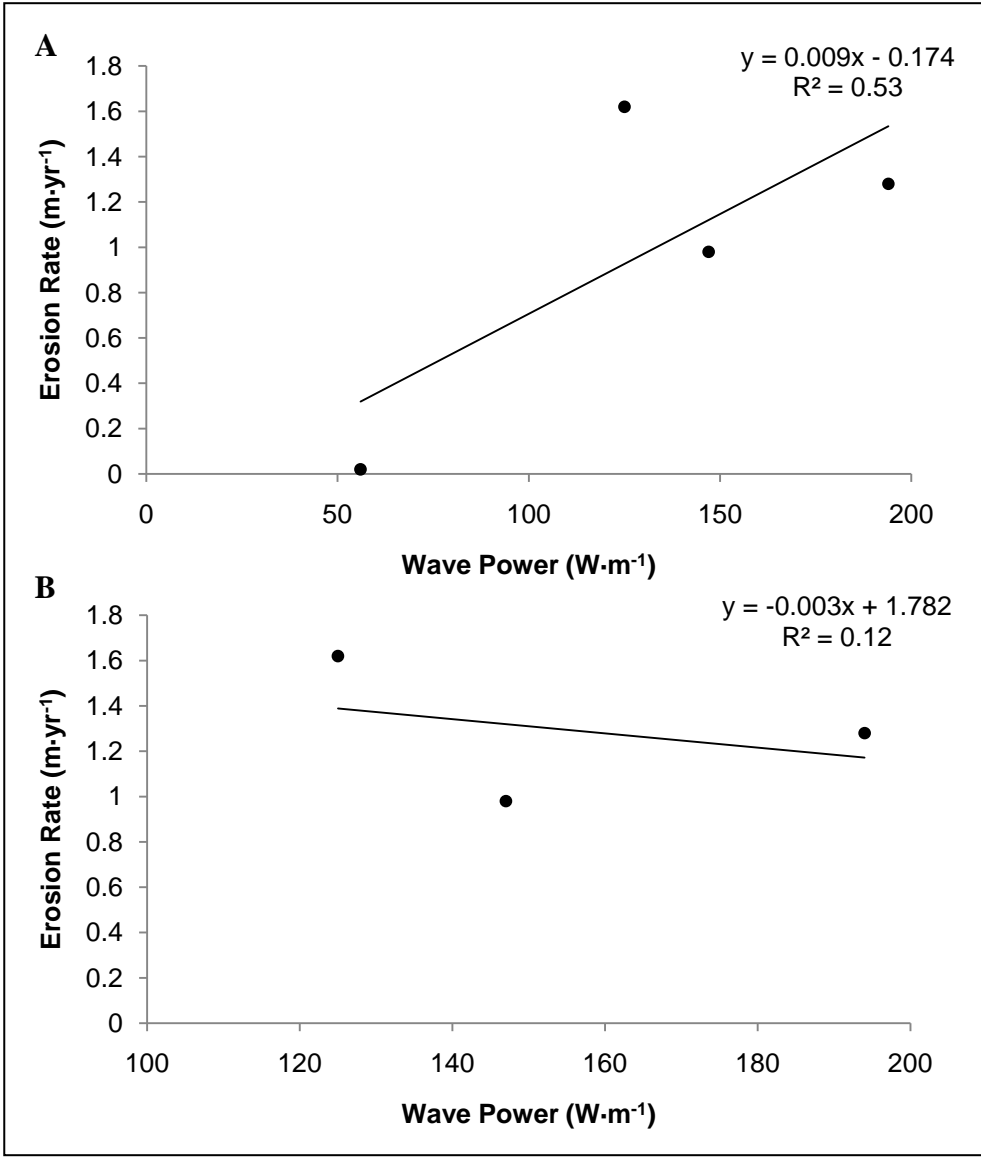


Figure 3.18. Relationship between estimated wave powers and erosion rates at the marsh edges with FP included (A) and excluded (B) from the analysis.

energies. Since this was not the case at the eroding sites, it suggests that other properties of the marsh edge influence erosion rates.

Waves in Hog Island Bay are depth-limited. Therefore, an increase in water depth as relative sea-level rises would likely lead to larger waves capable of promoting greater erosion along marsh edges (Mariotti et al. 2010). If RSLR has the added effect of channel widening and interior ponding at the marsh sites, as has been observed at marshes in Chesapeake Bay (Downs et al. 1994), then future rates of land loss will likely increase and the sustainability of these systems will become uncertain.

Elevation and Morphology

In order for salt marshes to survive, they must maintain vertical positions between mean sea-level (MSL) and mean higher high water (MHHW) (Fagherazzi et al. 2010). The four marshes in this study all had an average elevation above MSL, indicating a surface accretion rate that has kept pace with rising sea-levels. Surface elevation differences between the sites can be explained by the antecedent surfaces of the respective marshes, as well as differences in sediment inputs and accretional processes (Oertel and Woo 1994).

Cross-sectional profiles of the marsh flats provide information on how elevations change with distance from the edge. At all sites, a peak in elevation within the first 20 m of the marsh edge suggests the formation of levees. This is the result of high sediment deposition and rapid accretion that commonly occurs near the seaward edge of marshes (Reed 1988, Day et al. 1998). Sediment deposition near the marsh edge occurs through the settling of entrained sediment during daily flooding tides, with higher rates often

occurring during storm events (Goodbred and Hine 1995, Day et al. 1998). These levees may be similar to those commonly associated with tidal creek banks (e.g., Teal 1958, Reed et al. 1999, Christiansen et al. 2000).

Behind the levees, the marsh elevation tended to decrease towards the interior. This decrease was more dramatic at CP and HI than at MM. The marsh sites in this study are flooded during most high tides and fall completely within the *S. alterniflora* low marsh zone (Figure 3.19). The elevation profiles revealed similar patterns as those observed in the low marsh at Sapelo Island, GA (Teal 1958), where levees near the creek banks are backed by an area of lower elevation in the marsh interior. The more variable surface elevation pattern at FP may be a reflection of its development in swales of a former strand plain ridge (Oertel and Woo 1994).

The elevation profiles of the marsh edge can provide information about the morphologies of the edge at each of the sites and help to explain erosion processes. While the average edge elevations at MM, CP, and HI were all above MSL, the edge at FP was not. Because it did not have a clearly-defined edge in many areas, the vegetation line was used to demarcate the edge at FP. Growth of vegetation at low elevation areas may indicate expansion of *S. alterniflora* onto the adjacent mudflat, particularly if there has been an increase in sedimentation in the area (Schwimmer and Pizzuto 2000).

At the three eroding marshes, the profiles showed morphologies typical of those observed at the edge of each site. The northern portion of HI (Transects A-C, Figure 3.5b) is an area of significant terracing or root scalping (Fagherazzi et al. 2010), formed by the removal of the upper layer of root mat. At the southern end of the site (Transects

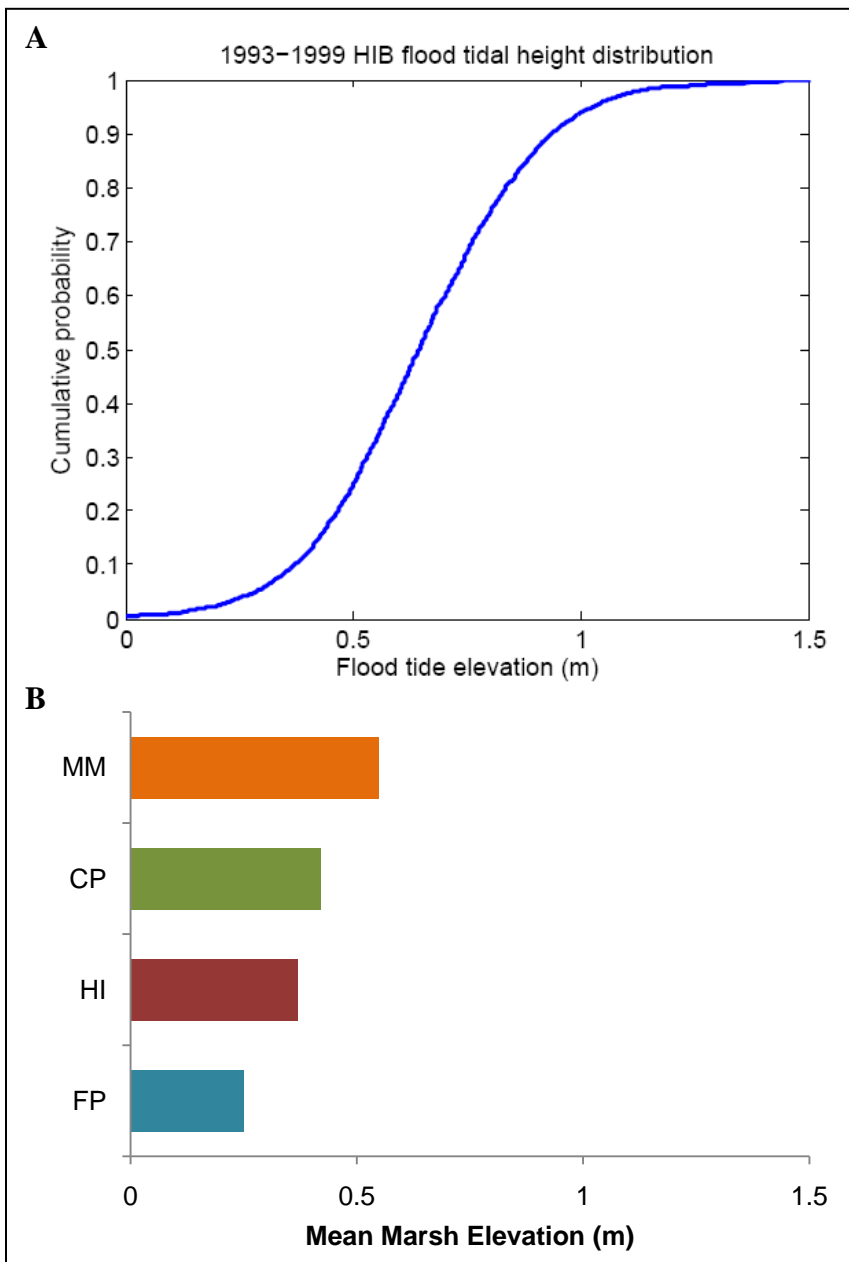


Figure 3.19. A) Cumulative probability distribution of peak flood tide elevation in Hog Island Bay. B) Mean elevation of the marsh flat at each of the sites.

E and F), a more vertical scarp is present, which is the result of cantilever failure commonly occurring in the region (a detailed explanation of erosion mechanisms is provided in Chapter 4). With the exception of an area where the edge gently slopes towards the mudflat (Transect D, Figure 3.4b), the marsh edge at MM is dominated by a vertical scarp. MM regularly experiences block detachment or slumping, and the morphology of the edge reflects that. The presence of an eroding edge is also evident at CP; however, the scarp does not tend to be as steep as that of MM. Root scalping also occurs at CP, whereby the uppermost layer of the root mat is removed from the edge, leaving the underlying sediment exposed (Transects A-C, Figure 3.3b). In some areas, this underlying sediment quickly erodes, causing a more vertical edge to form (i.e. Transect E). The shape of the marsh edge can be an indication of how marsh erosion occurs. Differences in edge morphologies between sites and variations across sites are the result of erosion mechanisms determined by local bathymetric and wave conditions, as well as individual properties of the marsh (Phillips 1986b).

Sediment Properties

Sediment grain sizes generally decrease with distance from the inlet towards the mainland in Hog Island Bay (Lawson 2004). It is expected that marsh sediments should follow a similar pattern. This is because there is not a large source of sediment input into the lagoon and most deposition occurs through the reworking of sediment within the system. Therefore, the primary sources of sediment for deposition on the marshes are the adjacent mudflats and lagoon bottom, as well as material eroded from the edge (Reed 1988). Grain sizes at the study sites decreased with distance from the inlet, with the

exception of Fowling Point. Fowling Point had the coarsest sediment of the four sites and possible reasons for this will be discussed later.

Porosity and bulk density are important to edge erosion because they are correlated with sediment cohesion (Winterwerp et al. 2004). Generally speaking, bulk density typically increases and porosity (of silts and clays) decreases with increasing grain size. Results from the marsh sites support this trend, as HI had the highest bulk densities and MM had the lowest. The spatial differences associated with porosity and bulk density at HI were likely the effect of differences in organic content between the edge and interior. Organic material lowers the bulk density of sediment (Feagin et al. 2009), which also has the effect of increasing porosity. The interior of HI had little near-surface organic matter in comparison to the edge, which caused disparities in bulk density and porosity between the locations.

The organic content at the marsh sites was within range of those found at other salt marshes on the Atlantic Coast (Odum 1988, Bradley and Morris 1990, Michaels 2004). Percent organic content was highly associated with sediment size at the marsh sites, with 71% of the variation in organic matter explained by median grain size. Lawson (2004) also found a positive relationship between percent organic matter and mean sediment size in the lagoon sediment of Hog Island Bay.

Feagin et al. (2009) argue that marshes with coarser sediments (higher bulk densities) will experience more rapid erosion. Results from this study do not support this claim, as a strong negative relationship existed between grain size and erosion rates ($r^2 = 0.97$, $p = 0.0085$, $n = 4$). This is not suggesting that the presence of finer sediments causes greater erosion rates, but it simply indicates that other factors are important in

controlling erosion, along with sediment type. Feagin et al. (2009) do suggest that a threshold bulk density ($0.9 \text{ g}\cdot\text{cm}^{-3}$) exists, above which edge erosion is regulated by the presence of coarse (sandy) sediments. If this threshold were to hold for Hog Island Bay marshes, it would suggest that erosion at HI may be controlled by its grain size, and that erosion at MM and CP, where bulk densities are less than $0.9 \text{ g}\cdot\text{cm}^{-3}$, may be controlled by some other condition besides sediment type. This might help to explain why undercutting was more prevalent at HI than at the other two sites; sandy sediment has been shown to be more susceptible to undercutting because it lacks the cohesiveness of finer grains (van Eerd 1985b, Allen 1989).

The marsh edge was much firmer than the interior locations at all of the marsh sites. Differences between the surface shear strengths of the edge and interior at each of the sites is most likely related to drainage of the marsh. The interior locations are more saturated because significant drainage of marsh ecosystems typically only occurs near the edge or creek banks or through crab burrows and cracks in the sediment (Bradley and Morris 1990). Crab burrows have been shown to be an important source of marsh drainage (e.g., Howes et al. 1981, Bertness 1985, Xin et al. 2009), and higher rates of burrowing near the seaward edge and creek banks help to explain the better drainage in these areas; less saturated, better drained sediments will have higher shear strengths.

Though poor drainage in the marsh interior is common across salt marshes, the interior substrate has been shown to be firmer than at the edge in some marshes (Bertness 1985). This has been found for both seaward edges at sheltered sites (Bertness 1985) and along creek banks (Teal 1958). However, to my knowledge, substrate hardness has never been documented for the marsh edge at exposed sites. This suggests that the firm marsh

edges found at the study sites may also be influenced by wave impact. As the edge is exposed to repeated wave attack, compaction of the surface sediments may occur, leading to the formation of harder substrate and greater shear strengths.

The only significant difference in sediment shear strength between edge sites existed between CP and MM. This may be due to both finer sediment at MM, as well as a dense upper layer of root mat at CP, which serves to strengthen the sediment. As dense root systems bind to sediment, they increase sediment shear strength and erosion resistance (Pestrong 1969). At CP, the firm surface substrate likely acts to stabilize the marsh against erosion.

Sediment shear strength along a scarp was greater near the surface than at lower locations. This is due to vegetation differences between the depths, as shear strength is higher in locations with denser root systems (Watts et al. 2003). Because root density and biomass typically decrease with depth (van Eerd 1985a), there is less root-related resistance to erosion at lower elevations on the scarp. The shear strength measurements within the upper root zone (0-5 cm) were probably underestimates because most of the sediment had been eroded from the belowground material; therefore, many of the measurements were taken in areas with exposed roots, which could more easily break under the torsional force of the shear vane than flat sediment surfaces. The difference in strengths between scarp locations indicates the importance of the top layer of belowground vegetation material to marsh stabilization, particularly in areas with a dense root mat, such as CP. The weaker sediment strength at lower scarp depths also suggests that this area is vulnerable to undercutting by wave activity (Schwimmer 2001), particularly in areas with sandy sediment, such as HI (van Eerd 1985b, Allen 1989).

Vegetation Characteristics

Feagin et al. (2009) have argued recently that vegetation is unlikely to be a primary control on edge erosion based on flume and field observations. However, the ability of belowground vegetation (roots and rhizomes) to stabilize marsh sediment and reduce erosion of the edge has been supported in other studies (e.g., Rosen 1980, van Eerdt 1985a, Allen 1989, Goodbred and Hine 1995). While aboveground vegetation is likely to have a lesser impact on erosion, studies have shown that it significantly reduces wave energies at the marsh edge (Knutson et al. 1982) and vegetation loss is thought to contribute to edge erosion in other areas (Day et al. 1998).

Results from aboveground and belowground sampling of *S. alterniflora* at the study sites suggest short-form *S. alterniflora* dominates at both the edge and interior locations of the marshes. Mean values for total belowground biomass, total aboveground biomass, stem density, and canopy height found at the three eroding sites were in agreement with those found in other short *S. alterniflora* marshes (Gross et al. 1991). The dominance of short *S. alterniflora* near the marsh edge of the study sites differs from observations at the edge of a New England salt marsh (Ellison et al. 1986), as well as typical findings along marsh creek banks (Valiela et al. 1978, Morris 1980), where the tall form of the grass is dominant. At the three eroding marshes, *S. alterniflora* remains in the short form throughout the landscape, with the exception of the band of tall *S. alterniflora* that forms along the interior creek banks (personal observations). It is beyond the scope of this research to explain why these unexpected vegetation distributions exist, however, sediment oxidation, nitrogen availability, interstitial salinity,

and pore-water drainage are all possible controls on *S. alterniflora* growth forms (Howes et al. 1986).

Biomass depth profiles from the sites generally showed a decrease in biomass with depth, with a couple of exceptions. This is consistent with depth profiles found for short *S. alterniflora* by Gallagher and Plumley (1979). The majority of belowground biomass is typically concentrated within the top 10-15 cm of the sediment for short-form *S. alterniflora* (Ellison et al. 1986, Gross et al. 1991). The top 5 cm at the edge of CP had significantly greater biomass than at any other location. Though it is unclear why this area contains a denser root mat, it helps to explain why the upper layer of the root mat appears to have a particularly large effect on the erosion mechanisms at this site.

Both aboveground biomass and vegetation height tended to be lower at the edges of CP and MM than at HI or any interior locations. In many areas along the edge of the two sites, the marsh was devoid of vegetation (up to 1-2 m in some areas on MM). Wave impact and grazing by *S. reticulatum* and *L. irrorata* have all been suggested as possible causes of vegetation die-off near the marsh edge (Day et al. 1998, Holdredge et al. 2009, Silliman and Bertness 2002). This loss of vegetation near the edge is significant to marsh stability because over fifty percent of wave energy may be dissipated within 2.5 m of the edge when *S. alterniflora* is present (Knutson et al. 1982). While aboveground vegetation does play an important role in reducing wave energy, it has less of an effect on edge erosion than belowground biomass. This is because belowground material has a direct control on the strength of the edge and most of the erosive wave energy is focused below the sediment surface.

The tensile strength of roots and rhizomes in the marshes was strongly correlated to their diameter, which is common among plant species (Tosi 2007). The strengths of the rhizomes were significantly less at MM than at CP and HI. However, analysis of the diameters of the rhizomes indicates that the rhizomes tested at MM were significantly thinner than those at CP and HI ($df = 2$, $SS = 0.1048$, $F = 9.25$, $p = 0.001$). Since rhizome strengths are affected by diameter, the difference in diameters between the sites likely explains the differences in strengths observed. This also indicates that rhizomes at the edge of MM tend to be thinner than those at the other marshes, which might suggest weaker root reinforcement of the sediment (van Eerd 1985a).

Tensile strengths of roots and rhizomes were higher in the marsh interior than at the edge. This is somewhat surprising and not well understood; however, one explanation might be related to live and dead material. Live and dead belowground material was not differentiated while sampling strengths. Since live roots and rhizomes tend to be turgid, and dead ones more flaccid (Darby and Turner 2008), dead material is weaker and more susceptible to breakage. If there is a greater proportion of dead material at the edge, possibly due to unsuitable conditions for new growth, then this could explain the location differences between root/rhizome tensile strengths. Although there may be differences in the strengths of individual roots and rhizomes between the marsh edge and interior, root density and belowground biomass likely serve as better measurements of the actual strength of the root mat and its ability to resist erosion (van Eerd 1985a).

Crab Burrows

Crab trappings indicated that *Uca pugnax* was the most abundant crab species in the studied marshes. Because traps were only set out for roughly twenty-four hours, it did not seem appropriate to run statistics on crab abundance. However, the results supported visual observations from the marshes, in that crabs appeared to be present in significantly lower numbers at HI than at the other two sites. *U. pugilator* was not the dominant crab species on HI, despite its sandy substrate. There is some evidence that suggests that *U. pugilator* populations are reduced in areas where *U. pugnax* are also present, even in marshes with sandy sediments (Teal 1958). This is thought to be related to the ability of *U. pugnax* to out-compete *U. pugilator* for space and resources. Because sand is not the preferred substrate of *U. pugnax* (Teal 1958), it explains its lower abundance at HI than at MM and CP. Both *Sesarma reticulatum* and *Panopeus herbstii* were found in traps on HI; this was unexpected considering the relative lack of their distinctive burrow structures along the marsh edge (Allen and Curran 1974).

Mud fiddler abundances were much higher at CP and MM than at HI. *U. pugnax* was the only fiddler species found at either marsh; this was expected due to the muddy substrate at these sites (Montague 1980). *S. reticulatum* inhabited both sites, though its relative abundance remains unclear, and *P. herbstii* was also present near the edge at MM. The presence of these species validated the findings of large burrow structures formed in the muddy substrate along the marsh edge (Edwards and Frey 1977). The lack of *P. herbstii* in traps at CP does not necessarily preclude its presence at the site. A larger-scale assessment is needed to more accurately quantify crab species populations

at the marshes in Hog Island Bay than that provided here. However, for the purposes of this study, the current results are sufficient to interpret burrowing activities at the sites.

Crab burrow densities were greater at the edge of MM than at the edges of CP and HI. The only spatial difference within the marshes occurred at CP, where densities were higher at the interior than the edge. Most density measurements fell within the ranges reported for fiddler crabs in salt marshes in previous studies (Basan and Frey 1977, Krebs and Valiela 1978, Bertness and Miller 1984, McCraith et al. 2003). Burrow densities were overestimated in areas where *S. reticulatum* burrows were present due to multiple surface openings associated with individual burrows. The low densities at HI were related to the site's lower crab abundance and sandier substrate, as previously discussed. Differences in densities at the edge and interior of CP was most likely the result of the dense root mat at the edge of this marsh; *U. pugnax* have greater difficulty burrowing in areas with highly dense root mats and hard substratum, as was found along the edge of CP (Bertness and Miller 1984). The upper layer of the root mat was less dense near the edge of MM, which provided a more suitable location for fiddler burrowing. While burrow densities were lower at the edge of CP, large burrow structures were still present there, as evident from burrow casts. This indicates that there was greater variability in burrow densities near the edge of CP compared to MM, where burrows were more uniformly abundant.

Burrow diameters and burrow coverage were greater at CP and MM than at HI. Again, this was related to the nature of the sandy substrate at HI. Despite low densities at the edge of CP, burrow coverage was fairly high due to the large burrow diameters there. Burrow coverage was very high at the edge of MM, where burrows were a prevalent

physical feature. Burrow diameters were greater at the marsh edge than the interior, and diameters were largest near the edges of CP and MM, due largely to the presence of *S. reticulatum* burrows; the openings of these burrows have been measured to range between 2.5 and 4 cm (Bertness et al. 2009).

Statistics were not performed on burrow volumes due to sampling methods. However, it is clear that burrow structures may be considerably larger at the edge of CP and MM than the edge of HI or the interior of any site. Burrow forms were much different at the edges of CP and MM compared with the other sample locations. These burrows were large, had multiple chambers, and had morphologies consistent with those communally inhabited by *S. reticulatum* and *P. herbstii* (Allen and Curran 1974). At the other sampling locations, burrow forms primarily consisted of individual *U. pugnax* burrows.

Burrow sampling results indicate that *S. reticulatum* burrows were common along the edge of MM and CP, while *U. pugnax* burrows dominated in other areas. The large intersecting, communal burrow structures of *S. reticulatum*, *P. herbstii*, and *U. pugnax* are a common feature along salt marsh edges (Allen and Curran 1974). These burrow structures are thought to influence erosion and slumping along marsh edges and creek banks in several other locations (Allen and Curran 1974, Edwards and Frey 1977, Bertness et al. 2009). This form of slumping and block detachment also appeared to be the primary mode of edge erosion at MM. The edge at MM was more susceptible to this form of erosion than that of CP because it possessed finer sediment and a less dense root mat. Therefore, conditions were more hospitable for widespread burrowing at MM, and as a result, bioerosion was common.

Mussel and Snail Densities

Ribbed mussels tended to be concentrated at higher densities at the marsh edge. This pattern is typical of *G. demissa* distributions in salt marshes along the East Coast (Franz 2001). *G. demissa* densities at the study sites were generally greater than those found in salt marshes in Georgia and North Carolina (Kuenzler 1961, Stiven and Gardner 1992), but substantially less than those found in marshes in Rhode Island and New York (Bertness 1984, Franz 2001). The measured densities were underestimated because only mussels observed at the sediment surface were counted. Ribbed mussels often live in dense aggregations, in which multiple individuals may live on top of one another (Bertness 1984). *G. demissa* populations were significantly greater at the edge of HI than the edge of CP. Though not statistically different, the mean density at the edge of HI was almost twice that of the edge at MM. It could be argued that a preference for sandy substrate might be the reason for larger densities at HI, considering similarly high numbers were found at the edge of FP.

Ribbed mussels in high abundance have the potential to reduce edge erosion and aid in seaward expansion and growth of the marsh (Bertness 1984). This is because the attachment of these bivalves to the marsh substrate provides greater sediment strength and stability. In marshes where mussels are at relatively high abundances, such as HI, these individuals may serve an influential role in controlling edge erosion. Dense aggregations may behave similarly to a dense root mat (Schwimmer 2001), such as that at CP, and act as a stabilizing mechanism for the upper layer of substrate. The presence of

G. demissa will not necessarily prevent erosion, but it may alter the mechanisms by which erosion occurs.

Periwinkle snail densities at the study sites were within the range of those found at most southern marsh sites reported in Silliman and Zieman (2001). It has been argued that *L. irrorata* have the ability to turn vegetated sections of marsh flats into barren mudflats through their grazing habits (Silliman and Bertness 2002, Silliman et al. 2005). However, periwinkle densities at the Hog Island Bay sites were much lower than those found to cause large-scale die-off, and therefore, likely have little effect on the erosion of the marsh edge.

Interpreting Fowling Point

Fowling Point differed from the other marsh sites in that it had a fairly stable edge and did not experience the high rates of erosion of the other three sites. Long-term analysis indicated that the marsh edge at FP eroded at a mean rate of $0.02 \text{ m}\cdot\text{yr}^{-1}$ (1957-2007), significantly less than that of any of the other marshes. This negligible edge movement (1 m over fifty years) is predominately due to a gently-sloping morphology and low wave energy near the edge. The low wave energy at FP is due to the presence of a large mudflat fronting the marsh, which prevents large waves from forming over the comparatively shallow water (Fagherazzi et al. 2006). Therefore, this marsh is not susceptible to the erosion processes experienced at the other three study sites.

One of the oddities at FP, when compared to other marshes in the lagoon, is its sediment type. FP had the coarsest sediment of all the sites, with a median grain size in the medium sand range. This defies expectations based on the findings of Lawson

(2004). Sediment within Hog Island Bay typically becomes finer with distance from the inlet towards the mainland. Since FP is a mainland marsh, with adjacent mudflats consisting of very fine sand (Lawson 2004), it is unusual that the marsh is dominated by coarser sediment. There is little input of sediment from fluvial sources into Hog Island Bay, and therefore most sediment is reworked, transported, and deposited from locations within the bay, itself. This suggests that the sediment observed might be a preexisting feature of the marsh. The sediment type, along with the variability in surface elevations throughout the marsh, supports the findings of Oertel and Woo (1994), that this is a hammock marsh.

Of the four sites studied, *S. alterniflora* was the most productive at FP. FP had the tallest vegetation canopy and the greatest shoot:root ratio. This indicates greater growth of aboveground vegetation at the marsh than at the other three sites. It is difficult to interpret why *S. alterniflora* performed better at FP without having measurements of specific edaphic conditions, such as nutrient levels, drainage, oxidation and redox potential, and salinity (Howes et al. 1986). Whether this was the result of the marsh's stable position, flooding frequency, sediment texture, or some other edaphic condition cannot be fully grasped based on the data collected during sampling. However, it was evident that vegetation at this site behaved differently than at the eroding sites; whether this is somehow related to larger-scale hydrologic or erosion processes needs to be determined.

Impacts on Erosion

Marsh characteristics may vary significantly between marshes of the same coastal lagoon, and the individual properties of the marsh edge can have a large impact on erosion. At each of the three eroding sites, erosion appeared to be facilitated by different properties of the edge. At Chimney Pole, the stability of the marsh was controlled by the upper layer of the root mat. The removal of this dense, firm substrate appeared to initiate the erosion and retreat of the edge. On the other hand, erosion at Matulakin Marsh appeared to be primarily controlled by the burrowing activities of crabs, namely *S. reticulatum* and *P. herbstii*. The widespread burrowing was facilitated by the fine sediment and comparatively weaker root mat at the site, leading to slumping and block detachment along the edge. Edge erosion at Hog Island was largely affected by the sandy substrate of the marsh, which allowed for greater undercutting of the scarp. The ultimate driving force behind these erosion processes was wave contact, which provided the energy necessary to remove sediment and material from the edge. When marshes are shielded from high wave energies, as was the case with Fowling Point, the morphology of the edge is transformed and scarp erosion becomes less prevalent.

CHAPTER 4: MECHANISMS OF MARSH EDGE EROSION

Previously Observed Mechanisms of Edge Erosion

It is well-established that wind-generated waves are the primary cause of marsh edge erosion in coastal bays and estuaries. Most marsh shoreline studies have focused on the trends, rates, and possible causes of erosion, and often their relationship to sea-level rise (e.g., Finkelstein and Hardaway 1988, Reed 1988, Downs et al. 1994, van der Wal and Pye 2004). Few studies, however, have examined the specific mechanisms of erosion along marsh boundaries, and even fewer have compared mechanisms between marshes within a single system. One of the objectives of this study was to compare the physical mechanisms of erosion at three eroding marshes within Hog Island Bay.

Though there may be several mechanisms of marsh edge erosion, relatively few have been discussed in detail in the literature. Schwimmer (2001) observed three styles of edge erosion at marshes in Rehoboth Bay, Delaware: cleft and neck formation, neck cut-off, and undercutting. Clefts and necks form an undulating pattern along the marsh edge, with clefts being V-shaped areas cut into the marsh shoreline, and necks being the shoreward area of marsh between clefts. Neck cut-off occurs when the neck is separated from the rest of the marsh at its base, resulting in rapid erosion of the isolated material. Undercutting is a common process along marsh edges, whereby the underlying sediment is more rapidly eroded than the dense, overlying root mat. This eventually leads to toppling of the root mat (beam failure) and an overall retreat of the edge; marshes with sandy sediment are particularly susceptible to this type of erosion due to the less cohesive nature of coarser sediments (van Eerd 1985b, Allen 1989). In marshes with relatively tall, muddy cliffs, such as those of the Severn Estuary (UK), rotational slipping may be

common (Allen 1989). Erosion at a marsh in Venice Lagoon occurred in two phases, whereby the aboveground vegetation was initially eroded from the edge through wave activity, followed by erosion of the underlying material (Day et al. 1998). Bioturbation, particularly by crabs, has also been shown to have an important influence on erosion. The burrowing and reworking of sediment by *S. reticulatum* and *P. herbstii* near marsh edges and creek banks often leads to sediment slumping and erosion in these areas (Edwards and Frey 1977, Bertness et al. 2009).

In this study, three eroding marshes in Hog Island Bay were examined to determine the mechanisms by which edge erosion occurs. It was discovered that the erosional processes differed between the three sites, despite their proximity within a single lagoon system. Bioerosion through *S. reticulatum* burrowing dominated the edge at Matulakin Marsh, which has been observed at other marshes on the Atlantic Coast (Edwards and Frey 1977, Bertness et al. 2009). Chimney Pole primarily experienced erosion through root scalping, whereby the upper root zone was removed from the marsh surface, and was followed by retreat of the underlying sediment. This form of erosion has not been previously reported for marshes outside of Hog Island Bay. The Hog Island site experienced two distinct forms of erosion. The southern portion of the site was dominated by undercutting, while root scalping and terrace formation persisted at the northern region. This form of root scalping differs from that of Chimney Pole in that it occurs over a much longer time period. A more detailed explanation of each of these erosion mechanisms follows.

Erosion Mechanisms in Hog Island Bay

Matulakin Marsh

The marsh edge has retreated at a rapid rate at Matulakin Marsh. Burrows were prevalent at the site, with high densities (200 m^{-2}) and coverage ($770 \text{ cm}^2 \cdot \text{m}^{-2}$) and large diameters (16 mm) and volumes. Erosion of the marsh's vertical scarp was facilitated by this widespread crab burrowing near the marsh edge by *S. reticulatum*, *P. herbstii*, and *U. pugnax* (Figure 4.1a). Matulakin Marsh had finer sediment (median grain size: $15 \mu\text{m}$) and a weaker upper root layer (top 5 cm: $2100 \text{ g} \cdot \text{m}^{-2}$), when compared with Chimney Pole, which caused the site to be more susceptible to sediment reworking and destabilization through burrowing. As water flowed through the large burrow structures during ebb and flood tides, at times enhanced by wave activity, cracks formed on the marsh surface; the orientations of the cracks were controlled by the paths of burrow structures (Figure 4.1b), which have also been observed along creek banks in Georgia (Edwards and Frey 1977). Over time, the cracks widened and deepened, creating distinct blocks that began to separate from the marsh (Figure 4.1c). Eventually these blocks were completely detached from the marsh and slumped onto the mudflat (Figure 4.1d). This likely occurred through the combination of wave attack and gravitational slipping. Waves appeared to be of critical importance both in increasing the depth and length of the cracks and ultimately removing these sections of marsh from the edge. Detachment of the block reestablished a vertical edge and the process could continue, provided active burrowing and sufficient wave exposure.

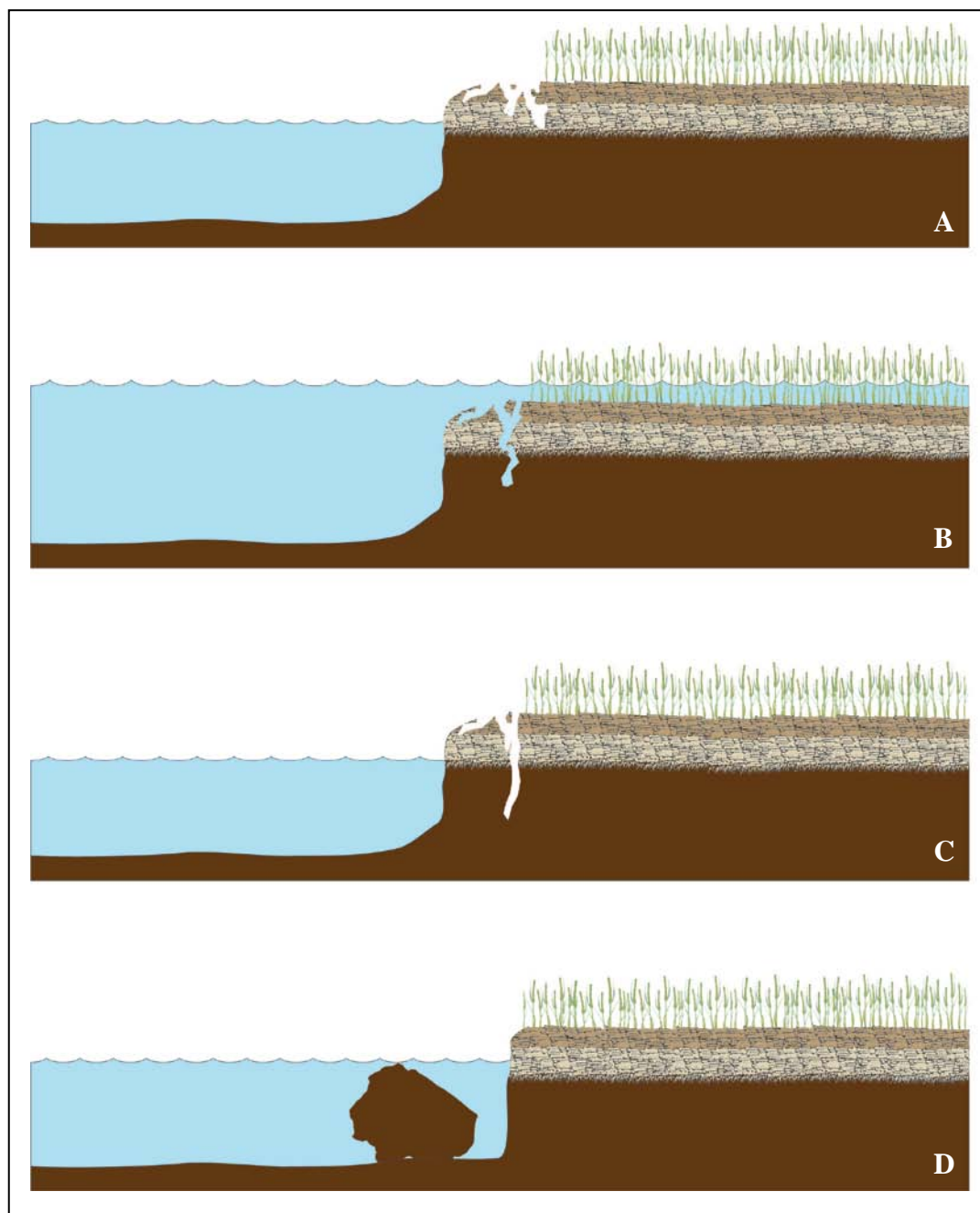


Figure 4.1. Schematic diagram of typical erosion process at Matulakin Marsh, whereby crab burrows facilitate block detachment and slumping.

Chimney Pole

At the Chimney Pole site, a different mechanism of edge erosion dominated. While large burrows were also present near the edge at CP (diameter: 18 mm, volume: $>10,000 \text{ cm}^3 \cdot \text{m}^{-2}$), they were not as widespread and abundant (density: 54 m^{-2}) as those found at MM. This, combined with the dense upper layer of root mat (top 5 cm: $3100 \text{ g} \cdot \text{m}^{-2}$) and relatively high surface shear strength ($0.4 \text{ kg} \cdot \text{cm}^{-2}$) at the site, provided greater resistance against bioerosion than at MM. The top 5 cm of the root zone appeared to have a significant control on erosion at CP, as this dense root mat served to stabilize the marsh edge (Figure 4.2a). As waves impacted the edge, they eventually penetrated the root mat through areas of weakness, such as large, interconnected burrows (Figure 4.2b). At some point, the persistent energy exerted by the waves removed the upper layer of substrate (Figure 4.2c), in a form of root scalping (Fagherazzi et al. 2010); the removed material was either transported into the marsh interior or slumped onto the fronting mudflat. This was followed by the gradual retreat of the exposed, underlying sediment (Figure 4.2d-e).

Though the rates of erosion may have varied spatially along the marsh edge, this process, whereby the upper root zone was initially removed from the marsh, persisted throughout the sampling location. The scarp did not appear to experience significant erosion via other mechanisms, such as undercutting, prior to or after the removal of the vegetation layer. This is likely related to both the cohesion of the sediment (median grain size: $49 \mu\text{m}$), which makes undercutting more difficult, and the slope of the scarp, which tended to be gentler than those found at MM and HI. The upper root mat served as a firm shield that stabilized the marsh surface. When this was removed, the weaker underlying sediment was exposed not only to horizontal erosion, but also to vertical erosion.

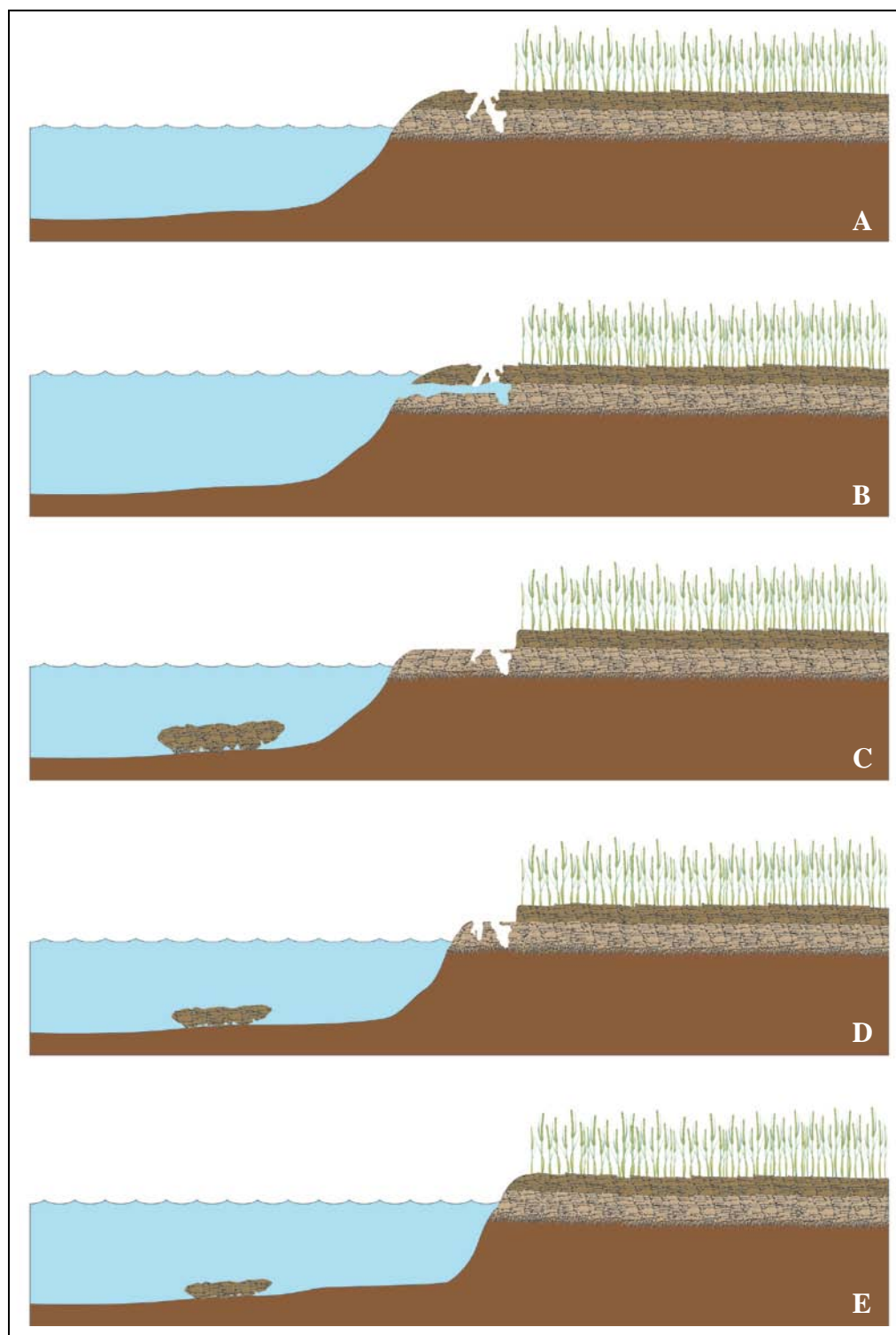


Figure 4.2. Schematic diagram of typical erosion process at Chimney Pole, whereby root scalping is followed by gradual erosion of the underlying sediment.

Observational Study at Chimney Pole

Erosion pins and semiannual surveys provide reliable estimates of short-term erosion rates along the marsh edge; however, they do not provide information about the specific conditions or processes under which erosion occurs. For that, a more detailed assessment is required. There are several logistical challenges associated with performing detailed temporal analyses at the marsh sites (i.e. time, distance, and weather) and erosion events are more likely to occur during poor weather conditions when access to the marshes is not feasible. Therefore, daily or weekly on-site observations of the marsh edge are impractical. In an attempt to bypass these logistical problems and still obtain high-frequency, long-term observations of the marsh edge, a network video camera was installed at Chimney Pole. Because there are several monetary, logistical, and time constraints associated with installing and monitoring a video camera on a marsh, a camera was only installed on one of the erosional sites. Chimney Pole was a logical choice due to both the mechanism of erosion present there and its proximity to a wireless access point tower.

A Vivotek IP7161 network camera (Vivotek, Chung-Ho, Taiwan) was installed at a fixed location near the edge of Chimney Pole in November 2009. The camera is powered by a solar panel and deep cycle marine battery, with a digital timer used to control hours of operation. The camera runs as a wireless network video camera (“webcam”), whereby a still image is taken once every thirty minutes, transmitted from the camera (through a radio bridge and panel antenna) to a nearby Wi-Fi access station (Machipongo Station) at the northern end of Hog Island (Porter and Smith 2008). From there, the image is sent to an FTP server in Charlottesville (VA), where it is stored. A live-feed of the camera can also be accessed over the internet. In the event that the

wireless network becomes unavailable, images are also stored directly onto a Secure Digital (SD) memory card in the camera.

The camera sits atop a stand at a height, roughly, 2.5 m above the marsh surface; a separate stand holds the solar panel and battery (Appendix 4). When the camera stand was initially installed in November 2009, it was 6.5-7 m from the marsh edge. It is focused onto a fixed section of the marsh edge, covering approximately 4 m. Two reference poles were placed at the marsh boundary 3.2 m apart on the day of installation. The camera operated fairly consistently from November 19, 2009 until January 28, 2010, when it malfunctioned. A leak in the weatherproof housing allowed water to infiltrate the camera causing the malfunction; this issue was eventually resolved and the camera became operational again on April 3, 2010.

Within the first week of deployment, a significant erosion event occurred at the marsh edge. Little change had occurred to the marsh surface between November 19 (the day of installation) and November 26. However, the first image taken on the morning of November 27 indicated that a portion of the root mat had been removed from the marsh edge at some point during the previous night or in the early morning (Figure 4.3a-b). Images from later that day suggest that rough weather conditions (i.e. waves) were present in the bay around that time (Figure 4.3c). Wind speeds (maximum: $8 \text{ m}\cdot\text{s}^{-1}$) and barometric pressure (minimum: 1000.6 mbar) from this period suggest foul weather and the possible presence of a moderate storm (Figure 4.4). Edge erosion events are often associated with storms (Day et al. 1998, Schwimmer 2001); however, they are more likely to occur during moderate storm conditions, when waves directly impact the edge (Wray et al. 1995). This is in contrast to high energy events, such as hurricanes and

Nor'easters, during which high water levels associated with storm surge prevent direct impact of waves on the marsh edge (Goodbred and Hine 1995).

After the root mat was removed from the surface of the edge, the underlying material began to slowly erode over time (Figure 4.3d-e). The camera malfunctioned on January 28, was repaired, and redeployed on April 3, upon which it was evident that the underlying edge material had largely eroded (Figure 4.3f). Unfortunately, no images were recorded during this time period, so it is not known whether the erosion occurred gradually or during a single large event. The edge remained fairly stable over the following months (Figure 4.3g-h). By August, the edge had eroded over 2 m at the southern reference marker (left pole in images). Erosion was triggered by the removal of the root mat nine months prior and was followed by the subsequent retreat of the remaining scarp.

Hog Island

While a single erosion mechanism tended to dominate the marsh edges at CP and MM, there appeared to be two distinct processes occurring at Hog Island. The southern portion of the site primarily experienced erosion through undercutting and root mat toppling. This process occurred as waves acted on the fairly vertical scarp (Figure 4.5a) and began to undercut the root mat and erode the underlying sandy sediment (median grain size: 130 μm) (Figure 4.5b). As undercutting continued, the weight of the overlying root zone, consisting of dense roots (total biomass: 5800 $\text{g}\cdot\text{m}^{-2}$) and ribbed mussels (400 m^{-2}), increased until the root mat began to bend downward and tension

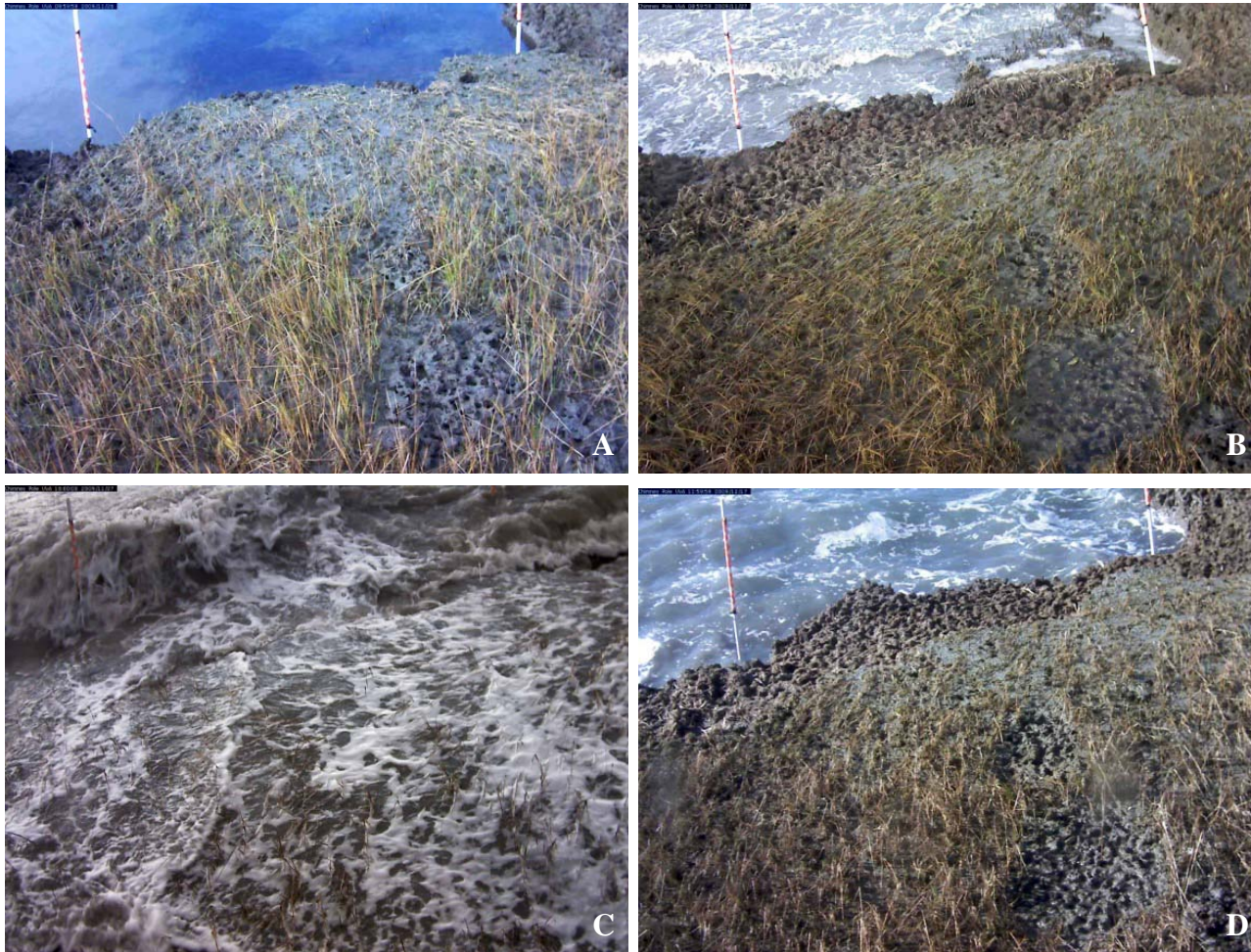


Figure 4.3. Images of the marsh edge at Chimney Pole on 11/26/09 at 10:00 AM (A), 11/27/09 at 9:00 AM (B), 11/27/09 at 4:00 PM (C), and 12/17/09 at 12:00 PM (D). Note the removal of the root mat between A and B.

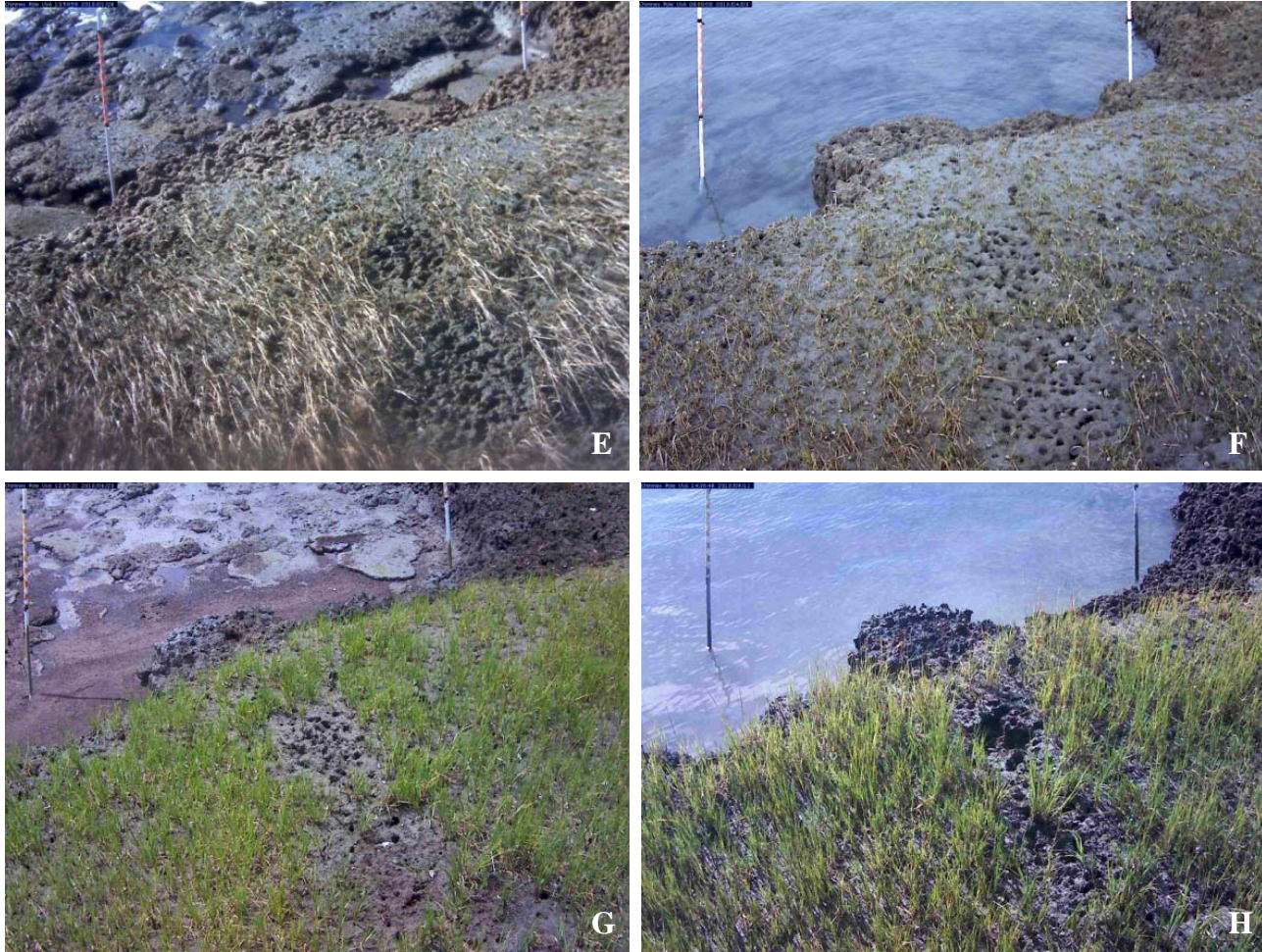


Figure 4.3 (cont.). Images of the marsh edge at Chimney Pole on 1/28/10 at 2:00 PM (E), 4/3/10 at 8:00 AM (F), 6/23/10 at 12:00 PM (G), and 9/11/10 at 2:30 PM (H).

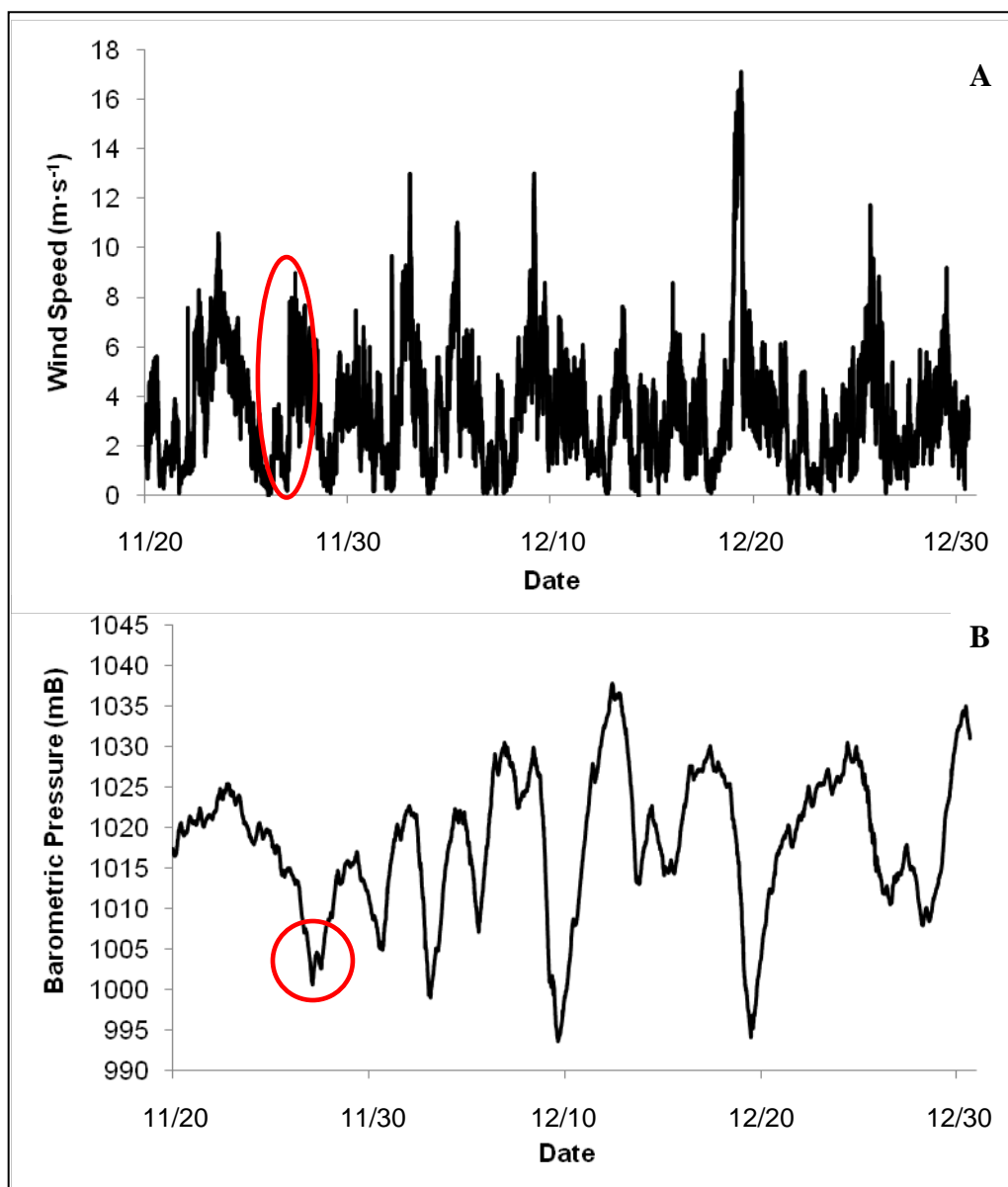


Figure 4.4. Wind speed (A) and barometric pressure (B) near Hog Island Bay from November 20, 2009 to December 30, 2009. Red circles indicate conditions during the initial erosion event.

cracks formed (Figure 4.5c-d). Eventually the overlying block broke from the marsh and fell onto the mudflat (Figure 4.5e). This type of beam failure is common on both salt marsh edges (van Eerd 1985b, Allen 1989, Schwimmer 2001) and river banks (Thorne and Tovey 1981, Pizzuto 1984). This process may continue once the detached block is eroded (Thorne and Tovey 1981, van Eerd 1985b). Unlike the mudflats at CP and MM, there was little evidence of slumped or toppled marsh material on the tidal flats at HI; this indicates that failed blocks erode fairly quickly here, likely due to higher sand content.

At the northern end of the study site, small terraces (5-6 m) had developed along the edge. This happened as the result of root scalping, whereby waves remove the root mat near the marsh edge (Figure 4.6a-b), leading to the formation of distinct step-like terraces along the edge. This process occurred more slowly than the other mechanisms previously discussed, which allowed *S. alterniflora* to begin to grow on the lower terrace (Figure 4.6c). This can have two possible consequences. The first is that expansion of *S. alterniflora* on the lower terrace can increase sediment deposition and vertical accretion of the marsh surface, allowing marsh rebuilding and growth in front of the eroded edge (Figure 4.6d, van de Koppel et al. 2005). The second is that the combined effects of wave attack on the sandy sediment and sea-level rise on vegetation growth will render marsh building unsustainable. As a result, the lower terrace may be eroded over time, allowing the root scalping to continue (Figure 4.6e). A terrace or elevated tidal flat was present in several aerial photographs at the site, but the edge had clearly retreated over time. Therefore, the latter mechanism of erosion is more probable, whereby the shape of the shoreline remains fairly consistent, but retreats landward over time. Marsh properties

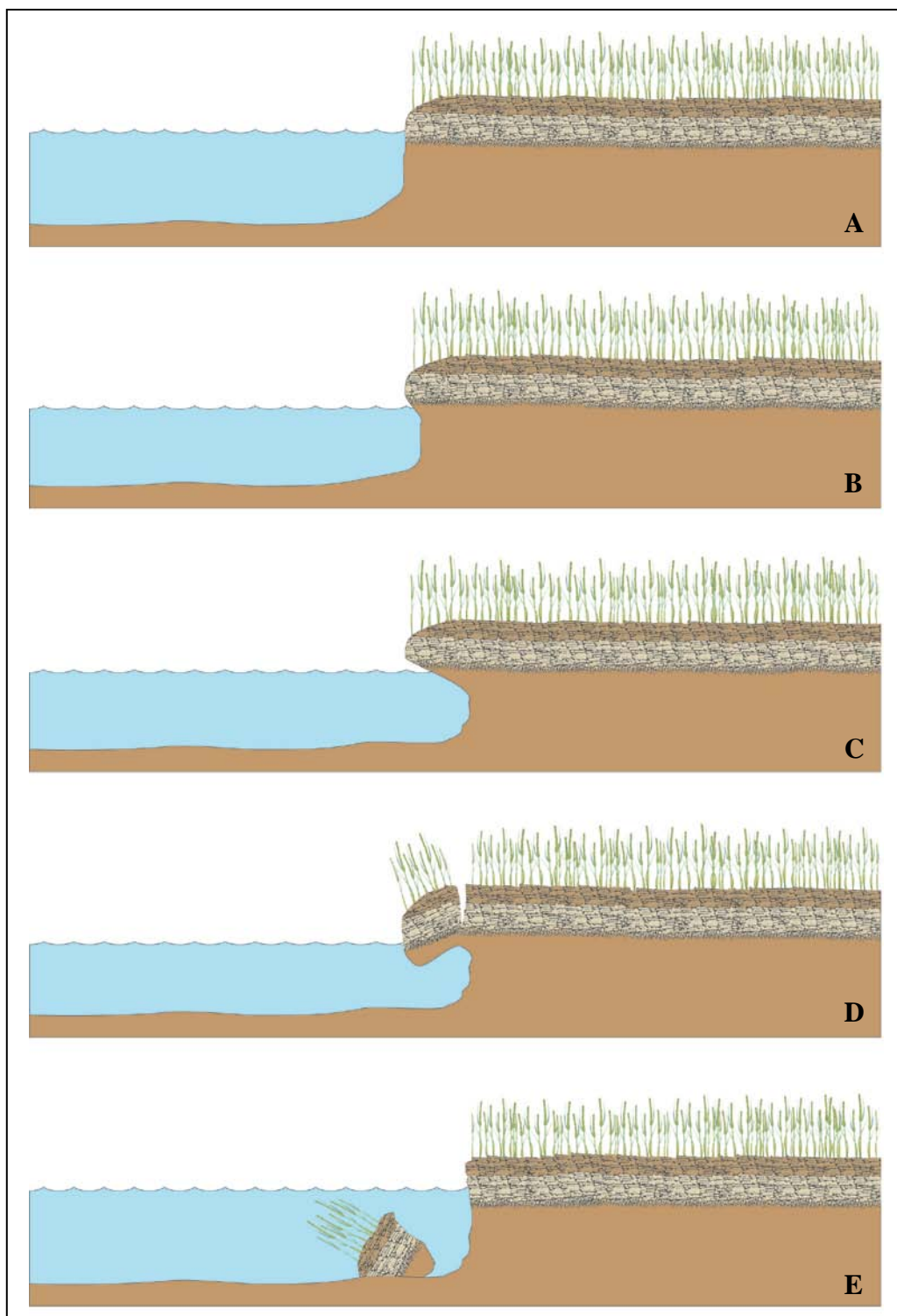


Figure 4.5. Schematic diagram of typical erosion process at the southern end of the Hog Island site, whereby undercutting and root mat toppling dominates.

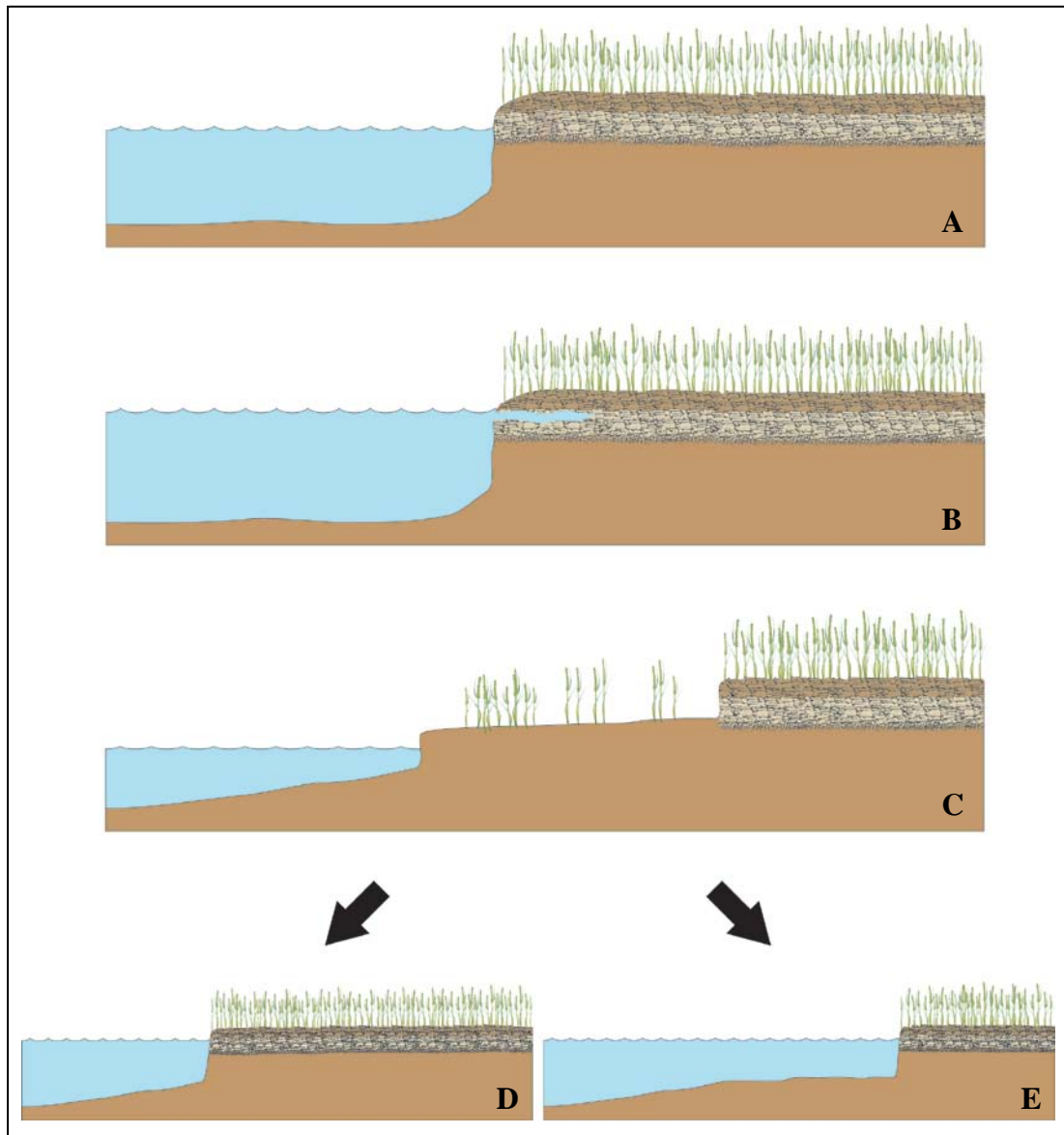


Figure 4.6. Schematic diagram of typical erosion process at the northern end of the Hog Island site, whereby root scalping and terracing dominate.

at the HI site were compared to determine if any spatial differences existed between the northern and southern edge that would account for the different patterns of erosion observed (Appendix 5). For the most part, no trends existed along the marsh edge. The only property to exhibit a noticeable spatial trend was the shear strength near the top of the scarp, which tended to be greater than $0.2 \text{ kg}\cdot\text{cm}^{-2}$ at the southern locations and less than $0.2 \text{ kg}\cdot\text{cm}^{-2}$ at the northern areas. This might indicate a firmer vegetation layer farther south, which could help to explain differences between undercutting and root scalping. Belowground cores were not taken along the length of the terrace, so it is difficult to quantitatively support this. Regardless, terrace formation has occurred at the site for at least twenty years (1989-present) and therefore, is more likely to be controlled by the interaction between the local bathymetry and wave impact than any spatial differences in sediment or ecological properties along the edge.

Mechanistic Significance

The results of this study indicate that erosional mechanisms varied between marsh sites within a single lagoon system, though the rates of erosion were high at each ($0.98 - 1.62 \text{ m}\cdot\text{yr}^{-1}$). Mechanisms may also vary within close proximity at an individual marsh, such as those at Hog Island. This is likely due to the differences in physical properties of the marsh edge observed at each of the sites, as well as differences in bathymetry, topography, orientation, and wave climate between the sites (Feagin et al. 2009). Salt marshes are often highly heterogeneous and complex, with significant variability in physical characteristics at an individual, local (i.e. lagoon), and regional scale (Phillips

1986b). For this reason, within-site or within-system comparisons can offer insights into patterns of erosion.

Future Sustainability

Marsh edges eroded rapidly at three of the studied marshes in Hog Island Bay; this trend has likely occurred at other sites in the VCR, as well. Between 1852 and 1968, there was a 16% loss of marsh land within the VCR lagoons (Knowlton 1971). Marsh loss is expected to increase as sea-levels rise, particularly at marsh islands and mid-lagoon marshes, where inorganic sediment sources for accretion may be scarcer (Hayden et al. 1991). With a predicted increase in relative sea-levels, water depths within Hog Island Bay will increase, leading to the formation of larger waves and potentially greater erosion rates (Mariotti et al. 2010). If the frequency of storms continues to increase on the Virginia coast, as has occurred over the past century (Hayden and Hayden 2003), it also has the potential to increase erosion rates due to higher wind speeds and larger waves that are associated with storm events.

Sea-level rise may have the added effect of interior marsh loss through ponding and creek widening, as has already been found in other mid-Atlantic marshes (Phillips 1986a, Downs et al. 1994, Wray et al. 1995), as well as throughout the Gulf Coast (e.g., Reed 1990, DeLaune et al. 1994). These interior erosion processes are not evident at any of the studied marshes; however, Kastler and Wiberg (1996) found that sedimentation rates on Chimney Pole did not offset rates of sea-level rise. Sediment Elevation Tables (SETs) are currently installed at two of the study sites, Chimney Pole and Fowling Point, to determine surface accretion rates on the marshes. These should help to determine if

the marshes are accreting sufficient material to keep pace with RSLR. If interior marsh loss begins, along with an acceleration of edge retreat, many of the marshes in the VCR will be in serious jeopardy. The sustainability of backbarrier marshes is difficult to predict based on the highly variable nature of these systems due to overwash (Hayden et al. 1991, Tyler and Zieman 1999). However, the vulnerability of the marsh islands and mid-lagoon marshes is much more certain.

CONCLUSIONS

Results from this study indicate that three of the marsh sites in Hog Island Bay experienced rapid edge erosion between 1957 and 2007, with rates near or greater than 1 m·yr⁻¹. Erosion rates differed significantly between the sites, with Matulakin Marsh experiencing the greatest erosion, followed by Chimney Pole and Hog Island. While average rates were high at each site, results indicated that erosion varied greatly across the length of the marsh edge. This variability is the result of differences in wave exposure, local bathymetry, and internal properties, such as sediment, vegetation, and invertebrate characteristics along the marsh edge. Unlike the other three marshes, the edge at Fowling Point remained relatively stable over the fifty-year period of the study. This is primarily due to the large mudflat fronting this mainland marsh, which protects the edge from the impact of high wave energy.

Hydrodynamic modeling results indicated that wave power alone cannot explain differences in erosion rates between the marshes. This suggests that other properties of the marsh edge influence erosion at the sites. Marsh edge characteristics showed significant differences between study sites, and these characteristics may have different effects on erosion rates at each of the sites. The mechanisms by which edge erosion occurred also varied between sites. At Matulakin Marsh, block detachment and slumping, facilitated by the burrowing of *S. reticulatum* and *P. herbstii*, was persistent along the edge. Erosion at Chimney Pole was initiated by the removal of the upper root mat and was followed by the gradual erosion of the underlying sediment. Two processes were evident at Hog Island. At the southern end of the sampling location, undercutting of the scarp and root mat toppling dominated, while at the northern portion of the site, root

scalping led to the formation of large terraces, which erode over time. These results indicate that within a single lagoon system, the characteristics of the marsh edge can vary greatly between marsh sites, and consequently, the mechanisms of edge erosion may differ between marshes.

Unlike in some previous studies where a single factor, such as waves (Day et al. 1998, Schwimmer 2001) or sediment type (Feagin et al. 2009), was considered to primarily control erosion rates, erosion at the marshes in this study was due to the complex interactions between different characteristics of the edge. This indicates that in lagoon systems where marshes are highly heterogeneous, no single factor can completely explain erosion processes. Instead, it is the interactions between sediment properties, vegetation structure, invertebrate behavior and abundance, edge morphology, and waves that determine the mechanism by which the marsh edge erodes. Differences in wave energy between marsh sites likely become more important in controlling erosion rates in more homogeneous systems, where properties and mechanisms of erosion along the edge are similar between sites.

This study has indicated that there are certain conditions along the marsh edge that affect the type of erosion experienced at a particular marsh site. This can be useful in determining what processes may potentially dominate the edge at other marsh sites within the VCR, as well as in other coastal systems. Marshes consisting of fine sediment ($< 62.5 \mu\text{m}$) and widespread burrowing near the edge by *S. reticulatum* and *P. herbstii* are likely to experience erosion through block detachment and slumping. On the other hand, undercutting and root mat toppling is most likely to be found along the edge at sandy marshes ($> 125 \mu\text{m}$) with vertical scarps. Root scalping, such as that observed at

Chimney Pole, may be found along marsh edges with a strong, dense upper root zone ($> 3000 \text{ g}\cdot\text{m}^{-2}$ in top 5 cm). Edges with gentler slopes are more likely to observe this form of erosion because more of the wave energy is directed at the root zone, unlike vertical scarps that are more susceptible to undercutting. It is very possible that these mechanisms of erosion exist along marsh edges in other systems, and the results of this study provide insight into identifying these processes.

Sea-level rise and an increase in storm frequencies are likely to increase marsh edge erosion in Hog Island Bay. Since the bay is depth-limited, an increase in water depth through RSLR will lead to larger wave formation and greater wave energy at the edges. Erosion events are also strongly associated with storms due to their effects on increasing wave energy, and therefore, edge erosion is expected to increase if the frequency of storms continues to rise. If greater edge erosion is in conjunction with interior marsh loss through ponding and creek widening, as has been reported for many marshes in the southern US, then the future sustainability of these vital ecosystems will be in doubt.

REFERENCES

- Allen, E. A. and H. A. Curran. 1974. Biogenic sedimentary structures produced by crabs in lagoon margin and salt marsh environments near Beaufort, North Carolina. *Journal of Sedimentary Petrology* 44:538-548.
- Allen, J. R. L. 1989. Evolution of salt-marsh cliffs in muddy and sandy systems: a qualitative comparison of British west-coast estuaries. *Earth Surface Processes and Landforms* 14:85-92.
- Basan, P. B. and R. W. Frey. 1977. Actual-palaeontology and neoichnology of salt marshes near Sapelo Island, Georgia. *Geological Journal* (Special Issue) 9:41-70.
- Bertness, M. D. 1984. Ribbed mussels and *Spartina alterniflora* production in a New England salt marsh. *Ecology* 65:1794-1807.
- Bertness, M. D. 1985. Fiddler crab regulation of *Spartina alterniflora* production on a New England salt marsh. *Ecology* 66:1042-1055.
- Bertness, M. D. and T. Miller. 1984. The distribution and dynamics of *Uca pugnax* (Smith) burrows in a New England salt marsh. *Journal of Experimental Marine Biology and Ecology* 83:211-237.
- Bertness, M. D., C. Holdredge, and A. H. Altieri. 2009. Substrate mediates consumer control of salt marsh cordgrass on Cape Cod, New England. *Ecology* 90:2108-2117.
- Botto, F. and O. Iribarne. 2000. Contrasting effects of two burrowing crabs (*Chasmagnathus granulata* and *Uca uruguayensis*) on sediment composition and transport in estuarine environments. *Estuarine, Coastal and Shelf Science* 51:141-151.
- Bradley, P. M. and J. T. Morris. 1990. Physical characteristics of salt marsh sediments: ecological implications. *Marine Ecology Progress Series* 61:245-252.
- Byrne, R. J. and G. L. Anderson. 1978. Shoreline erosion in tidewater Virginia. Special Report in Applied Marine Science and Ocean Engineering. No. 111, Virginia Institute of Marine Science, Gloucester Pt, VA, 102p.
- Christiansen, T., P. L. Wiberg, and T. G. Milligan. 2000. Flow and sediment transport on a tidal salt marsh surface. *Estuarine, Coastal and Shelf Science* 50:315-331.
- Cox, R., R. A. Wadsworth, and A. G. Thomson. 2003. Long-term changes in salt marsh extent affected by channel deepening in a modified estuary. *Continental Shelf Research* 23:1833-1846.

- Darby, F. A. and R. E. Turner. 2008. Below- and aboveground *Spartina alterniflora* production in a Louisiana salt marsh. *Estuaries and Coasts* 31:223-231.
- Day Jr., J. W., F. Scarton, A. Rismondo, and D. Are. 1998. Rapid deterioration of a salt marsh in Venice Lagoon, Italy. *Journal of Coastal Research* 14:583-590.
- DeLaune, R. D., R. H. Baumann, and J. G. Gosselink. 1983. Relationships among vertical accretion, coastal submergence, and erosion in a Louisiana Gulf Coast marsh. *Journal of Sedimentary Petrology* 53:147-157.
- DeLaune, R. D., J. A. Nyman, and W. H. Patrick, Jr. 1994. Peat collapse, ponding and wetland loss in a rapidly submerging coastal marsh. *Journal of Coastal Research* 10:1021-1030.
- Downs, L. L., R. J. Nicholls, S. P. Leatherman, and J. Hautzenroder. 1994. Historic evolution of a marsh island: Bloodsworth Island, Maryland. *Journal of Coastal Research* 10:1031-1044.
- Edwards, J. M. and R. W. Frey. 1977. Substrate characteristics within a Holocene salt marsh, Sapelo Island, Georgia. *Senckenbergiana maritima* 9:215-259.
- Ellison, A. M., M. D. Bertness, and T. Miller. 1986. Seasonal patterns in the belowground biomass of *Spartina alterniflora* (Gramineae) across a tidal gradient. *American Journal of Botany* 73:1548-1554.
- Erwin, R. M., G. M. Sanders, and D. J. Posser. 2004. Changes in lagoonal marsh morphology at selected northeastern Atlantic Coast sites of significance to migratory waterbirds. *Wetlands* 24:891-903.
- Escapa, M., D. R. Minkoff, G. M. E. Perillo, and O. Iribane. 2007. Direct and indirect effects of burrowing crab *Chasmagnathus granulatus* activities on erosion of southwest Atlantic *Sarcocornia*-dominated marshes. *Limnology and Oceanography* 52:2340-2349.
- Fagherazzi, S., L. Carniello, L. D'Alpaos, and A. Defina. 2006. Critical bifurcation of shallow microtidal landforms in tidal flats and salt marshes. *Proceedings of the National Academy of Sciences* 103:8337-8341.
- Fagherazzi, S. and P. L. Wiberg. 2009. Importance of wind conditions, fetch, and water levels on wave-generated shear stresses in shallow intertidal basins. *Journal of Geophysical Research* 114:F03022. doi: 10.1029/2008JF001139.
- Fagherazzi, S., D. M. FitzGerald, R. W. Fulweiler, Z. Hughes, P. L. Wiberg, K. J. McGlathery, J. T. Morris, T. J. Tolhurst, L. A. Deegan, and D. S. Johnson. 2010. Ecogeomorphology of salt marshes and tidal flats. In *Treatise on Geomorphology*. Elsevier (submitted).

- Feagin, R. A., S. M. Lozanda-Bernard, T. M. Ravens, I. Moller, K. M. Yeager, and A. H. Baird. 2009. Does vegetation prevent wave erosion of salt marsh edges? *Proceedings of the National Academy of Sciences* 106:10109-10113.
- Finkelstein, K. and C. S. Hardaway. 1988. Late Holocene sedimentation and erosion of estuarine fringing marshes, York River, Virginia. *Journal of Coastal Research* 4:447-456.
- Franz, D. R. 2001. Recruitment, survivorship, and age structure of a New York ribbed mussel population (*Geukensia demissa*) in relation to shore level – a nine year study. *Estuaries* 24:319-327.
- Gabet, E. J. 1998. Lateral migration and bank erosion in a saltmarsh tidal channel in San Francisco Bay, California. *Estuaries* 21:745-753.
- Gallagher, J. L. and F. G. Plumley. 1979. Underground biomass profiles and productivity in Atlantic coastal marshes. *American Journal of Botany* 66:156-161.
- Gallagher, J. L., G. F. Somers, D. M. Grant, and D. M. Seliskar. 1988. Persistent differences in two forms of *Spartina alterniflora*: a common garden experiment. *Ecology* 69:1005-1008.
- Garofalo, D. 1980. The influence of wetland vegetation on tidal stream channel migration and morphology. *Estuaries* 3:258-270.
- Goodbred Jr., S. L. and A. C. Hine. 1995. Coastal storm deposition: salt-marsh response to a severe extratropical storm, March 1993, west-central Florida. *Geology* 23:679-682.
- Grimes, B. H., M. T. Huish, J. H. Kerby, and D. Moran. 1989. Species profiles: life histories and environmental requirements of coastal fishes and invertebrates (Mid-Atlantic) – Atlantic marsh fiddler. U.S. Fish and Wildlife Service Biological Report 82(11.114). U.S. Army Corps of Engineers, TR EL-82-4. 18pp.
- Gross, M. F., M. A. Hardisky, P. L. Wolf, and V. Klemas. 1991. Relationship between aboveground and belowground biomass of *Spartina alterniflora* (smooth cordgrass). *Estuaries* 14:180-191.
- Harmsworth, G. C. and S. P. Long. 1986. An assessment of saltmarsh erosion in Essex, England, with reference to the Dengie Peninsula. *Biological Conservation* 35:377-387.
- Hayden, B. P., R. D. Dueser, J. T. Callahan, and H. H. Shugart. 1991. Long-term research at the Virginia Coast Reserve. *BioScience* 41:310-318.

- Hayden, B. P. and N. R. Hayden. 2003. Decadal and century-long changes in storminess at Long-Term Ecological Research sites. In *Climate variability and ecosystem response at Long-Term Ecological Research sites*, eds. D. Greenland, D. G. Goodin, and R. C. Smith, 262-285. Oxford, UK: Oxford University Press.
- Higinbotham, C. B., M. Alber, and A. C. Chalmers. 2004. Analysis of tidal marsh vegetation patterns in two Georgia estuaries using aerial photography and GIS. *Estuaries* 27:670-683.
- Holdredge, C., M. D. Bertness, and A. H. Altieri. 2009. Role of crab herbivory in die-off of New England salt marshes. *Conservation Biology* 23:672-679.
- Howes, B. L., R. W. Howarth, J. M. Teal, and I. Valiela. 1981. Oxidation-reduction potentials in a salt marsh: spatial patterns and interactions with primary production. *Limnology and Oceanography* 26:350-360.
- Howes, B. L., J. W. Dacey, and D. D. Goehring. 1986. Factors controlling the growth form of *Spartina alterniflora*: feedbacks between above-ground production, sediment oxidation, nitrogen and salinity. *Journal of Ecology* 74:881-898.
- Hughes, M. L., P. F. McDowell, and W. A. Marcus. 2006. Accuracy assessment of georectified aerial photographs: Implications for measuring lateral channel movement in a GIS. *Geomorphology* 74:1-16.
- Kastler, J. A. 1993. Sedimentation and landscape evolution of Virginia salt marshes. MS Thesis. University of Virginia, Charlottesville, VA.
- Kastler, J. A. and P. L. Wiberg. 1996. Sedimentation and boundary changes of Virginia salt marshes. *Estuarine, Coastal and Shelf Science* 42:683-700.
- Kearney, M. S. and J. C. Stevenson. 1991. Island land loss and marsh vertical accretion rate evidence for historical sea-level changes in Chesapeake Bay. *Journal of Coastal Research* 7:403-415.
- Krebs, C. T. and I. Valiela. 1978. Effect of experimentally applied chlorinated hydrocarbons on the biomass of the fiddler crab, *Uca pugnax* (Smith). *Estuarine and Coastal Marine Science* 6:375-386.
- Knowlton, S. M. 1971. Geomorphological history of tidal marshes, Eastern Shore, Virginia, from 1852-1966. MS Thesis. University of Virginia, Charlottesville, VA.
- Knutson, P. L., R. A. Brochu, W. A. Seelig, and M. Inskeep. 1982. Wave damping in *Spartina alterniflora* marshes. *Wetlands* 2:87-104.

- Kuenzler, E. J. 1961. Structure and energy flow of a mussel population in a Georgia salt marsh. *Limnology and Oceanography* 6:191-204.
- Lawson, S. E. 2004. Sediment suspension as a control on light availability in a coastal lagoon. MS Thesis. University of Virginia, Charlottesville, VA.
- Mariotti, G., S. Fagherazzi, P. L. Wiberg, K. J. McGlathery, L. Carniello, and A. Defina. 2010. Influence of storm surges and sea level on shallow tidal basin erosive processes. *Journal of Geophysical Research*. doi: 10.1029/2009JC005892 (in press).
- McCraith, B. J., L. R. Gardner, D. S. Wethey, and W. S. Moore. 2003. The effect of fiddler crab burrowing on sediment mixing and radionuclide profiles along a topographic gradient in a southeastern salt marsh. *Journal of Marine Research* 61:359-390.
- McGlathery, K. J., I. C. Anderson, and A. C. Tyler. 2001. Magnitude and variability of benthic and pelagic metabolism in a temperate coastal lagoon. *Marine Ecology Progress Series* 216:1-15.
- McIvor, C. C. and T. J. Smith III. 1995. Differences in the crab fauna of mangrove areas at a southwest Florida and a northeast Australia location: implications for leaf litter processing. *Estuaries* 18:591-597.
- Michaels, R. E. 2004. The effects of *Uca pugnax* on the porewater biogeochemistry in a *Spartina alterniflora* salt marsh. MS Thesis. University of Virginia, Charlottesville, VA.
- Micheli, E. R. and J. W. Kirchner. 2002. Effects of wet meadow riparian vegetation on streambank erosion. 2. Measurements of vegetated bank strength and consequences for failure mechanics. *Earth Surface Processes and Landforms* 27:687-697.
- Möller, I. 2006. Quantifying saltmarsh vegetation and its effect on wave height dissipation: Results from a UK East coast saltmarsh. *Estuarine, Coastal and Shelf Science* 69:337-351.
- Möller, I., T. Spencer, J. R. French, D. J. Leggett, and M. Dixon. 1999. Wave transformation over salt marshes: A field and numerical modeling study from North Norfolk, England. *Estuarine, Coastal and Shelf Science* 49:411-426.
- Montague, C. L. 1980. A natural history of temperate western Atlantic fiddler crabs (Genus *Uca*) with reference to their impact on the salt marsh. *Contributions in Marine Science* 23:25-55.

- Moore, L. J. 2000. Shoreline mapping techniques. *Journal of Coastal Research* 16:111-124.
- Moreira, M. E. S. D. A. 1992. Recent saltmarsh changes and sedimentation rates in the Sado Estuary, Portugal. *Journal of Coastal Research* 8:631-640.
- Morris, J. T. 1980. The nitrogen uptake kinetics of *Spartina alterniflora* in culture. *Ecology* 61:1114-1121.
- Odum, W.E. 1988. Comparative ecology of tidal freshwater and salt marshes. *Annual Review of Ecology, Evolution, and Systematics* 19:147-176.
- Oertel, G. F. 2001. Hypsographic, hydro-hypsographic, and hydrological analysis of coastal bay environments, Great Machipongo Bay, Virginia. *Journal of Coastal Research* 17:775-783.
- Oertel, G. F. and H. J. Woo. 1994. Landscape classification and terminology for marsh in deficit coastal lagoons. *Journal of Coastal Research* 10:919-932.
- Pennings, S. C. and M. D. Bertness. 2001. Salt marsh communities. In *Marine community ecology*, eds. M. D. Bertness, S. Gaines, and M. E. Hay, 289-316. Sunderland, Massachusetts: Sinauer.
- Pestrong, R. 1969. The shear stress of tidal marsh sediments. *Journal of Sedimentary Petrology* 39:322-326.
- Pethick, J. S. 1992. Saltmarsh geomorphology. In *Saltmarshes: morphodynamics, conservation, and engineering significance*, eds. J. R. L. Allen and K. Pye. Cambridge, UK: Cambridge University Press.
- Phillips, J. D. 1986a. Coastal submergence and marsh fringe erosion. *Journal of Coastal Research* 2:427-436.
- Phillips, J. D. 1986b. Spatial analysis of shoreline erosion, Delaware Bay, New Jersey. *Annals of the Association of American Geographers* 76:50-62.
- Pizzuto, J. E. 1984. Bank erodibility of shallow sandbed streams. *Earth Surface Processes and Landforms* 9:113-124.
- Porter, J. P. and D. E. Smith. 2008. Live from the field: managing live-image databases at the Virginia Coast Reserve. Environmental Information Management Conference. Albuquerque, NM, USA.
- Reed, D. J. 1988. Sediment dynamics and deposition in a retreating coastal salt marsh. *Estuarine, Coastal and Shelf Science* 26:67-79.

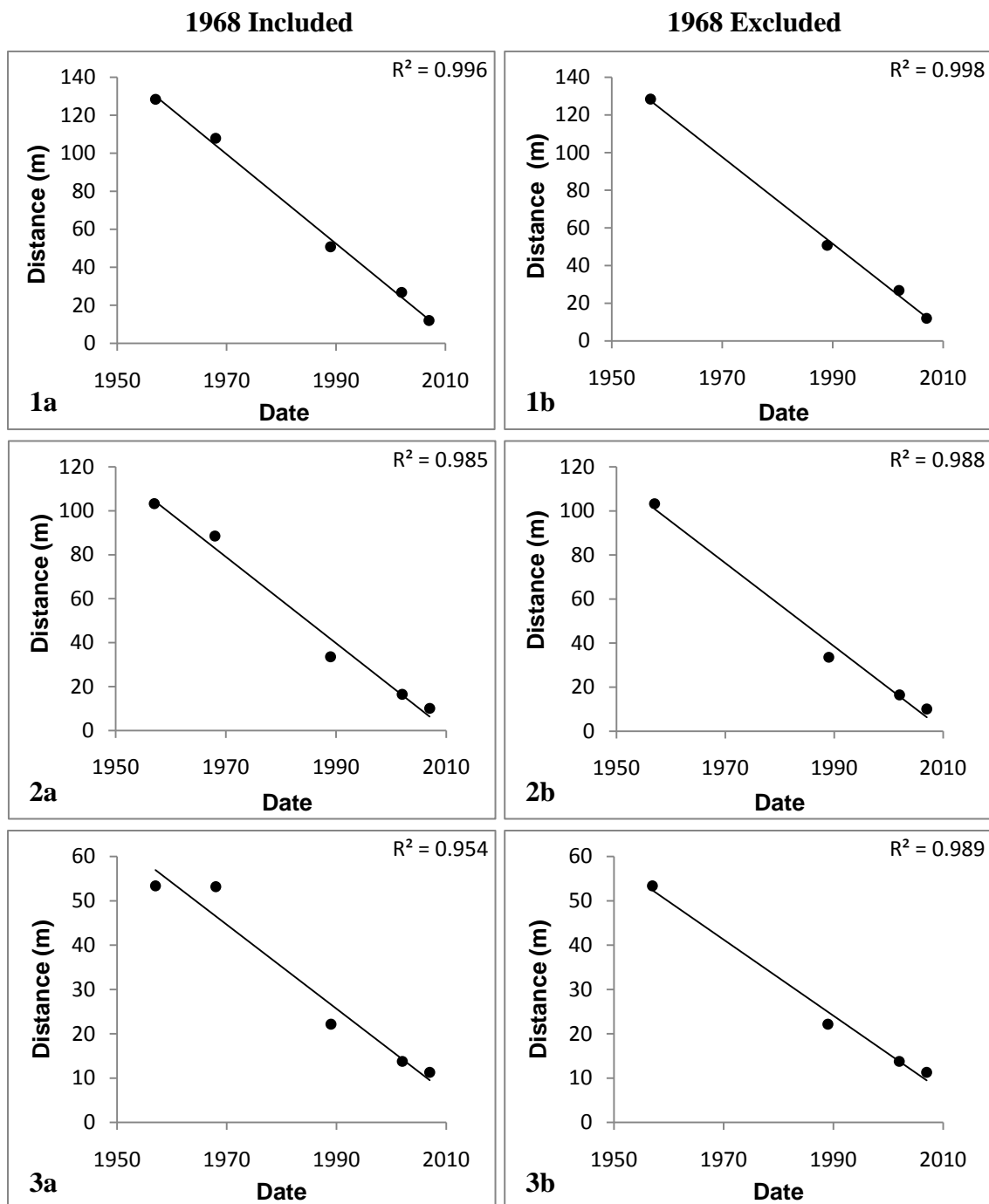
- Reed, D.J. 1990. The impact of sea-level rise on coastal salt marshes. *Progress in Physical Geography* 14:465-481.
- Reed, D. J., T. Spencer, A. L. Murray, J. R. French, and L. Leonard. 1999. Marsh surface sediment deposition and the role of tidal creeks: implications for created and managed coastal marshes. *Journal of Coastal Conservation* 5:81-90.
- Rosen, P. S. 1980. Erosion susceptibility of the Virginia Chesapeake Bay shoreline. *Marine Geology* 34:45-59.
- Schwimmer, R. A. 2001. Rates and processes of marsh shoreline erosion in Rehoboth Bay, Delaware, U.S.A. *Journal of Coastal Research* 17:672-683.
- Schwimmer, R. A. and J. E. Pizzuto. 2000. A model for the evolution of marsh shorelines. *Journal of Sedimentary Research* 70:1026-1035.
- Shinn, E. A. 1968. Burrowing in recent lime sediments of Florida and the Bahamas. *Journal of Paleontology* 42:879-894.
- Silliman, B. R. and J. C. Zieman. 2001. Top-down control of *Spartina alterniflora* production by periwinkle grazing in a Virginia salt marsh. *Ecology* 82:2830-2845.
- Silliman, B. R. and M. D. Bertness. 2002. A trophic cascade regulates salt marsh primary productivity. *Proceedings of the National Academy of Sciences* 99:10500-10505.
- Silliman, B. R., J. van de Koppel, M. D. Bertness, L. E. Stanton, and I. A. Mendelssohn. 2005. Drought, snails, and large-scale die-off of Southern U.S. salt marshes. *Science* 310:1803-1806.
- Sokal, R. R. and F. J. Rohlf. 1995. *Biometry: the principles and practice of statistics in biological research*, 3rd edition. New York: W. H. Freeman and Company.
- Stiven, A. E. and S. A. Gardner. 1992. Population processes in the ribbed mussel *Geukensia demissa* (Dillwyn) in a North Carolina salt marsh tidal gradient: spatial pattern, predation, growth and mortality. *Journal of Experimental Marine Biology and Ecology* 160:81-102.
- Stoodley, J. A. 1998. Saltmarsh sediments as indicators of changing environmental conditions: Thames Estuary, UK. PhD Dissertation. University of Reading, Reading, UK.
- Teal, J.M. 1958. Distribution of fiddler crabs in Georgia salt marshes. *Ecology* 39:185-193.

- Thieler, E. R., E. A. Himmelstoss, J. L. Zichichi, and A. Ergul. 2009. Digital Shoreline Analysis System (DSAS) version 4.0 — An ArcGIS extension for calculating shoreline change. U.S. Geological Survey Open-File Report 2008-1278.
- Thorne, C. R. and N. K. Tovey. 1981. Stability of composite river banks. *Earth Surface Processes and Landforms* 6:469-484.
- Tosi, M. 2007. Root tensile strength relationships and their slope stability implications of three shrub species in the Northern Apennines (Italy). *Geomorphology* 87:268-283.
- Tyler, A. C. and J. C. Zieman. 1999. Patterns of development in the creekbank region of a barrier island *Spartina alterniflora* marsh. *Marine Ecology Progress Series* 180:161-177.
- Valiela, I., J. M. Teal, and W. G. Deuser. 1978. The nature of growth forms in the salt marsh grass *Spartina alterniflora*. *The American Naturalist* 112:461-470.
- van de Koppel, J., D. van der Wal, J. P. Bakker, and P. M. J. Herman. 2005. Self-organization and vegetation collapse in salt marsh ecosystems. *The American Naturalist* 165:E1-E12.
- van der Wal, D., and K. Pye. 2004. Patterns, rates and possible causes of saltmarsh erosion in the Greater Thames area (UK). *Geomorphology* 61:373-391.
- van Eerd, M. M. 1985a. The influence of vegetation on erosion and accretion in salt marshes of the Oosterschelde, The Netherlands. *Vegetatio* 62:367-373.
- van Eerd, M. M. 1985b. Salt marsh cliff stability in the Oosterschelde. *Earth Surface Processes and Landforms* 10:95-106.
- Wang, J. Q., X. D. Zhong, L. F. Jiang, M. D. Bertness, C. M. Fang, J. K. Chen, T. Hara, and B. Li. 2010. Bioturbation of burrowing crabs promotes sediment turnover and carbon and nitrogen movements in an estuarine salt marsh. *Ecosystems* 13:586-599.
- Watts, C. W., T. J. Tolhurst, K. S. Black, and A. P. Whitmore. 2003. In situ measurements of erosion shear stress and geotechnical shear strength of the intertidal sediments of the experimental managed realignment scheme at Tollesbury, Essex, UK. *Estuarine, Coastal and Shelf Science* 58:611-620.
- Wilson, C. A. and M. A. Allison. 2008. An equilibrium profile model for retreating marsh shorelines in southeast Louisiana. *Estuarine, Coastal and Shelf Science* 80:483-494.

- Winterwerp, J. C., and W. G. M. van Kesteren. (2004). *Introduction to the Physics of Cohesive Sediment in the Marine Environment*. Amsterdam: Elsevier.
- Wray, R. D., S. P. Leatherman, and R. J. Nicholls. 1995. Historic and future land loss for upland and marsh islands in the Chesapeake Bay, Maryland, U.S.A. *Journal of Coastal Research* 11:1195-1203.
- Xin, P., G. Jin, L. Li, and D. A. Barry. 2009. Effects of crab burrows on pore water flows in salt marshes. *Advances in Water Resources* 32:439-449.

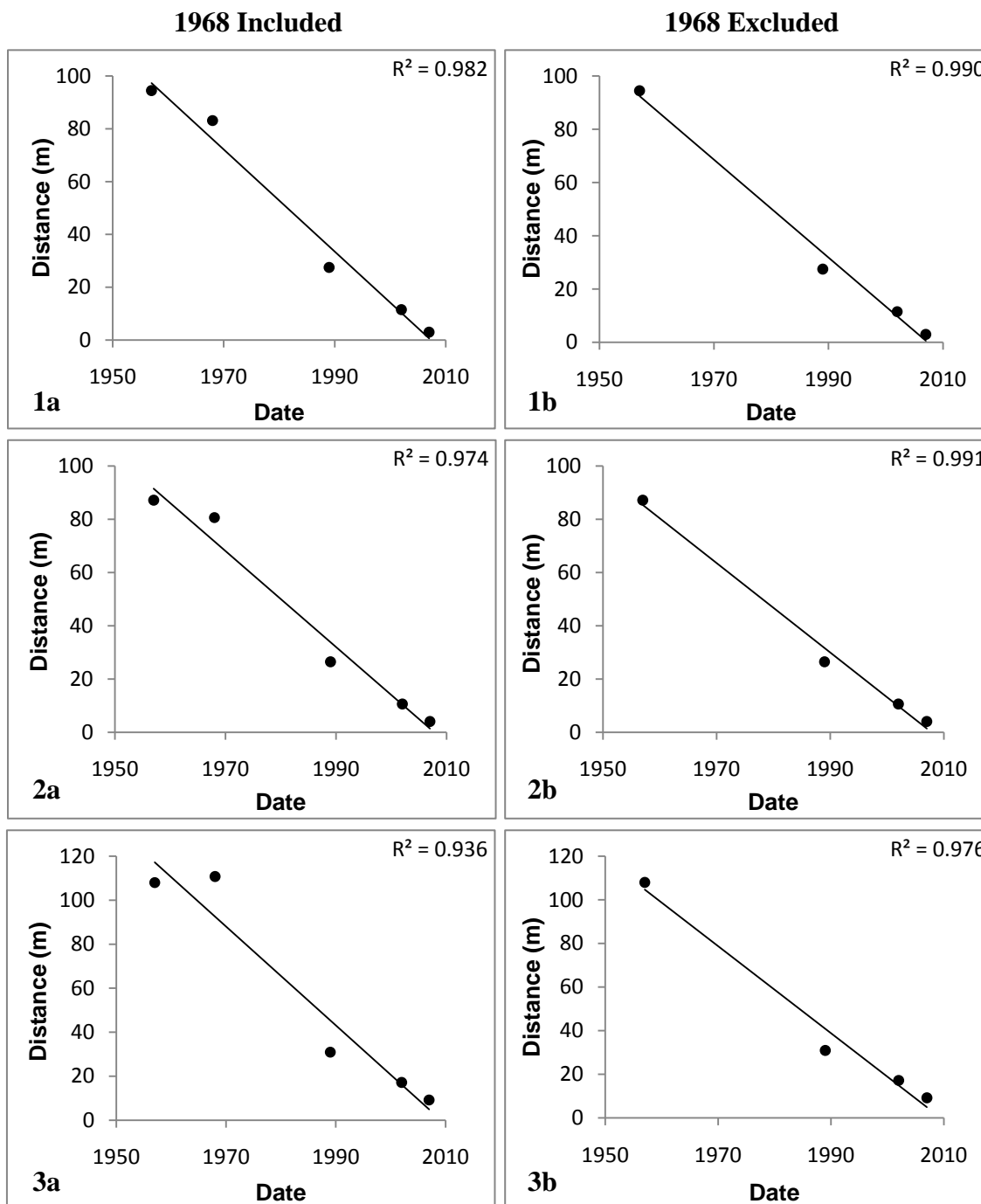
Appendix 1: Shoreline locations along selected transects

Chimney Pole



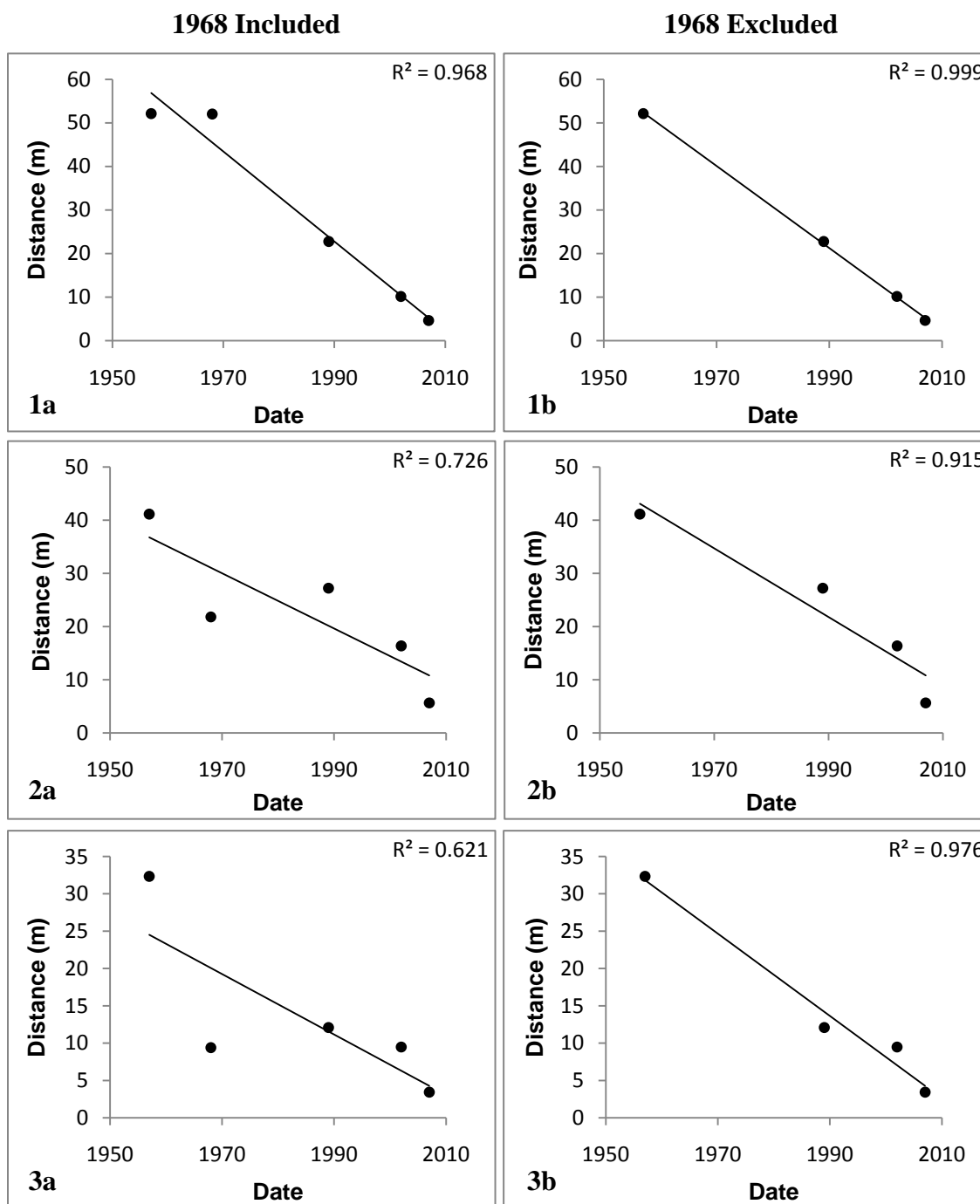
Positions of marsh shorelines with respect to the baseline at CP with 1968 included (a) and excluded (b). Selected transect numbers are: 1) 36, 2) 116, and 3) 264.

Matulakin Marsh



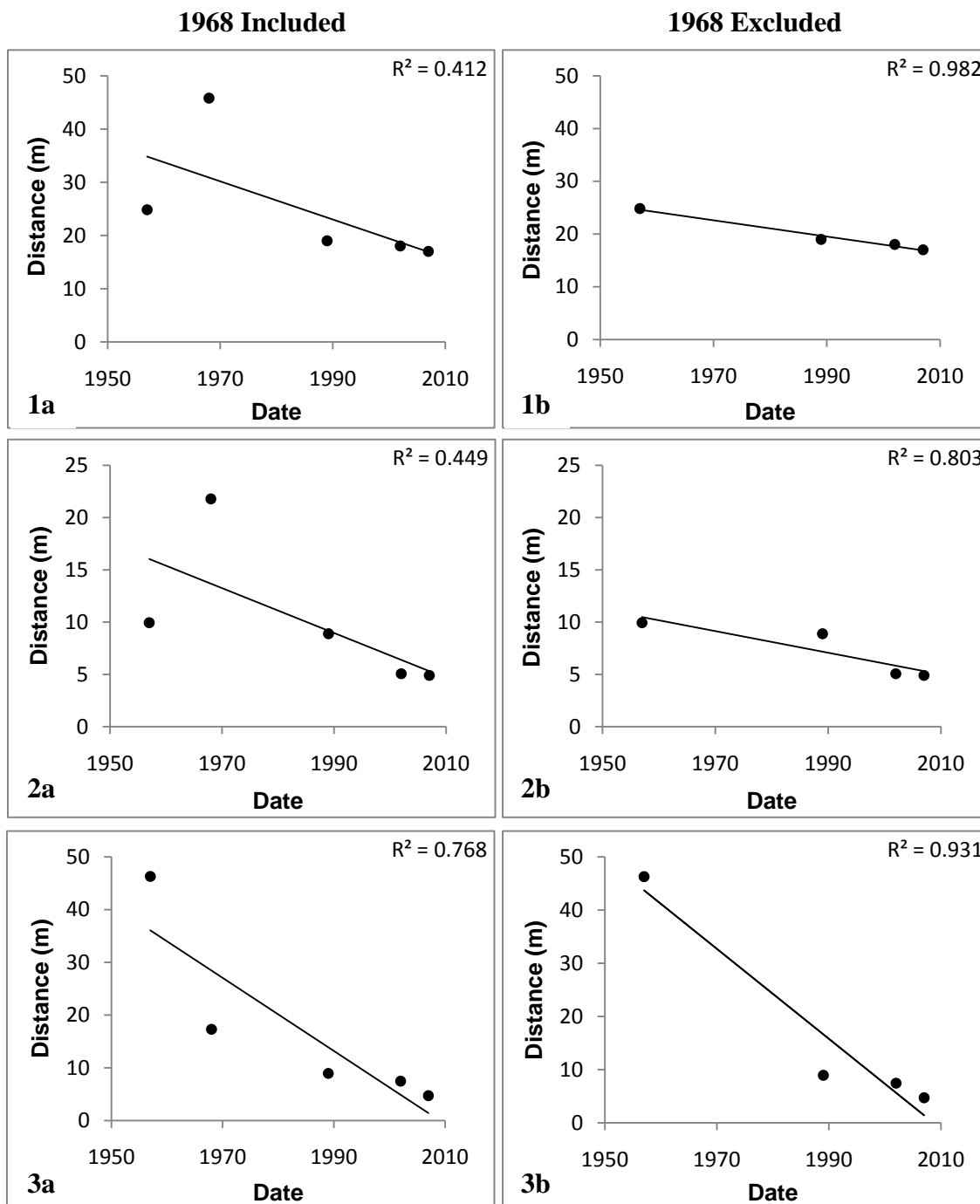
Positions of marsh shorelines with respect to the baseline at MM with 1968 included (a) and excluded (b). Selected transect numbers are: 1) 27, 2) 111, and 3) 321.

Hog Island



Positions of marsh shorelines with respect to the baseline at HI with 1968 included (a) and excluded (b). Selected transect numbers are: 1) 112, 2) 179, and 3) 298.

Fowling Point



Positions of marsh shorelines with respect to the baseline at FP with 1968 included (a) and excluded (b). Selected transect numbers are: 1) 70, 2) 136, and 3) 273.

Appendix 2: June and August 2009 vegetation results (mean values)

Marsh Location	Total Belowground Biomass (g·cm ⁻²)	Total Aboveground Biomass (g·cm ⁻²)	Shoot: Root	Canopy Height (cm)	Stem Density (m ⁻²)
FP Edge					
June	3997	519	0.16	31.7	985
August	4508	467	0.16	29.4	996
FP Interior					
June	5508	340	0.1	28.8	651
August	4901	585	0.26	27.1	894
HI Edge					
June	6384	320	0.05	16.3	1222
August	5162	528	0.1	23.7	770
HI Interior					
June	4595	265	0.06	17.3	736
August	3680	380	0.1	17.8	1019
CP Edge					
June	N/A	193	N/A	11	1460
August	7190	255	0.04	15.5	1177
CP Interior					
June	N/A	384	N/A	20.6	815
August	7280	353	0.05	15.6	1053
MM Edge					
June	6772	108	0.02	7.1	1120
August	6024	152	0.03	8.3	407
MM Interior					
June	6463	320	0.05	16.5	1109
August	6829	368	0.06	13.9	1222

Appendix 3: Means (± 1 SE) for burrow characteristics.

Marsh	Burrow Density (m ⁻²)	Burrow Diameter (mm)	Burrow Area (cm ² ·m ⁻²)	Burrow Volume (cm ³ ·m ⁻²)
<i>Fowling Point</i>				
Edge	112 \pm 32	9.1 \pm 0.2	78.8 \pm 22.3	2718
Interior	115.2 \pm 28.4	7.9 \pm 0.8	77.1 \pm 30.9	84
<i>Hog Island</i>				
Edge	48 \pm 18.2	9.6 \pm 2.4	80.9 \pm 66.5	338
Interior	28.8 \pm 11.8	6.5 \pm 2.0	16.0 \pm 6.8	145
<i>Chimney Pole</i>				
Edge	54.4 \pm 12.0	18.0 \pm 4.2	349.2 \pm 191.6	10592
Interior	179.2 \pm 52.4	10.9 \pm 1.4	221.0 \pm 74.2	487
<i>Matulakin Marsh</i>				
Edge	201.6 \pm 54.6	16.1 \pm 2.5	769.3 \pm 324.3	7700
Interior	128 \pm 29.9	10.8 \pm 0.7	167.4 \pm 60.2	604

Appendix 4: Chimney Pole camera design.



Appendix 5: Hog Island characteristics

Selected sediment properties (numbered sequentially from north to south; grain size and shear strength sampling not performed at same locations):

Sample Location	Median Grain Size (μm)	Surface Shear Strength ($\text{kg}\cdot\text{cm}^{-2}$)	Scarp Shear Strength (0-5 cm depth) ($\text{kg}\cdot\text{cm}^{-2}$)
1	127	0.46	N/A
2	155	0.20	0.12
3	152	0.26	0.14
4	118	0.34	0.33
5	120	0.30	0.22
6	N/A	0.32	0.49

Tensile strengths:

Sample Location	Rhizome Strength (N)	Root Strength (N)
1	17	1.5
2	16.5	1.8
3	10	0.6
4	15	1.8
5	15	1.8

Invertebrate characteristics (crab and mussel sampling not performed at same locations):

Sample Location	Burrow Density (m^{-2})	Burrow Coverage ($\text{cm}^2\cdot\text{m}^{-2}$)	Mussel Density (m^{-2})
1	16	7	400
2	112	346	384
3	64	31	80
4	32	16	896
5	16	4	816
6	N/A	N/A	112
7	N/A	N/A	64
8	N/A	N/A	416

Appendix 6: Mean values for selected marsh characteristics

Sediment Properties:

Marsh	Median Grain Size (μm)	Mean Grain Size (μm)	Surface Stress ($\text{kg}\cdot\text{cm}^{-2}$)
Fowling Point			
Edge	271.1	260.1	0.34
Interior	237.5	248.8	0.08
Hog Island			
Edge	134.2	124.9	0.32
Interior	146.4	135.5	0.07
Chimney Pole			
Edge	49.4	64.3	0.41
Interior	42.8	55.7	0.05
Matulakin Marsh			
Edge	14.9	32.0	0.26
Interior	14.1	27.7	0.12

Vegetation Characteristics:

Marsh	Total Aboveground Biomass ($\text{g}\cdot\text{m}^{-2}$)	Total Belowground Biomass ($\text{g}\cdot\text{m}^{-2}$)	Root Strength (N)	Rhizome Strength (N)
Fowling Point				
Edge	493	4252	1.62	23.73
Interior	476	5171	1.52	12.40
Hog Island				
Edge	424	5773	1.51	14.76
Interior	323	4138	2.23	18.47
Chimney Pole				
Edge	224	7190	1.58	16.67
Interior	369	7280	2.14	20.53
Matulakin Marsh				
Edge	130	6398	1.39	8.65
Interior	344	6646	1.65	10.77

Belowground Biomass by Depth:

Marsh	Location	Depth (cm)	Belowground Biomass (g·cm ⁻²)
CP	Edge	0-5	3132
CP	Edge	5-10	1785
CP	Edge	10-15	1245
CP	Edge	15-20	1027
CP	Interior	0-5	1755
CP	Interior	5-10	2357
CP	Interior	10-15	1806
CP	Interior	15-20	1363
FP	Edge	0-5	1272
FP	Edge	5-10	1134
FP	Edge	10-15	904
FP	Edge	15-20	943
FP	Interior	0-5	1841
FP	Interior	5-10	1544
FP	Interior	10-15	984
FP	Interior	15-20	802
HI	Edge	0-5	1768
HI	Edge	5-10	1857
HI	Edge	10-15	1203
HI	Edge	15-20	945
HI	Interior	0-5	680
HI	Interior	5-10	870
HI	Interior	10-15	1217
HI	Interior	15-20	1371
MM	Edge	0-5	2118
MM	Edge	5-10	1788
MM	Edge	10-15	1504
MM	Edge	15-20	987
MM	Interior	0-5	1893
MM	Interior	5-10	1875
MM	Interior	10-15	1710
MM	Interior	15-20	1167

Mussel and Snail Densities

Marsh	Mussel Density (m ⁻²)	Snail Density (m ⁻²)
Fowling Point		
Edge	398	54
Interior	88	154
Hog Island		
Edge	396	32
Interior	4	86
Chimney Pole		
Edge	102	216
Interior	2	146
Matulakin Marsh		
Edge	200	148
Interior	58	194

Appendix 7: Grain size distributions

Diameter (μm)	FP Edge	FP Interior	HI Edge	HI Interior	CP Edge	CP Interior	MM Edge	MM Interior
0.3752	0.0351881	0.0448785	0.0314207	0.0264363	0.0780004	0.0732951	0.119589	0.103116
0.41188	0.0643956	0.0800227	0.0579524	0.0501963	0.138541	0.130365	0.212685	0.183512
0.45214	0.100703	0.118679	0.0917265	0.0838365	0.203797	0.192049	0.313094	0.270532
0.49635	0.141372	0.168462	0.128132	0.114632	0.290081	0.273616	0.445561	0.385673
0.54487	0.177344	0.209947	0.160107	0.142748	0.361294	0.340888	0.554219	0.480809
0.59814	0.209804	0.246045	0.18875	0.167733	0.422717	0.399355	0.647972	0.56409
0.65662	0.239477	0.278518	0.21443	0.189285	0.477435	0.451846	0.731427	0.639539
0.72081	0.267319	0.309641	0.237725	0.207113	0.529547	0.502213	0.81083	0.712682
0.79128	0.291606	0.335948	0.256851	0.221114	0.572365	0.543628	0.875127	0.773697
0.86863	0.311796	0.356651	0.271609	0.231262	0.604	0.574788	0.922224	0.821373
0.95355	0.328314	0.372911	0.282299	0.237698	0.626202	0.597371	0.955043	0.858302
1.0468	0.3417	0.386134	0.289289	0.240635	0.6412	0.613465	0.977286	0.887728
1.1491	0.352722	0.39784	0.293018	0.240627	0.651724	0.625231	0.992848	0.91253
1.2614	0.360933	0.407061	0.29329	0.238187	0.655841	0.630833	0.999091	0.930483
1.3848	0.366844	0.414889	0.290835	0.233762	0.655796	0.632596	1.00015	0.945076
1.5201	0.370876	0.422115	0.286214	0.227731	0.653354	0.632285	0.999326	0.959059
1.6688	0.374149	0.430861	0.280505	0.220413	0.653077	0.634284	1.0041	0.978731
1.8319	0.376745	0.440796	0.273719	0.212166	0.655017	0.63824	1.01431	1.00361
2.011	0.379053	0.452072	0.266489	0.203448	0.660254	0.645327	1.03213	1.03557
2.2076	0.381609	0.46473	0.259557	0.194976	0.669633	0.656405	1.05915	1.07593
2.4234	0.385437	0.47954	0.25417	0.187738	0.685258	0.673739	1.09914	1.12814
2.6603	0.391523	0.496881	0.251154	0.182985	0.70847	0.698089	1.1533	1.19284
2.9204	0.400501	0.516662	0.251214	0.181975	0.739405	0.729289	1.22129	1.26965
3.2059	0.412604	0.538637	0.254905	0.185645	0.777777	0.766871	1.30204	1.35751

3.5193	0.427284	0.562031	0.262285	0.194198	0.822071	0.809586	1.39321	1.45467
3.8634	0.443453	0.586111	0.272945	0.206853	0.871325	0.856655	1.49291	1.55938
4.2411	0.459157	0.609283	0.285584	0.221838	0.923182	0.905945	1.5972	1.66811
4.6557	0.47202	0.629668	0.298622	0.236698	0.975106	0.955354	1.702	1.77724
5.1109	0.479623	0.644991	0.310268	0.248913	1.02344	1.00194	1.80226	1.88239
5.6105	0.480372	0.653676	0.319381	0.256564	1.06553	1.044	1.89483	1.9809
6.159	0.47394	0.654874	0.325498	0.258979	1.09967	1.08025	1.97729	2.07043
6.7611	0.461333	0.648792	0.328916	0.256842	1.1257	1.11039	2.04876	2.14986
7.4221	0.444309	0.636409	0.330579	0.251831	1.14451	1.13477	2.10916	2.21852
8.1477	0.424662	0.619	0.3316	0.246186	1.15648	1.15366	2.15865	2.27621
8.9443	0.40373	0.59811	0.33343	0.242137	1.16205	1.16784	2.19739	2.32267
9.8187	0.382291	0.57517	0.336732	0.24106	1.16119	1.17782	2.22526	2.35738
10.779	0.361549	0.552672	0.342498	0.243657	1.1572	1.18668	2.24452	2.38166
11.832	0.343668	0.53375	0.351252	0.250304	1.15511	1.19867	2.26051	2.39961
12.989	0.33145	0.522015	0.364316	0.261685	1.16183	1.22015	2.2818	2.41851
14.259	0.326585	0.519122	0.38285	0.278951	1.18104	1.25587	2.31514	2.44427
15.653	0.327661	0.523499	0.407078	0.301628	1.21166	1.30749	2.36115	2.47754
17.183	0.329395	0.530558	0.435553	0.327027	1.24897	1.37371	2.4128	2.51215
18.863	0.325211	0.534909	0.4649	0.350582	1.28769	1.45176	2.45932	2.53891
20.707	0.312447	0.534705	0.493614	0.370504	1.32888	1.54277	2.49369	2.55279
22.732	0.294459	0.532693	0.523141	0.390508	1.37892	1.65117	2.51606	2.55609
24.954	0.27868	0.53538	0.55802	0.416339	1.44865	1.78462	2.53278	2.55703
27.393	0.272346	0.548707	0.60461	0.456082	1.54615	1.94851	2.54899	2.56202
30.071	0.277879	0.574364	0.667129	0.513363	1.67311	2.14237	2.56218	2.56897
33.011	0.290678	0.608958	0.744315	0.582158	1.82516	2.3598	2.5612	2.56613
36.239	0.30134	0.645137	0.832036	0.653743	1.9948	2.59045	2.52957	2.53583
39.781	0.301932	0.675953	0.924436	0.719196	2.17915	2.82619	2.45421	2.46374

43.67	0.290727	0.698528	1.01485	0.771863	2.38234	3.06274	2.33136	2.34542
47.94	0.274008	0.715713	1.10068	0.814092	2.61432	3.29798	2.16787	2.18738
52.626	0.265576	0.733991	1.18652	0.863784	2.88309	3.52548	1.97725	2.00236
57.771	0.275389	0.755964	1.28285	0.947652	3.18442	3.7275	1.7726	1.80162
63.419	0.294558	0.77452	1.39592	1.06725	3.49541	3.87433	1.56293	1.59142
69.619	0.297915	0.774303	1.52886	1.19083	3.77426	3.92994	1.35325	1.37457
76.425	0.280382	0.747358	1.71997	1.32929	3.97062	3.86615	1.14828	1.15639
83.897	0.264632	0.706909	2.07792	1.605	4.04215	3.67833	0.957746	0.951052
92.099	0.265677	0.680702	2.7585	2.21731	3.97125	3.39179	0.797073	0.7804
101.1	0.2833	0.702717	3.89219	3.37125	3.77356	3.05709	0.683019	0.665463
110.99	0.340941	0.81148	5.48296	5.18086	3.4868	2.72443	0.625421	0.613932
121.84	0.502334	1.04657	7.32317	7.50964	3.15058	2.41803	0.620531	0.61508
133.75	0.819926	1.43898	9.00179	9.82287	2.78396	2.12887	0.649331	0.640824
146.82	1.32773	1.98813	10.0247	11.3593	2.37955	1.8232	0.677238	0.649983
161.18	2.08298	2.63602	10.0048	11.5573	1.92586	1.47587	0.664566	0.607103
176.93	3.12488	3.27396	8.8558	10.3447	1.42722	1.09129	0.584836	0.502408
194.23	4.40126	3.79154	6.84254	8.10441	0.925408	0.711388	0.443399	0.353709
213.22	5.75498	4.13322	4.41545	5.29756	0.500965	0.392871	0.273755	0.19952
234.07	6.9767	4.31845	2.08371	2.45534	0.227471	0.182558	0.13091	0.0863656
256.95	7.86132	4.42114	0.616059	0.682898	0.107617	0.08253	0.0542366	0.0316062
282.07	8.2731	4.53135	0.0892229	0.10211	0.087065	0.0539257	0.035875	0.0165184
309.64	8.18754	4.70554	0.00462722	0.00448481	0.126916	0.0596866	0.0576873	0.0160645
339.92	7.67244	4.92077	0	0	0.205791	0.084654	0.110062	0.0204912
373.15	6.82962	5.06495	0	0	0.280307	0.114537	0.169814	0.0236359
409.63	5.70921	4.98221	0	0	0.303644	0.128132	0.197593	0.0216258
449.67	4.35271	4.56262	0	0	0.260526	0.113602	0.179512	0.0142221
493.63	2.96296	3.83119	0	0	0.172559	0.0720352	0.122204	0.00621431

541.89	1.7714	2.92063	0	0	0.0850106	0.0300584	0.0580174	0.00130063
594.87	0.832232	2.00568	0	0	0.0293845	0.00601512	0.0164062	0.0001119
653.02	0.259696	1.23163	0	0	0.00857322	0.0004891	0.00233617	0
716.87	0.0603143	0.685922	0	0	0.00442744	0	0.00011156	0
786.95	0.0124867	0.392003	0	0	0.00435528	0	0	0
863.88	0.0015657	0.245921	0	0	0.0037361	0	0	0
948.34	7.33E-05	0.193868	0	0	0.00130119	0	0	0
1041	0	0.191534	0	0	0.00019812	0	0	0
1142.8	0	0.141901	0	0	0	0	0	0
1254.6	0	0.0661488	0	0	0	0	0	0
1377.2	0	0.0142467	0	0	0	0	0	0
1511.8	0	0.001232	0	0	0	0	0	0
1659.6	0	0	0	0	0	0	0	0
1821.9	0	0	0	0	0	0	0	0
2000								